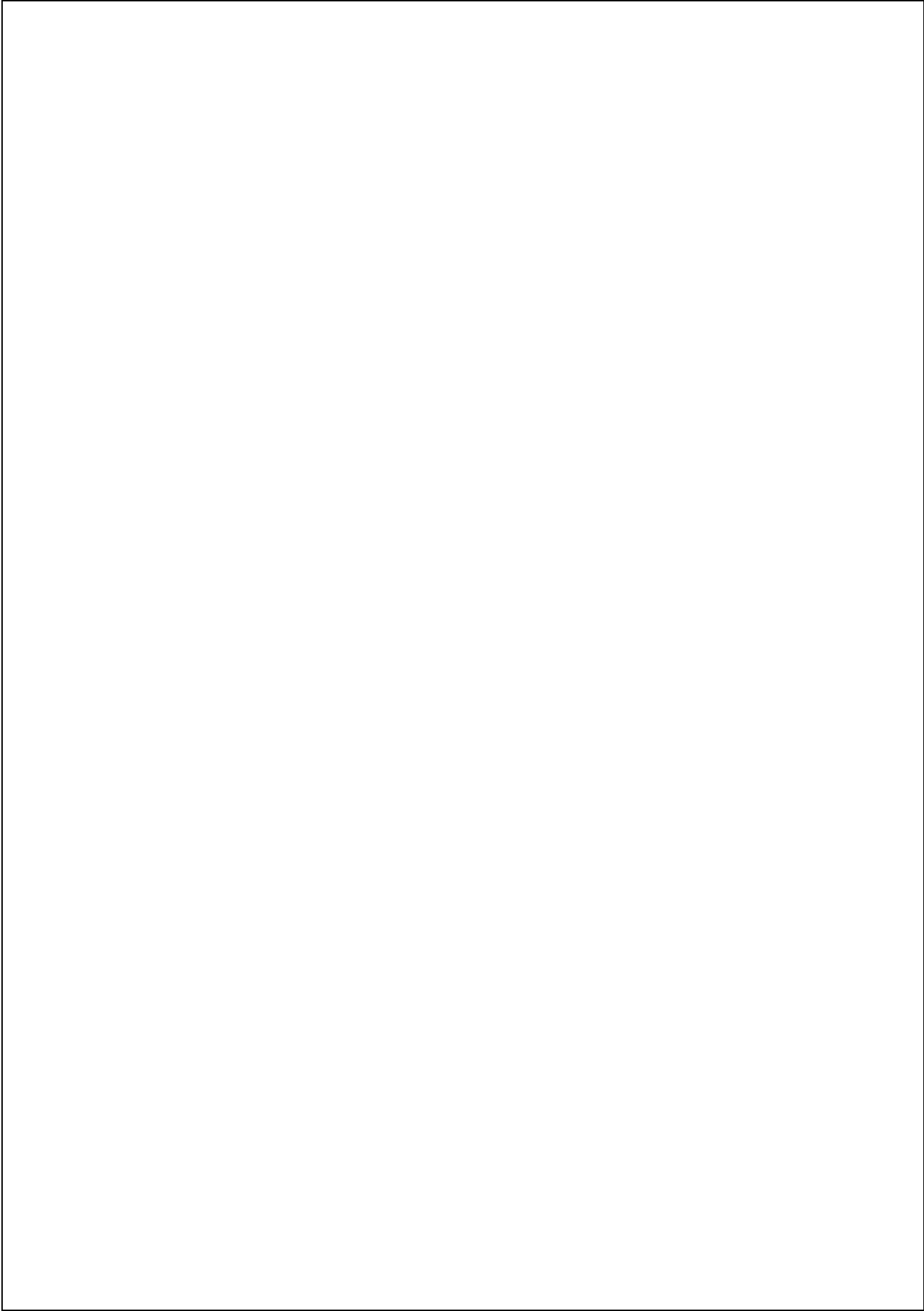




Scientific Report

2010-2011



Scientific Report
2010-2011

Cover image: *CTAB crystals on carbon grid, self-arranged during solvent evaporation.*
Valerio Voliani, Nest, Pisa. Artwork: Lucia Covi.

Table of contents

foreword	<i>pag. 1</i>
organization	<i>pag. 2</i>
people	<i>pag. 3</i>
summary of research activities	<i>pag. 8</i>
highlights	<i>pag. 13</i>
equipment	<i>pag. 57</i>
publications	<i>pag. 63</i>
projects and grants	<i>pag. 73</i>
collaborations	<i>pag. 79</i>
CnrNano life	<i>pag. 83</i>
outreach and communication	<i>pag. 91</i>

The Nanoscience Institute of the National Research Council (CnrNano) has been recently established (February 2010) from the merging of three former INFM centers: NEST in Pisa, NNL in Lecce, and S3 in Modena.

The primary objective of the Institute is the fundamental study and the manipulation of systems at the nanometric scale. Its wide and multidisciplinary research activities include the synthesis and fabrication of nanostructures and devices, the experimental and theoretical-computational study of their properties and functionality, and of their interfaces at a microscopic and mesoscopic scale, as well as their integration in complex functional systems. Knowledge and expertise are used to develop applications in several fields, from energy and environment to nanomechanics, nano(bio)technologies, nanomedicine, with special attention to projects and advanced technologies of industrial interest. Among the main features of the Institute we point out its number of research infrastructures at high technological content and the presence of a critical mass able to pursue research activities in the framework of the program Horizon 2020. The Institute is also strongly committed to the promotion of communication and education in the area of nanoscience.

Besides Scuola Normale Superiore of Pisa, University of Salento of Lecce, and University of Modena and Reggio Emilia, which host the Institute centers, we share common projects with several Italian and foreign research institutions and companies. It is also worth mentioning the strong interaction with the Istituto Italiano di Tecnologia (IIT).

Prominent in this Institute is the presence of young researchers and students. The Institute has 59 permanent and 21 fixed-term staff members, and about 50 young researchers among PhD students and post doctoral fellows. Furthermore, 130 affiliated researchers (50 of which with a permanent position) participate in the research activities of the Institute.

This is the first Activity Report of the new Nanoscience Institute. The following pages intend to offer an overview of its activities and facilities, as well as of its main achievements in the first two years of research activity.

I would like to thank Franco Calabi, Elisa Molinari, Paola Luches, Vittorio Pellegrini, Daniele Sanvitto, Roberta De Donatis, Luisa Neri, and Maddalena Scandola for their precious help in the preparation of this Report.

A full description of CnrNano activity, production, news and events, is available on our website <http://www.nano.cnr.it>.

Lucia Sorba
Director of the CNR Nanoscience Institute



Organization

Director of the Institute Lucia Sorba

Directors of the Centers

Pisa NEST	Lucia Sorba
Lecce NNL	Franco Calabi
Modena S3	Elisa Molinari

Administrative Secretary Maria Grazia Angelini

Communication Maddalena Scandola

Executive Board

CnrNano Researchers Franco Calabi, Milena De Giorgi, Paola Luches, Marco Polini, Gian Michele Ratto, Massimo Rontani

Administrative and Technical Staff Ciro Urso

Affiliated researchers Andrea Alessandrini, Massimo De Vittorio, Stefano Frabboni, Giuseppe Grosso



People

People

CnrNano Researchers

Valentina Arima NNL	Paolo Facci S3	Deborah Prezzi S3
Daniele Arosio NEST	Riccardo Farchioni NEST	Alessandra Quarta NNL
Valerio Bellini S3	Andrea Ferretti S3	Gian Michele Ratto NEST
Andrea Bertoni S3	Gian Carlo Gazzadi S3	Aurora Rizzo NNL
Laura Blasi NNL	Francesco Giazotto NEST	Massimo Rontani S3
Giorgia Brancolini S3	Vincenzo Grillo S3	Carlo Andrea Rozzi S3
Franco Calabi NNL	Roberto Grisorio NNL	Daniele Sanvitto NNL
Arrigo Calzolari S3	Stefan Heun NEST	Lucia Sorba NEST
Andrea Camposeo NNL	Shilpi Karmakar NNL	Fabio Taddei NEST
Andrea Candini S3	Stefano Leporatti NNL	Vittorianna Tasco NNL
Luigi Carbone NNL	Paola Luches S3	Maria Teresa Todaro NNL
Riccardo Castagna NEST	Vincenzo Maiorano NNL	Valentina Tozzini NEST
Marco Cecchini NEST	Carmela Martinelli NNL	Alessandro Tredicucci NEST
Stefano Corni S3	Riccardo Nifosi NEST	Paolo Emilio Trevisanutto NNL
Valdis Corradini S3	Guido Paolicelli S3	Filippo Troiani S3
Milena De Giorgi NNL	Adriana Grazia Passaseo NNL	Stefano Veronesi NEST
Loretta Laureana Del Mercato NNL	Vittorio Pellegrini NEST	Alessandro Vezzani S3
Fabio Della Sala NNL	Teresa Pellegrino NNL	Ilenia Viola NNL
Alessandro di Bona S3	Luana Persano NNL	
Rosa Di Felice S3	Marco Pieruccini S3	
Eduardo Fabiano NNL	Marco Polini NEST	

CnrNano Post-docs

Alessandra Aloisi NNL	Filippo Fabbri NNL	Mariela Rodriguez Otazo S3
Mario Amado Montero NEST	Elena Favilla NEST	Miguel Royo Valls S3
Patrizia Andreozzi NNL	Giulio Ferrari S3	Anna Giovanna Sciancalepore NNL
Luca Bellucci S3	Andrea Gamucci NEST	Heiko Seeger S3
Maria Rosa Belviso NNL	Alberto Ghirri S3	Wenming Sun S3
Andrea Benassi S3	Donata Iandolo NNL	Elisabetta Tarentini NNL
Enrico Benassi S3	Carola La Tegola NNL	Aleksandrs Terentjevs NNL
Stefania Benedetti S3	Francesca Lezzi NNL	Dimitrios Toroz S3
Monica Bianco NNL	Lucia Marra NNL	Sandro Usseglio Nanot NNL
Igor Bodrenko NNL	Elisabetta Marulli NNL	Viviana Vergaro NNL
Agostina Lia Capodilupo NNL	Giovanni Morello NNL	Valeria Videtta NNL
Giuseppe Caretto NNL	Concetta Nobile NNL	Michele Virgilio NEST
Oliver Carrillo S3	Daniela Parisi NEST	Orazio Vittorio NEST
Ciro Cecconi S3	Marialilia Pea NEST	Antonella Zacheo NNL
Paola Serena D'Agostino S3	Alessandro Polini NNL	Alessandra Zizzari NNL
Pino D'Amico S3	Marco Polo NNL	
Alain Delgado Gran S3	Giovanni Potente NNL	
Antonio Della Torre NNL	Elisabetta Primiceri NNL	

Affiliated Researchers

Marco Affronte S3
 Andrea Alessandrini S3
 Giuseppe Amoretti S3
 Athanasia Athanasiou NNL
 Fabio Beltram NEST
 Carlo Maria Bertoni S3
 Roberto Biagi S3
 Mariano Biasiucci NNL
 Diego Bisero S3
 Olmes Bisi S3
 Ranieri Bizzarri NEST
 Martino Bolognesi S3
 Annalisa Bonfiglio S3
 Paolo Bordone S3
 Virginio Bortolani S3
 Rossella Brunetti S3
 Marilia Junqueira Caldas S3
 Franco Carillo NEST
 Giovanni Carlotti S3
 Claudia Carlucci NNL
 Stefano Carretta S3
 Alessandra Catellani S3
 Carlo Cavazzoni S3
 Giuseppe Ciccarella NNL
 Roberto Cingolani NNL
 Maurizio Enrico Corti S3
 Pantaleo Davide Cozzoli NNL

Sergio D'Addato S3
 Valentina De Renzi S3
 Umberto del Pennino S3
 Francesca De Rienzo S3
 Massimo De Vittorio NNL
 Elena Degoli S3
 Nicolas Didier NEST
 Alberto Di Lieto NEST
 Daniele Ercolani NEST
 Rosario Fazio NEST
 Mauro Ferrario S3
 Stefano Frabboni S3
 Anna Maria Garbesi S3
 Giuseppe Gigli NNL
 Vittorio Giovannetti NEST
 Guido Goldoni S3
 Giuseppe Grosso NEST
 Carlo Jacoboni S3
 Biswajit Karmakar NEST
 Silvia Landi NEST
 Alessandro Lascialfari S3
 Stefano Luin NEST
 Rita Magri S3
 Franca Manghi S3
 Giuseppe Maruccio NNL
 Marco Mazzeo NNL
 Claudia Menozzi S3

Elisa Molinari S3
 Umberto Muscatello S3
 David Neilson NEST
 Stefano Ossicini S3
 Gioacchino Massimo Palma NEST
 Giuseppe Pastori Parravicini NEST
 Pasqualantonio Pingue NEST
 Dario Pisignano NNL
 Stefano Pugnetti NEST
 Angelo Rettori S3
 Maria Clelia Righi S3
 Rosaria Rinaldi NNL
 Stefano Roddaro NEST
 Davide Rossini NEST
 Alice Ruini S3
 Andrea Sacchetti S3
 Bruno Samorì S3
 Paolo Santini S3
 Marco Sola S3
 Alessandra Toncelli NEST
 Mauro Tonelli NEST
 Sergio Valeri S3
 Daniele Varsano S3
 Paolo Vavassori S3
 Cristiano Viappiani NEST
 Miriam Vitiello NEST
 Giampaolo Zuccheri S3

People

Affiliated Post-Docs

Amit Kumar Agarwal NEST
Michele Amato S3
Antonella Battisti NEST
Subhajt Biswas NEST
Igor Bodrenko NNL
Luca Chirolli NEST
Francesco Ciccarello NEST
Piero Cosseddu S3
Riccardo Degl'Innocenti NEST
Fabio Deon NEST
Antonella De Pasquale NEST
Luisa De Vivo NEST
Armida Di Fenza NEST
Mariagrazia Di Luca NEST
Roberto Guerra S3
Emanuela Jacchetti NEST
Silvia Landi NEST
Giovanna Lucarelli NNL
Laura Marchetti NEST
Maria J. Martinez Perez NEST
Simone Montangero NEST
Daniela Parisi NEST
Alessandro Pitanti NEST
Andrea Pucci NEST
Fernanda Ricci NEST
Mariela Rodriguez Otazo S3
Marcello Rosini S3
Alberto Rota S3
Magdalena Elzbieta Siwko S3
Attila Szallas S3
Ilaria Tonazzini NEST
Davide Venturelli NEST

Affiliated PhD students

Lorenzo Albertazzi NEST
Christian Alvino S3
Andrea Arcangeli NEST
Gaelle Françoise Arnaud S3
Laura Basiricò S3
Maria Rosa Belviso NNL
Luca Bergamini S3
Matteo Bertocchi S3
Francesca Branzoli S3
Marco Brondi NEST
Marialuisa Caiazzo S3
Maria Camarasa G. NEST (CNR funded)
Matteo Carrega NEST
Maria Serena Chiriaco NNL
Caterina Cocchi S3
Alessandro Di Cerbo S3
Riccardo Di Corato NNL
Raffaele Faoro NEST
Francesco Ferrara NNL
Tahereh Ghane S3
Marco Gibertini NEST
Laura Gioia Passione NNL
Sarah Goler NEST
Marco Govoni S3
Karina A. Guerrero Becerra S3
Mirgender Kumar NEST
Savio Laricchia NNL
Ang Li NEST
Anna Louidice NNL
Giulia Lorusso S3
Farah Mahwish S3
Francesco Malara NNL
Letizia Mariotti NEST
Simone Marocchi S3
Luca Masini NEST
Claudio Manzato S3
Giorgio Mattana S3
Sandro Meucci NEST
Maria Moffa NNL
Anna Grazia Monteduro NNL
Massimo Morandini NEST
Mariangela Mortato NNL
Stefano Pagliara NNL
Federico Pagliuca S3
Ilaria Elena Palamà NNL
Nicola Paradiso NEST
Sebastiano Peotta NEST
Paolo Petrangolini S3
Silvio Pipolo S3
Ferruccio Pisanello NNL
Giovanni Potente NNL
Elisabetta Primiceri NNL
Alessandro Principi NEST
Rosario Profumo NEST
Diego Rainis NEST
Marco Reguzzoni S3
Alberto Ronzani NEST
Marta Rosa S3
Massimo Rovatti S3
Angela Scrascia NNL
Andrea Secchi S3
Ilaria Siloi S3
Barbara Storti NEST
Sebastian Sulis Sato NEST
Marco Travagliati NEST
Manoj Tripathi S3 (CNR funded)
Fabio Trovato NEST
Giuseppe Valletta NEST
Valerio Voliani NEST
Antonella Zacheo NNL
Simone Zanotto NEST
Giovanna Zilibotti S3

Administrative Staff

Maria Grazia Angelini S3
Elisa Bolognesi S3
Francesca Cristofaro NEST
Lucia Francini NEST
Patrizia Pucci NEST
Federica Rapposelli S3
Maria Giovanna Santoro NNL
Anna Grazia Stefani S3
Ciro Urso NNL
Alessandro Zammillo NNL

Technical Staff

Antonio Graziano Antico NNL
Benedetta Antonazzo NNL
Paolo Barbieri NNL
Ivana Bianco NNL
Davide Calanca S3
Adriana Campa NNL
Sonia Carallo NNL
Giorgio Casalini S3
Paolo Cazzato NNL
Eliana D'Amone NNL
Stefania D'Amone NNL
Gianvito De Iaco NNL
Gianmichele Epifani NNL
Vittorio Federico Fiorelli NNL
Antonio Domenico Gigante NNL
Diego Mangiullo NNL
Mariangela Margarito NNL
Luisa Neri S3
Riccardo Pallini NEST
Silvia Rizzo NNL
Maddalena Scandola S3
Gabriella Zammillo NNL

Support Staff @ Genova

Since its origin, CnrNano can rely on further support from offices in Genova, which serve simultaneously the IOM, SPIN and NANO Institutes of CNR.

CNR coworkers in Genova are:

Maria Chiara Andreoli	Paola Corezzola	Danilo Imperatore
Matilde Bolla	Monica Dalla Libera	Tatiana Marescalchi
Barbara Cagnana	Roberta De Donatis	Marco Punginelli
Enrico Camauli	Fabio Distefano	Giovanna Savoldi
Marco Campani	Francesca Fortunati	Liliana Sciaccaluga

The focus of the Nanoscience Institute ranges from fundamental nanoscale phenomena to materials and systems for frontier applications. A strength of our research comes from convergent contributions of scientists with background in different disciplines, and from combining advanced experiments and simulations.

1. **Fundamental nanoscience studies** are mostly concerned with **low-dimensional systems as laboratories** to study and control many body states and interactions. Key structures that are investigated include:

- **two-, one-, and zero-dimensional semiconductor objects**, and their electronic, optical, magnetic, and vibrational excitations. In quantum Hall systems, properties of edge channels and interactions between them for edge-state interferometry are studied by transport measurements and scanning gate microscopy;
- **graphene and its nanostructures**: of special interest are electron-electron interactions, as well as optics and magneto-phonon resonances;
- **hybrid superconducting systems**: we investigate quantum transport and phase coherence effects in hybrid nanostructures such as superconductors and normal metals (or semiconductors), as well as hybrid graphene structures and resonators;
- **molecular magnetism**: low temperature spin states and interactions of isolated and coupled systems.

In addition, **fundamentals of nanoscale imaging and spectroscopies** are also investigated, together with basic phenomena controlling **molecular aggregation and recognition processes at surfaces and in complex supramolecular structures**.

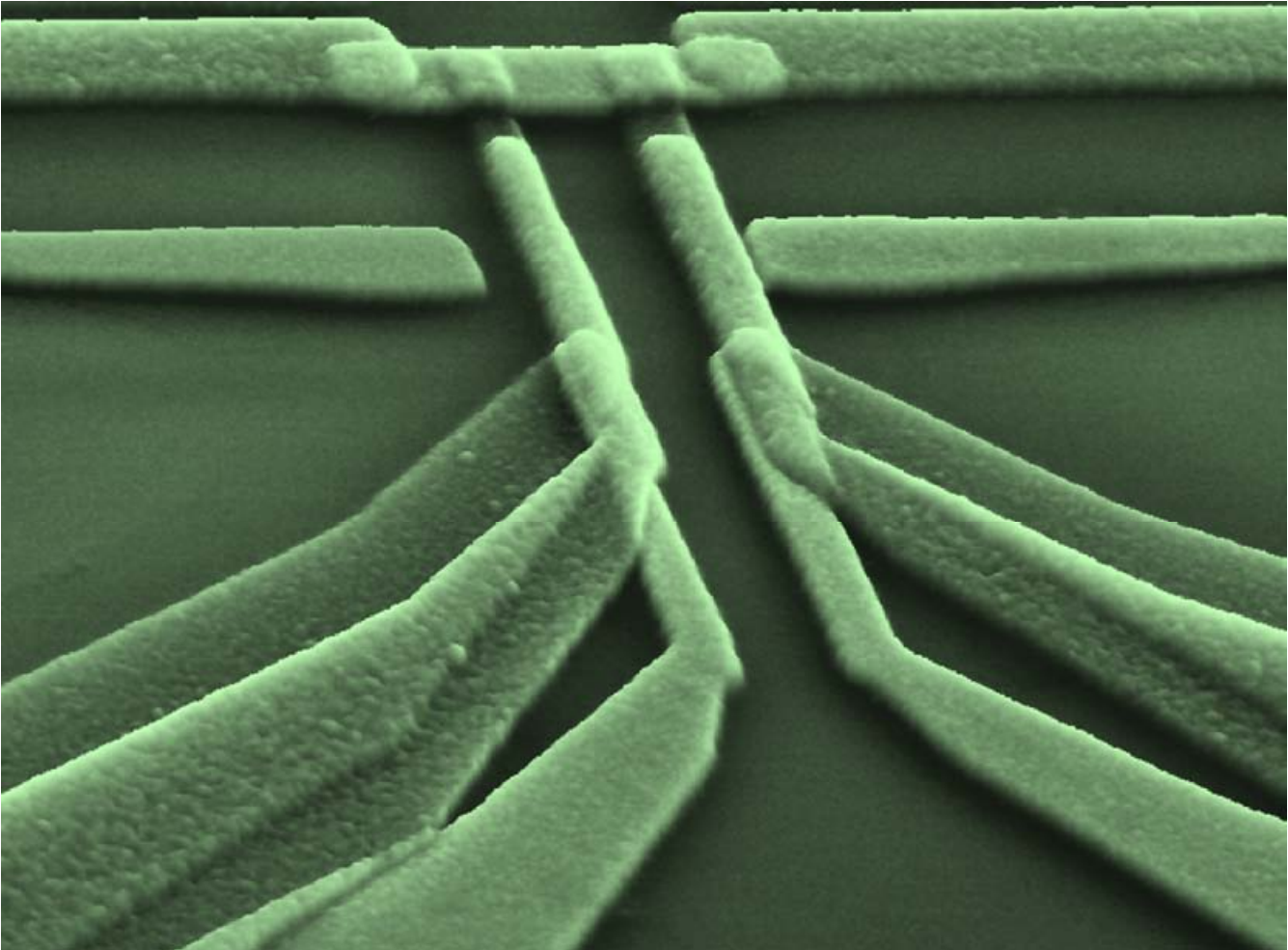
2. We study implications of novel nanoscience for **frontier technologies** in different fields:

- **advanced photonics and optoelectronics, focus activities**:
 - **THz photonics**: development of THz photonics building blocks, addressing issues such as emission, propagation and detection of light at THz frequencies. The experimental investigations deeply involve fundamental physics aspects, working in-between quantum photonics and radiofrequency semi-classical physics;
 - **polaritonics**: quantum hydrodynamics based on exciton polaritons: optical dynamic control of quantum flow and high Q-factor GaAs-based microcavities. Signatures of ultra-strong coupling contributions to intersubband polariton energies, as well as the non-adiabatic sub-cycle modulation of the coupling strength and the formation of intersubband polaritons in one-dimensional surface plasmon photonic crystals.

- **materials** developed and investigated include: **InAs/GaAs quantum dot (QD) systems** (structural and optoelectronic properties of QD for applications in polarization-insensitive optical amplifiers and solar cells); **GaN and GaAs-based free-standing structures** (development of metamaterials and studies of innovative non-linear optical effects); **Nanofibers** (polymer nanofibers, supramolecular crystalline fibers combining high charge mobility and intense fluorescence, nanocomposite light-emitting CdS nanocrystal-containing polymer fibres for laser and field effect applications); **silicon-germanium optoelectronics** (theoretical research aiming at exploring the potential of SiGe nanostructures as Si-compatible optically active materials for optoelectronic devices); **fluoride and oxide crystals for optoelectronics** (Czochralski growth of fluoride and oxide crystals, doped with rare earth trivalent ions, and their spectroscopic characterization);
- **energy-related applications, focus activities:**
 - **organic photovoltaics:** design and synthesis of novel organic polymers as donors for bulk-heterojunction solar cells, development of new organic dyes for dye-sensitized solar cells (DSSCs), studies of the optical properties of LED conjugated polymers and organic semiconductor single crystals by polarization-, time-, and temperature-resolved spectroscopy, ab-initio simulations of interface structure and functionalization, energy states and dynamics since the earliest stages of photoinduced charge separation;
 - study and control of the atomic scale properties of model systems based on **oxides**, combined with molecules and metal nanoparticles, for photovoltaic applications, fuel cells and environmental catalysts;
 - **graphene** for photovoltaics and for H storage;
- **mechanics and tribology-related processes, focus activities:**
 - **friction control** through multifunctional coatings and patterned hierarchical surfaces; understanding and controlling friction and tribo-chemical phenomena at the nanoscale;
 - **nanocomposites:** development of nanocomposites based on organic polymers, TiO₂ nanorod fillers, flexible nanocomposite foils, due to their enhanced thermal stability, reversible increase of hydrophilicity upon exposure to UV and vacuum storage and multifunctional properties (superhydrophobicity, magnetism, luminescence, antimicrobial activity). Development of a novel low-cost, lightweight and flexible nanocomposite foil (thin plates of multiwalled carbon nanotubes dispersed in polypropylene);

- **electronics, spintronics, information technologies**, *focus activities*:
 - **hybrid graphene-nanomagnets structures** for spintronics; electron and scanning probe spectroscopies combined with transport characterization;
 - **magnetic oxides**, films and nanoparticles, for spintronics and recording;
 - **quantum dots, nanotubes and graphene-based nanosystems**: correlation and few-electron phenomena;
 - **quantum information**: many areas of quantum information ranging from quantum communication to solid state implementations in semiconductor structures or molecular nanomagnets;
- **nanobioscience and nanobiotechnologies**, *focus activities*:
 - **visualization of the brain function and structure in the living mouse**: this research is a platform for the in-vivo testing of nano-engineered compounds;
 - **lipid-protein interactions in model membranes**: supported lipid bilayers as models for the influence of hosting lipid on the activity of membrane proteins;
 - **cell mechano-transduction**: study of the cell molecular mechanisms regulating nano-environment sensing. Nanostructures fabricated by nanoimprint lithography are exploited to: improve peripheral nerve regeneration; study neuronal and glial cell response in selected pathological models; drive adult stem cell differentiation and enhance endothelial cell adhesion and spreading. Collagen-derivatized or composite polymeric electrospun fibers are also investigated as scaffolds for tissue engineering, to promote cell adhesion and proliferation;
 - **nanoparticle/nanocapsules for cell biology**: preparation of nanobeads consisting of, or coated with, “smart” polymers (pH- or temperature sensitive) for the controlled uptake and release of drugs (cancer chemotherapeutics, siRNA) or of optical labels (gold NPs or thiophenes). Chemical strategies for the fabrication of multifunctional composite nanobeads such as NPs with magnetic or optical properties or of superparamagnetic nanoparticles coupled to silica nanoparticles for dual mode imaging MRI/ultrasonography;
 - **lab-on-a-chip technologies**: design and development of portable microfluidic devices based on surface-acoustic-wave integrated micro-pumps. Fabrication and modeling of fluidic microsystems for gradient generation in cell culture microchambers. Development of microfluidic systems for synthetic chemistry based on glass or polymeric materials. LabOnChip systems for medical diagnostics and cell biology applications. Design of an improved fluorescence read-out system for biochips based on photonic crystal nanocavities.

- **nanoscale and single-molecule spectroscopy and imaging of soft matter:** engineering synthetic fluorescent indicators of nanoenvironment characteristics (e.g., polarity, viscosity, aggregation), nanodevices based on dendrimers or metallic nanoparticles (NP), optical switches based on synthetic probes and autofluorescent proteins, and high-sensitivity (down to single-molecule) imaging techniques; scanning-probe and optical tweezers studies of individual biomolecules and their folding and interactions;
 - **structure and electron transfer processes** at biomolecular and hybrid bio-inorganic interfaces: understanding protein-surface interactions by scanning probe spectroscopies and simulations, exploiting electron-transfer molecules for bioinspired nanodevices;
 - **DNA-based self-assembling nanostructures:** biological constituents and bioinspired strategies to induce the aggregation of complex functional architectures based on nanoscale components.
3. A strategic endeavor for the institute is the **development of novel experimental and computational tools**, which are required for frontier research and technologies. These include:
- **growth and nanofabrication.** Current chemical beam epitaxy growth developments focus on the realization of radial and axial heterostructured metal-catalyzed nanowires with extreme control of morphological and structural properties. Nanofabrication developments focus on non-conventional functionalizations and applications of focused electron and ion beams and their combinations;
 - **imaging, quantitative microscopies, spectroscopies.** High-resolution transmission electron microscopies developments for strain field measurements, tomography, as well as spin-polarization filtering. Frontiers in scanning probe microscopies and in electron spectroscopies, both in-house and at large-scale facilities;
 - **molecular modeling and simulation:** this transversal activity spans over inorganic, organic, and biological structures and their hybrids. The used methods include Quantum Chemistry calculations, Density Functional Theory (DFT) (i.e., Exchange-correlation functionals; Orbital-dependent functional; Classical and quantum-mechanical embedding methods) and many-body perturbation theory, all-atom Force Field and Coarse Grained simulations, either applied singularly or combined in multi-scale approaches. Correlation and excitonic effects are included at various levels. Open source codes are developed for the investigation of transport, optics, plasmonics, including the effects of environment.



Highlights Nanotechnology

Hydrogen in Graphene

Graphene is currently considered one of the most promising materials for new technologies, potentially as revolutionary as plastic was in the middle of past century. It is extremely robust and light, capable of being modeled in a number of different shapes and has unique electronic properties that make it an extremely efficient heat and current conductor. It was recently proposed that combining graphene with hydrogen could enhance its versatility, considering that the completely hydrogenated graphene equivalent (i.e., graphane) displays different electronic and structural properties. In order to further explore this possibility, we theoretically studied two specific aspects of the hydrogenated graphene systems: the electronic and structural properties of hybrid graphane/graphene systems and the possibility of using graphene for chemisorption-based hydrogen storage systems. The main results are: (i) the electronic properties of graphene/graphane hybrid systems can be finely tuned by controlling the hydrogenation down to the single atom level; (ii) an efficient hydrogen storage and release process can be achieved at room conditions by controlling the curvature of graphene sheets. These results point towards the possibility of building all-graphene-based integrated self-powered electronic devices.

Graphene is a two dimensional sp^2 hybridized honeycomb lattice of carbon atoms. It can be obtained from graphite by mechanical or chemical exfoliation, or by deposition of carbon on substrates. Due to its peculiar band structure with linear dispersion at K points, it is potentially a very fast and efficient conductor. Its hydrogen saturated version, graphane, is an insulator. These circumstances open the possibility of building graphene/graphane based nanoelectronics by “sculpting” graphene-like structures within a graphane matrix. We studied graphene nanoribbons (GNR) sculpted in graphane by means of Density Functional Theory (DFT) and Car-Parrinello molecular dynamics. GNRs in graphane are very stable, with minimal structural distortion rapidly decreasing with the distance from the edge (Fig. 1A).

More interestingly, along the edge within the nanoribbon we observe a Peierls distortion manifesting with a bond-length alternation (BLA). This is a very subtle effect emerging only with density functionals including explicit exchange.

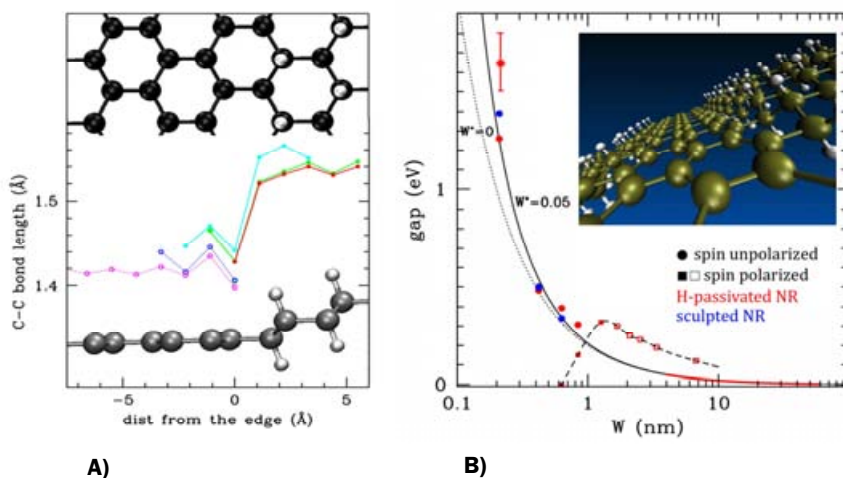


Figure 1. Structural and electronic properties of graphene nanoribbons sculpted in graphane. A) Top view (top) and lateral view (bottom) of the graphene/graphane edge. The plots report the C-C bond-length as a function of the distance from the edge. B) Band-gap as a function of the GNR width in the inset, a pictorial view of a zig-zag nanoribbon within the graphane matrix.

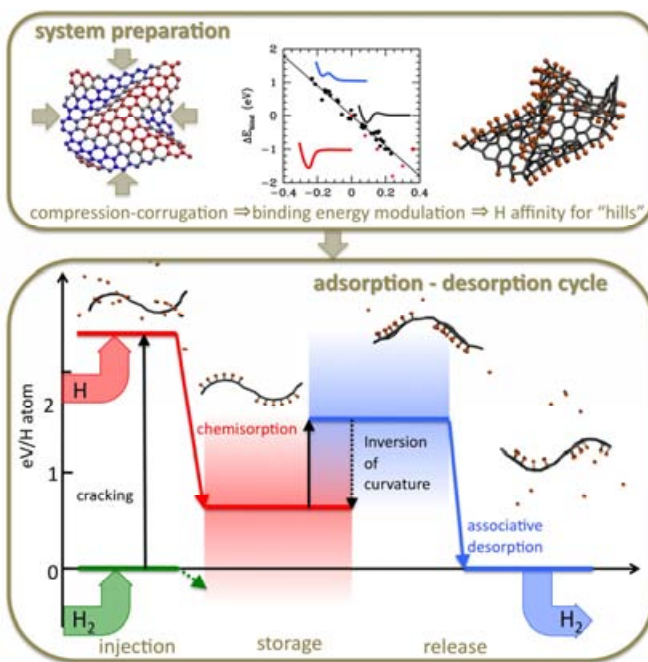
Contact Person Valentina Tozzini (valentina.tozzini@nano.cnr.it)

Collaborator V. Pellegrini

The Peierls distortion turns out to be related to opening of the band gap, being ultimately the cause of the semiconducting nature of the zig-zag graphene nanoribbons (Fig. 1B). In fact, the BLA and the gap tend to vanish as the nanoribbon width increases and the graphene bulk behavior prevails. For nanoribbon widths larger than ~ 1 nm this effect is masked by the emergence of spin polarization at the edge orbitals, that adds a “magnetic” symmetry breaking to the “structural” one, inducing an additional gap opening. The gap can be tuned between 1.5 and ~ 0.2 eV, by varying the nanoribbon width in the range 0.5–10 nm, allowing the engineering of non trivial nano-electronic devices by controlling at the atomic level the dehydrogenation of a graphane matrix. The versatility of graphene suggests exploring its properties when mechanically deformed. Using DFT and Car-Parrinello, we produced a corrugated graphene (multi)layer by laterally compressing an approximately squared ~ 2 nm large supercell (Fig. 2, top). The rippled structure has variable local curvature (concave and convex). Hydrogen binding energy (evaluated on sampled sites) is linearly dependent on the local curvature, spanning a range of ~ 2 eV. This implies that hydrogen binds very favorably to the convex sites, while it is weakly bound or unstable on concave sites. This naturally suggests a scheme for a possible hydrogen storage device based on the control of the graphene corrugation (Fig. 2, bottom). In the injection phase the corrugation of the graphene sheet must be created and maintained. Hydrogen will then bind to the convex sites ensuring a stable storage. The release can be obtained inverting the local curvature of the graphene sheet: the hydrogen will find itself in the concave regions and spontaneously detach. Both the binding and release phases were observed in simulations. *In silico*, the curvature inversion is forced by an external mechanical displacement field simulating a transverse mechanical wave. Practical ways to create and control ripples in the real system are currently under study, and include the coupling to mechanical waves generators, and the functionalization with optically or electro-magnetically controllable molecular switches.

Figure 2.

Hydrogen storage in rippled graphene. Top Panel: preparation of the system for H binding. From left: graphene corrugation by lateral compression (color code: red=convex, blue=concave); variation of the binding energy as a function of the curvature; qualitative binding energy profiles are reported with the same color code as the curvature (with black=flat); a view of the graphene. Bottom panel: Scheme for the adsorption-desorption cycle. During injection, hydrogen is cracked and chemisorbed on convex sites. Then the curvature of the sheets is inverted and the hydrogen detaches from concave sites in molecular form.



Related publications *Electronic structure and Peierls instability in graphene nanoribbons sculpted in graphane.* V. Tozzini and V. Pellegrini, *Phys Rev B* **81**, 113404 (2010).

Reversible Hydrogen Storage by Controlled Buckling of Graphene Layers. V. Tozzini and V. Pellegrini, *J. Phys. Chem. C* **115**, 25523 (2011).

A quasi-crystal semiconductor laser

Semiconductor lasers have had a huge impact on everyday life: they are the defining element of optical storage systems, fibre optics communications, optical sensors, etc. When high spectral purity is desired, this is typically achieved inserting in the laser cavity a grating that produces a periodic variation of the refractive index. This grating selects the lasing mode whose wavelength matches its periodicity. Here, we have instead employed a special grating following the Fibonacci sequence, realizing what is called an optical quasi-crystal. These structures, though based on a precise mathematical rule, are not periodic and already display many properties of disordered systems. It is the first time a laser diode is produced with this approach, allowing greater flexibility in the design and novel functionalities. In this work, the grating was realized in the metallic waveguide of a so-called quantum cascade laser to demonstrate the possibility of independently controlling emission angle and frequency, as well as to develop multi-colour devices operating contemporarily at two or more, specifically chosen, frequencies. These characteristics are presently of great interest for lasers in the THz spectral range (i.e., between microwave and infrared), intensively investigated for security applications. The result also opens the way toward the development of semiconductor lasers in completely disordered materials, where light propagation is dominated by diffusion.

We have demonstrated the realization of a quasi-crystal semiconductor injection laser, using a Fibonacci sequence, in the one-dimensional grating geometry of conventional distributed feedback (DFB) lasers. The device employs a quantum-cascade active region in the Terahertz frequency range and is electrically pumped. Single-mode emission at a specific angle from the device surface is obtained, showing an elegant fundamental solution to the known difficulties of achieving lasing on vertically radiating modes in this type of lasers. As further proof of concept of aperiodic DFB versatility, we have also shown dual-wavelength operation with about 210 GHz separation (close to the typical ~ 1 meV intersubband transition linewidths in this frequency range), by implementing a device with a double gap configuration. The quasi-periodic arrangement is formed according to the Fibonacci generation scheme: $S_{j+1} = \{S_j, -1S_j\}$ for $j \geq 1$, with $S_0 = \{B\}$ and $S_1 = \{A\}$, where the index j is called order of the sequence. In THz quantum cascade lasers (QCL), the waveguide typically consists of the gain material sandwiched between two metallic layers and has a confinement factor close to unity.

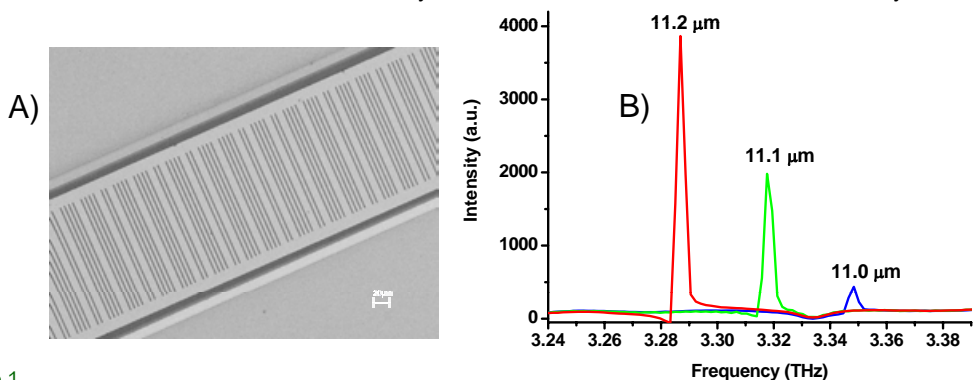


Figure 1.

Emission spectra from devices with different grating periods and duty cycles. A) Top view of a fabricated device. B) Emission spectra of three different devices, each with a different quasiperiod. The emission scales perfectly, demonstrating laser operation on the grating resonance.

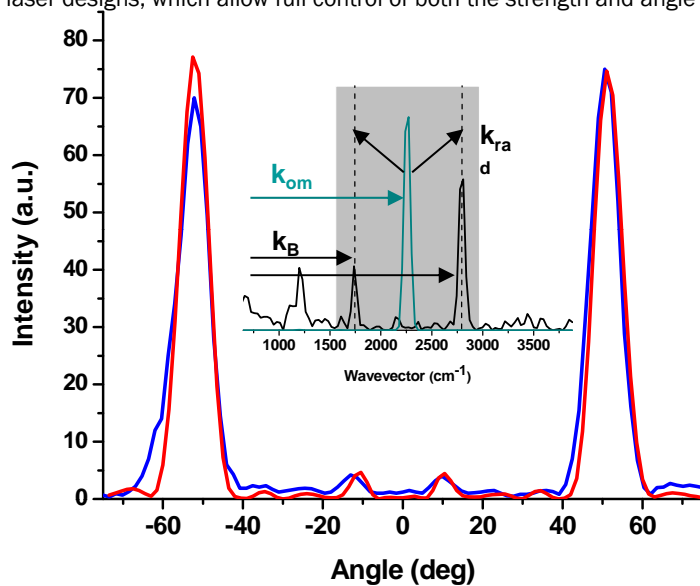
Contact Person Alessandro Tredicucci (alessandro.tredicucci@nano.cnr.it)

Collaborators L. Mahler, F. Beltram, C. Walther, J. Faist, H.E. Beere, D.A. Ritchie, D. Wiersma

The two surface-plasmons at the metal-dielectric interfaces form a mode of transverse-magnetic (TM) nature, which ideally matches the selection rules of intersubband transitions. The Fibonacci sequence is integrated into this metallic waveguide by replacing every interface between element A and B by a slit in the top metallization. Fig. 1A shows a top view of a processed device. A photonic band-gap of about 160-170 GHz is computed to develop at the chosen Bragg resonance for a wide parameter range, corresponding to 5% of the Bragg frequency, which shows the strong coupling between forward and backward traveling waves necessary for selective laser action. Most lasers fabricated in this way indeed showed single-mode emission under all operating conditions. Fig. 1B plots spectra of three devices with different grating periods. The emission frequency scales perfectly with the quasi-period, which proves the grating to be the origin of the modes. Comparison with calculations shows that these devices are lasing on the high-energy band-edge of the photonic crystal structure. Fig. 2 shows the far-field of another such laser ($\nu=3.27$ THz). This device on the other hand lases on the lower band-edge and we see that the photons are emitted at an angle of 51° with respect to the surface normal. Exactly the same far-field pattern is predicted by applying the Stratton-Chu formula to the near-field of the computed eigenmode, an even stronger evidence for the laser operating on the resonance of the quasi-crystalline structure. To illustrate how the interaction of the optical mode and the grating can lead to surface emission under a particular desired angle, we consider in the inset of Fig. 2 an enlarged section of the Fourier transform of our grating, together with a Fourier transform of the computed optical eigenmode. The emission angle is given by the relation $\sin(\theta)k_{\text{rad}}=|k_{\text{B}}-k_{\text{om}}|$, where θ is the angle between the surface normal and the wavevector k_{rad} of the emitted photon; k_{B} is the Bragg peak wavevector and k_{om} is the optical mode wavevector. We believe the present devices could pave the way towards more advanced DFB laser designs, which allow full control of both the strength and angle of the surface emission.

Figure 2.

Far-field pattern of a device operating on the lower band-edge. The red and blue line show computed and measured far-field, respectively. Both data show distinct peaks at 11° and 51° and are symmetric with respect to the surface normal. The inset shows the interaction of the optical mode with the grating, both represented by their Fourier transform in black and cyan respectively. Unlike in a conventional first order DFB, the grating has resonances close to the wavevector of the guided mode, which generates surface emission.



Radiating modes are possible by scattering on grating wavevectors within the gray rectangle, where the condition $|k_{\text{B}} - k_{\text{om}}| < k_{\text{rad}}$ is fulfilled. This geometrical consideration predicts emission at 50° with respect to the surface normal. Further grating peaks very close to the optical mode, causing the emission at 11° , are barely visible.

Related publication *Quasi-periodic distributed feedback laser*. L. Mahler, A. Tredicucci, F. Beltram, C. Walther, J. Faist, H.E. Beere, D.A. Ritchie, and D.S. Wiersma, *Nature Photonics* **4**, 165 (2010).

Active role of oxide layers in the polarization of plasmonic nanostructures

In this paper a theoretical study of polarization properties of a silver nanosphere touching a homogeneous silver substrate and covered by oxide layers of increasing thickness is reported. Oxide layers are often deposited on metallic nanostructures in metal-enhanced fluorescence (MEF) or surface-enhanced Raman scattering experiments to avoid nonradiative energy transfer from emitters to the metal, and to increase the nanoparticles stability against thermal processes and laser exposure. Not much has been said on the effect of the oxide on the field enhancement of such kind of plasmonic systems. This work aims at filling this gap by shedding light on the effects of the oxide coverage on the near and far field behavior: numerical simulations performed in the framework of the discrete dipole approximation show the presence of new resonances in the absorption spectra and, of major importance for MEF applications, a strong enhancement of the near field around the nanosphere.

Recent developments in nanoparticle synthesis, innovations in the characterization procedures, and theoretical understanding, have spread out the interest of scientists in surface plasmon-based photonics or plasmonics. The focus is to manipulate and/or to strongly enhance the electromagnetic fields by means of surface plasmons (SPs) or localized surface plasmons (LSPs). In metal nanoparticles (MNPs) the properties of LSPs can be tuned by changing the particle shape, size and the environment.

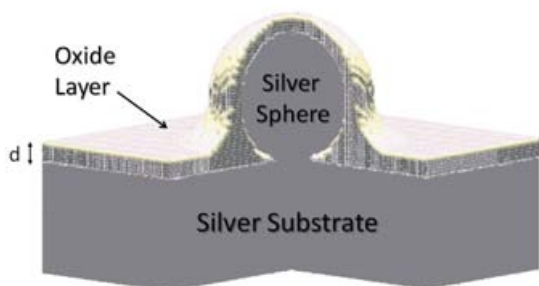


Figure 1.

System under investigation: a silver nanosphere with a diameter of 75 nm is lying on a 70 nm thick silver substrate and the whole system is covered by a thin layer of Al_2O_3 with different thicknesses ($d=5, 10$ and 20 nm).

Several plasmonics applications aim at increasing the Raman scattering of organic molecules (SERS, surface enhanced Raman scattering) or the fluorescence of emitters (MEF, metal-enhanced fluorescence).

However, at short emitter-metal distances a resonant energy transfer to the metal occurs, which increases the nonradiative (NR) rate of the emitter and quenches the fluorescence. To avoid NR quenching, non-absorbing oxide layers are often used as bare spacers.

In this work, we show that oxide layers play instead an important active role in the optical response of plasmonic nanostructures, strongly modifying the electromagnetic field enhancement factor. The presented theoretical analysis is based on the discrete dipole approximation (DDA) calculations.

Contact Person Fabio Della Sala (fabio.dellasala@nano.cnr.it)

Collaborator S. D'Agostino

The considered system is shown in Fig. 1. Here the attention is focused on the perturbations induced by oxide layers on the properties of the LSPs. In particular two main important features are underlined: i) the red-shift in the extinction spectra and the appearance of an additional resonance at low energy (690 nm), localized at the sphere-substrate interface (Fig. 2), and ii) the strong modification of the near-field enhancement which increases and spreads out in the whole space above the substrate (Fig. 3).

Moreover it is demonstrated that the near-field enhancement does not necessary decay rapidly from the MNP surface, and therefore oxide coatings thicker than those commonly used can be considered in SERS/MEF applications with the possibility of engineering the plasmonics response. In conclusion, we have shown the importance of an oxide layer in enlarging the interaction effects between a MNP and a metal substrate.

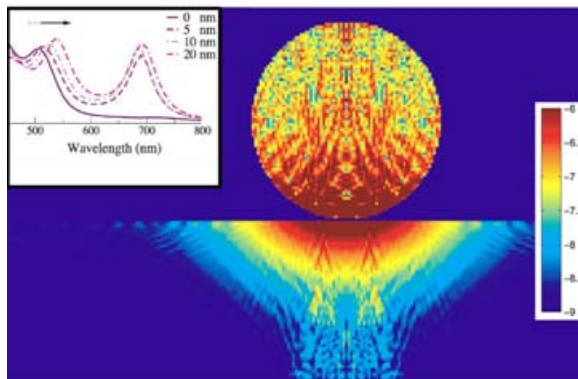


Figure 2.

Computed local absorption cross section (color-map log-scale) of the system covered with a 5 nm-thick Al_2O_3 layer and excited at the oxide induced resonance (690 nm); (inset) Absorption spectra for different oxide thicknesses (d). The arrow indicates the direction of the shift of the peak-wavelengths.

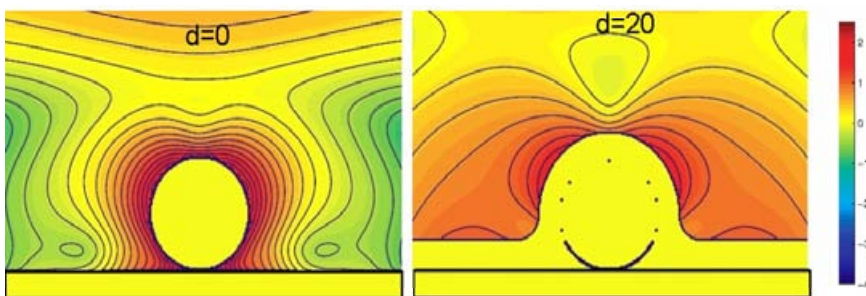


Figure 3.

Field enhancement map (log-scale) for the system without (left panel) and with the oxide layer (right panel).

Related publication *Active Role of Oxide Layers on the Polarization of Plasmonic Nanostructures.* S. D'Agostino and F. Della Sala, *ACS NANO* **4**, 4117 (2010).

Shaping white light through electroluminescent fully organic coupled microcavities

White organic light emitting diodes (white-OLEDs) have shown the potential to replace commercial sources for lighting applications because of their high efficiency and superior color quality. The most conventional architectures used to maximize the performances of such devices consist in the employment of three kinds of emitting phosphorescent or fluorescent molecules and modified glass substrates for the optical management of light outcoupling. Although very promising, these approaches are still based on the use of expensive and relatively low conductive indium tin oxide (ITO) substrates, thus leading to high fabrication costs and poor color emission homogeneity on large area devices. Here we report an innovative high performance ITO-free white-OLED architecture based on the coupling of two organic microcavities constituted by only thermally evaporated metallic and organic layers. In the proposed structure two cavities are coupled through a thin high reflective metal layer, to result in the generation of two electromagnetic modes sustained by the whole cavity. If white light emitting molecules are inserted properly into the structure as active layer, the color emission, the outcoupling efficiency, and the color rendering index (CRI) can be simultaneously optimized in the same cavity structure. This opens new pathways to fabricate a novel class of very cheap, high color quality, and ITO-free devices for the next generation of “plastic-light” sources.

The coupled microcavity – OLEDs (CM-OLEDs) are constituted of two cavities (C1 and C2), each made by two metallic mirrors (silver or aluminum) separated by sub-micrometric organic stacks. The common metallic layer works as the coupler of the two cavities and the degree of coupling is determined by its thickness. The structure is realized by depositing on a transparent glass substrate the following layer sequence: AgB/OS1/AgM/OS2/AgT, where AgB is a semitransparent silver bottom layer, OS1 the first active organic stack where the emitters are placed, AgM the middle coupler silver layer, OS2 a second passive organic stack, and AgT a thick reflective silver layer (Fig. 1). The anode and the cathode are AgB and AgM, respectively. White light is emitted through the semitransparent bottom electrode. OS2 is filled with a standard organic material which should have a high energy gap to avoid the absorption of light.

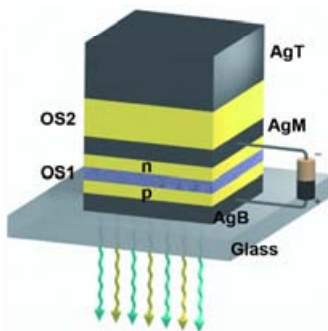


Figure 1.

Schematic view of the CM configuration used in this work, exclusively made of metallic and organic layers. The blue layer indicates the emitting layer. p and n represent the hole- and the electron-conductive sides of the OLED. Photo of a working CM3 device at 10.000 Cd/m².

Once the materials to employ as white emitters are established, the cavity can be designed in order to amplify just the modes that correspond to the peak wavelengths of the white emission spectrum and/or to change completely the spectral shape. This is mainly due to the concentration of Photonic Mode density (PMD) around the selected wavelengths. White-OLEDs have been fabricated using two complementary color fluorescent materials. The structures consist of the following sequences: ITO/p/EBL/Y/B/HBL/n/AgT for the reference structures (R) and AgB/p/EBL/Y/B/HBL/n/AgM/OS2/AgT for the CM devices.

Contact Person Marco Mazzeo (marco.mazzeo@unisalento.it)

Collaborators F. Della Sala, R. Cingolani, G. Gigli, F. Mariano, G. Melcarne, S. D'Agostino, Y. Duan

Here p and n layers are the hole and electron conductive transport layers, while EBL and HBL are the electron and the hole blocking layer, respectively. Three series of devices have been realized with white color emission. In the first series of devices (coupled-microcavity, CM1, and reference cavity-less, R1) the efficiency has been optimized regardless of the CRI. In the second series, both the CM and the reference structures (CM2 and R2) have been optimized fixing the angular-averaged CRI at 70, which still corresponds to an acceptable luminance. Finally, in the third series (CM3) we have maximized the CRI of the CM configuration regardless of the efficiency. In Fig. 2A,B) the electroluminescence (EL) spectra (blue lines) of the CM1 and R1 devices are displayed. The CM1 architecture results in better current efficiency (11Cd/A) values than the R1 structure (6.6Cd/A) with an enhancement around 67%. This strong improvement is ascribed to the cavity effect. Such better electro-optical performances result in higher power efficiencies of about 15 lm/W in cavity device. The electro-optical performances of devices R2 and CM2 are also reported. As we can see a CRI value as high as 86 has been obtained in CM2, similar to the best so far reported. At 1000 Cd/m², the microcavity device still shows a remarkable increase of current efficiency by a factor 1.45 compared to the reference cavity-less device, going from 5.1 to 7.4 Cd/A. Moreover, a brightness of 10.000 Cd/m² is reached at 3.5 V in CM2, which is the lowest voltage so far reported in white-OLEDs. A maximum power efficiency value of 12.6 lm/W is obtained in the CM2 device, with respect to 8.4 lm/W shown by the reference structure, which corresponds to an enhancement of around 50%. In the third class of devices (CM3), the CRI has been optimized regardless of the efficiency value. An impressive CRI of 94 in the forward direction is achieved (Fig. 2), which is similar to the highest value so far reported for conventional ITO-based white-OLEDs.

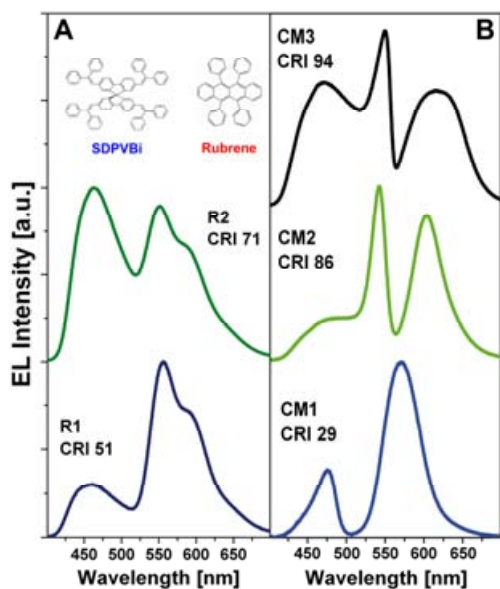


Figure 2.

A) Reference devices EL spectra. B) Cavity devices EL spectra. Blue lines correspond to the spectra shown by the series 1. Green lines correspond to the spectra of series 2. The black line is the high CRI device spectrum (series 3). The chemical structures of the emitters employed (spiro-DPVBi and rubrene) are also shown.

Related publication *Shaping white light through electroluminescent fully organic coupled-microcavities*. M. Mazzeo, F. Della Sala, F. Mariano, G. Melcarne, S. D'Agostino, Y. Duan, R. Cingolani, and G. Gigli, *Adv Mat.* **22**, 4696 (2010).

Electrical currents through polymer nanostructures

Molecular electronics is the solution of choice proposed for electronic circuits beyond nowadays silicon-based electronics. Intense research efforts aim at identifying suitable organic components that might be anchored to inorganic supports and integrated in electronic circuits. A molecular wire must fulfill two basic requirements for the construction of complex devices: it should transport charge with a low resistance and should have structuring capabilities, based on the self-assembly of its building blocks. Very few molecular systems match both requirements. MMX nanoribbons do.

MMX polymers are a key to the implementation of future, powerful and highly-integrated electronic devices and computing architectures. In collaboration with chemistry and physics experimental groups at the Universidad Autonoma de Madrid, we have conducted research on MMX polymers with different metal, halide and organic-ligand species. Our investigations based on organics synthesis, atomic force microscopy, transport measurements, magnetic characterization and density functional theory calculations, indicate that MMX nanostructures sustain high currents and that their conductivity may be controlled by adjusting the atomic structure through physico-chemical parameters.

A joint experimental-theoretical investigation of electrically conductive MMX coordination polymers - $[\text{Pt}_2(\text{S}_2\text{CCH}_3)_4]_n$ - self-assembled on an insulating substrate by direct sublimation of polymer crystals was carried out. The main characteristic of these polymers is the embedding of metal centers into the organic matrix in a controlled, modular manner and the realization of 3-, 2-, and 1-dimensional arrangements. The electrical measurements were obtained with the conductive atomic force microscopy (AFM) technique at room temperature.

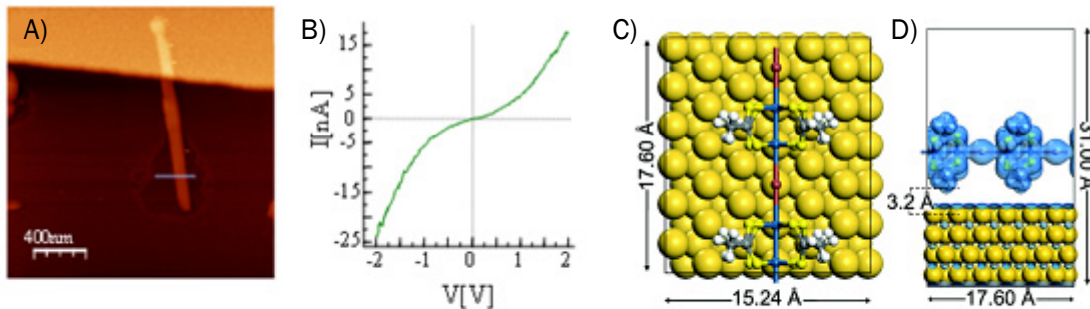


Figure 1.

A) AFM topography showing a MMX wire ($[\text{Pt}_2(\text{S}_2\text{CCH}_3)_4]_n$) adsorbed on mica. B) Current versus voltage characteristic taken by contacting the nanoribbon 100 nm from the gold electrode. Image adapted from original paper. C) Top view of an infinite (by periodic boundary conditions) MMX chain on Au(111). D) Side view of the simulated system, with an isosurface plot of the total charge density. The empty region with no charge density demonstrates that there is no charge coupling between the polymer and the surface that represents the gold electrode.

Contact Person Rosa Di Felice (rosa.difelice@nano.cnr.it)

Collaborators A. Calzolari, F. Zamora, J. Gómez-Herrero

The theoretical characterization of the electronic structure was based on density functional theory (DFT) approaches. Our results show that one-dimensional MMX chains can be isolated and exhibit striking electrical transport properties (Fig. 1). The observed currents exceed those sustained in other organic and metal-organic assemblies on surfaces by orders of magnitude and over longer distances. Theory in particular elucidates the structure and electronic coupling at the hybrid interface, we discussed the contact resistance and the effect of disorder on the conductivity trends (Fig. 1). MMX polymers of the same Pt-I family obtained with different side ligands - $[\text{Pt}_2(\text{n-pentylCS}_2)_4]_n$ - exhibit a variety of electrical behaviors in the bulk crystal phase (Fig. 2), depending, e.g., on the thermal treatment. These polymers can also be deposited as nanostructures on surfaces, suggesting the possibility of constructing nanoelectronic components with controlled electrical response.

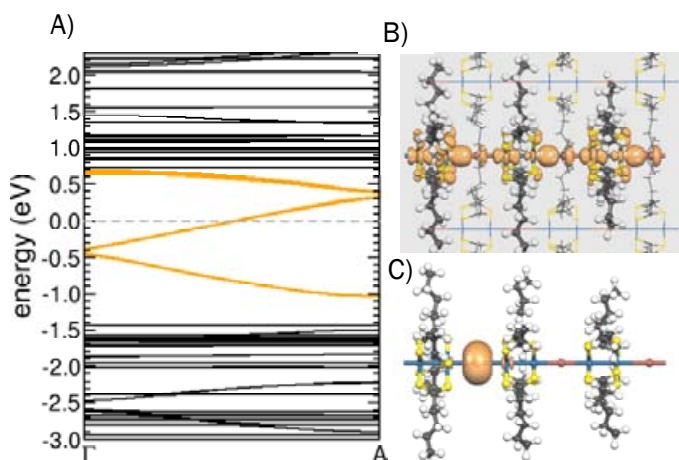


Figure 2.

A) Calculated bandstructure for the RT (room temperature) crystalline phase. The orange metallic band crosses the Fermi level (dashed line). B) Isosurface plot of a single particle orbital for the LT (low temperature) crystal structure, belonging to the metallic band. C) Top-of-valence-band orbital state for an individual distorted chain (spin-up), revealing charge localization.

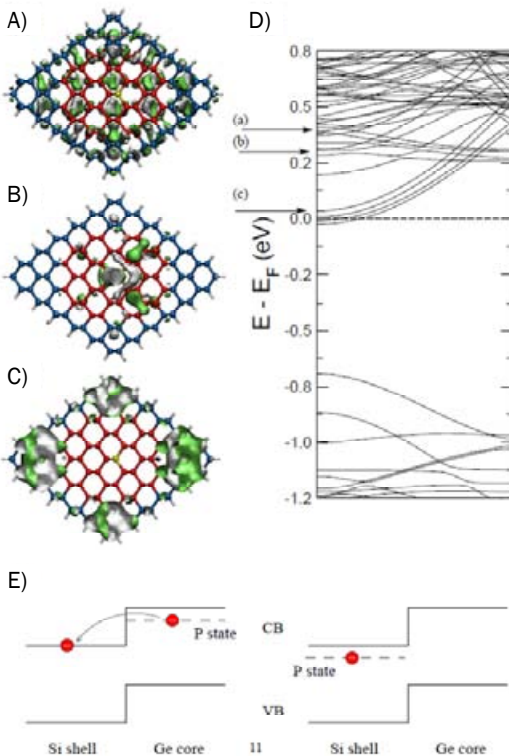
Related publications *Highly conductive nanoribbons of coordination polymers.* L. Welte, A. Calzolari, R. Di Felice, F. Zamora, and J. Gómez-Herrero, *Nature Nanotech.* **5**, 110 (2010).

MMX as conductors: from single crystal to nanostructures. A. Guijarro, O. Castillo, L. Welte, A. Calzolari, P.J. Sanz Miguel, C.J. Gómez-García, D. Olea, R. Di Felice, J. Gómez-Herrero, and F. Zamora, *Adv. Funct. Mater.* **20**, 1451 (2010).

Band-Offset Driven Efficiency of the Doping of SiGe Core-Shell Nanowires

Impurity doping of semiconducting nanowires has been predicted to become increasingly inefficient as the wire diameter is reduced. We show that efficient n- and p-type doping can be achieved in SiGe core-shell nanowires as thin as 2 nm, taking advantage of the band offset at the Si/Ge interface. A one-dimensional electron (hole) gas is created at the band-edge and the carrier density is uniquely controlled by the impurity concentration with no need of thermal activation. Additionally, SiGe core-shell nanowires naturally provide the separation between the different types of carriers, electrons and holes, and are ideally suited for photovoltaic applications.

One of the main limits of doping of pure Si and Ge nanowires (NWs) is its inefficiency when the diameter is reduced, as a consequence of surface segregation, quantum confinement and dielectric mismatch. In the case of doping with B or P atoms, the impurity state is deep in the band gap and cannot be activated at typical device temperatures. The results of our ab-initio DFT calculations on SiGe core-shell NWs show how this limit can be overcome by appropriate doping with B and P.



In these NWs, in fact, the band offset between the two materials causes a localization of the valence states in Ge and of conduction states in Si.

As a consequence of this property, with particular doping conditions, a one-dimensional electron (hole) gas at the band edge is created and the carrier density is uniquely controlled by the impurity concentration without need of thermal activation.

As shown in Fig. 1 (left) in the case of a GeSi core-shell wire with a P impurity in the core, the impurity level falls inside the conduction band, yielding an electron at its bottom. This is related to the type II band-offset that results at the Si/Ge interface. In a pure Ge NW of the size of the core, the impurity level would have been deep in the band gap and very difficult to activate.

Figure 1.

Top. Band structure of a GeSi core-shell NW with a P impurity in the Ge core. The arrows indicate the real space wave localization. Bottom. A band-offset scheme of the creation of the electron gas is shown.

Contact Person Stefano Ossicini (stefano.ossicini@unimore.it)

Collaborators M. Amato, R. Rurali

Here, instead, analyzing the wave function localization, we found that the bottom of the conduction band is in the Si shell, which is below all Ge core states; this means that the impurity needs to be thermally activated. This indicates the formation of a one-dimensional electron gas that might be relevant for device applications.

A further interesting case spots a B atom in the Si shell of a GeSi core-shell NW. As shown in Fig. 2 (right), the impurity level is deep in the valence states: the valence band is made by Ge core states at higher energy than the B state and this causes the formation of a one-dimensional hole gas. These results can be easily extended to the case of SiGe core-shell NWs. Therefore, the spatial carrier localization of electrons and holes together with the chance of making both carriers active from an electrical point of view renders SiGe core-shell NWs ideally suited for photovoltaic applications.

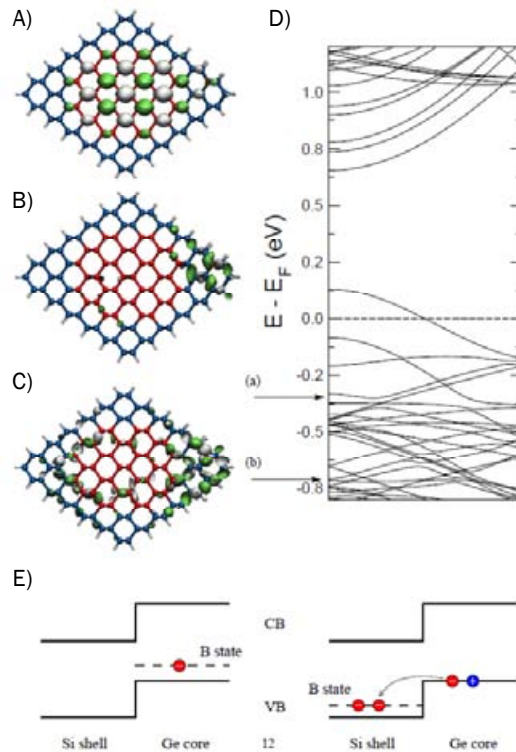


Figure 2.

Top. Band structure of a GeSi core-shell NW with a B impurity into the Si shell. Bottom. A band-offset scheme of the creation of a hole gas.

Related publication *Band-Offset Driven Efficiency of the Doping of SiGe Core-Shell Nanowires.* M. Amato, S. Ossicini, and R. Rurali, *Nanoletters* **11**, 594 (2011).

Molecular nanomagnets and graphene: steps towards spintronic devices

The possibility to graft nano-objects directly on its surface makes graphene particularly appealing for device and sensing applications. Here, we report the design and the realization of a novel device made by a graphene nano-constriction decorated with TbPc₂ magnetic molecules (Pc = phthalocyanine), to electrically detect the magnetization reversal of the molecules in proximity with graphene. A magnetoconductivity signal as high as 20% is found for the spin reversal, revealing the uniaxial magnetic anisotropy of the TbPc₂ quantum magnets. These results depict the behaviour of multiple-field-effect nano-transistors with sensitivity at the single-molecule level.

Single-molecule magnets (SMMs) have been demonstrated to possess well-defined quantum states and quantum behavior at single molecule level and their usage as active units in spintronic devices was recently proposed. Sp²-carbon substrates, such as graphene or carbon nanotubes, have been proven to act as integrating base for embedding nano-scale molecular properties into device environments, due to their unique conductivity properties and the direct exposure to the external world. Here, we present the design, realization and characterization of a novel hybrid spintronic nano-device (Fig. 1A) made by the integration of a graphene nano-constriction, working in the Coulomb blockade regime, and Terbium(III) bis(phthalocyanine) - SMMs. Low-temperature experiments show evidence for the electrical detection of the magnetization reversal of the TbPc₂ SMMs through magnetoconductivity.

Our devices consist of ~20 nm-wide graphene nano-constriction obtained by Electron Beam Lithography and plasma etching. The low-temperature conductivity as a function of backgate and bias voltages shows the typical behavior of one or few quantum dots in series, in agreement with what is reported for similar systems.

The pyrene-substituted Terbium (III) bis(phthalocyanine) single-molecule magnets (TbPc₂ hereafter) are deposited from the liquid phase. Combined Raman and conductance studies show that the electronic properties of the graphene sheets remain intact after SMM deposition. An averaged SMMs density of ~10 molecules can be estimated for the nanoconstriction.

The effects of the molecule grafting on our graphene devices become visible considering the low-temperature magnetoconductivity, G(H), shown in Fig. 1B obtained at a fixed back gate voltage, which shows the opening of a hysteresis loop. The emergence of a hysteresis in the magnetoconductivity indicates the presence of “external” magnetic moments coupled with the graphene device and it is a signature that the transport can be effectively tuned by the deposition of the TbPc₂ SMMs. Indeed, all the main characteristics of the TbPc₂ hysteresis loops are found in the G(H) signal of our devices, in particular the signature of the uniaxial anisotropy typical for the TbPc₂ SMMs. This case is also very different from the reported observation of hysteresis loops in the magnetoconductivity of pristine graphene devices, since the hysteresis remains even for very slow rates, it is strongly anisotropic and does not change sign with the backgate voltage.

Contact Person Andrea Candini (andrea.candini@nano.cnr.it)

Collaborators M. Affronte, S. Klyatskaya, M. Ruben, W. Wernsdorfer

The hybrid nanodevice behaves similarly to conventional spin valves, however it makes no use of ferromagnetic electrodes and a molecular magnetic gate is used instead. Further tunability can be obtained by employing different molecular gates with different functionalities. This prototype depicts the behavior of a novel class of molecular devices with sensitivity at the single-molecule and single-electron levels.

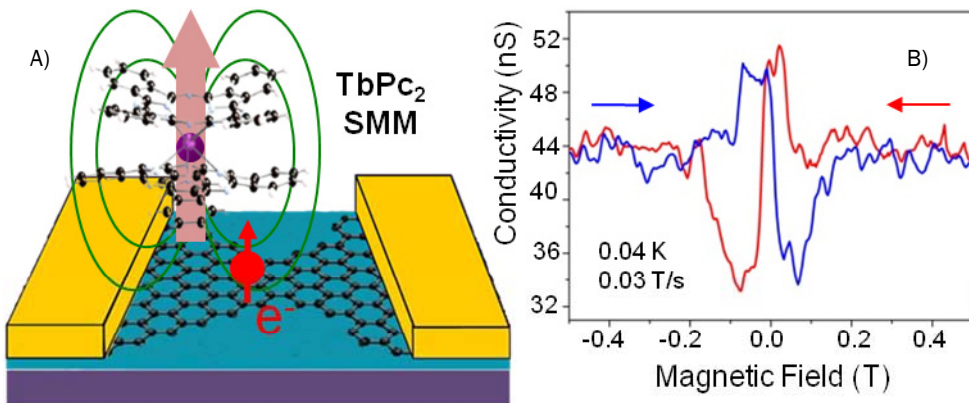


Figure 1.

A) Schematic view of the nanodevice: TbPc₂ single molecule magnets are coupled with a graphene nanoconstriction. B) Magnetoconductivity of the graphene-based device showing the opening of the hysteresis loop given by the magnetization reversal of the magnetic molecules.

Related publication *Graphene Spintronic Devices with Molecular Nanomagnets.* A. Candini, S. Klyatskaya, M. Ruben, W. Wernsdorfer, and M. Affronte, *Nano Letters* **11**, 2634 (2011).

Understanding microscopic mechanisms in frictional phenomena

Friction is a hot topic for scientific and technological reasons; yet, five centuries after Leonardo da Vinci, much effort is still devoted to understanding the underlying physics, particularly in new directions including nanosystems. Employing "molecular dynamics" simulation studies, CNR researchers have unraveled the microscopic mechanisms at play in two important frictional phenomena: i) The dynamics of fast nano-objects sliding on crystalline surfaces; ii) The onset of slip for interlocked surfaces.

i) Ballistic nanofriction.

Most fundamental physical tribology and nanofrictional studies focus on exceedingly low speeds. Yet, there are situations where it may be important to know what exactly happens when for example an adsorbed molecule or cluster slides over a solid surface at hundreds of meters per second. CNR researchers have chosen for the prototype study of fast nano-objects a gold nanoparticle on graphite—small gold clusters are in fact known to be thermally mobile when deposited on the very "slippery" graphite surface.

Simulating the motion of diffusing and slowly drifting, and of fast moving "kicked" gold clusters on graphite, the study demonstrates analogies and differences between low speed sliding, which is diffusive and long understood, and high speed sliding, so far unexplored. At high speed, a novel frictional regime, freshly designated as "ballistic", emerges. The slowing down of the cluster's speed appears as the result of successive collisions with thermal excitations of the surface; as a result, ballistic friction increases with temperature, unlike standard diffusive friction, which is well known to decrease.

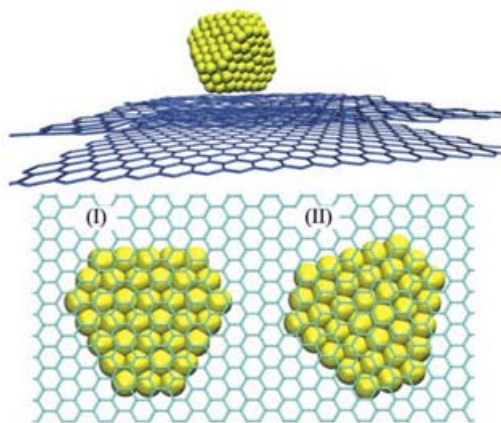


Figure 1. Simulated gold cluster sliding over a graphite surface. In-registry (I) and out-of-registry (II) geometries for the cluster's (111) contact facet and the graphite.

Also, the interplay of rotations and translations is completely opposite in low speed friction, where the two work in phase, and in ballistic friction, where they are out of phase, and kinetic energy bounces back and forth between translation and rotation. A broad crossover regime of intermediate speeds between ballistic and diffusive friction is identified and described. Finally, and perhaps surprisingly in view of their different mechanisms, the ballistic frictional force grows roughly linearly with speed, similar to low speed "viscous" friction. While these results highlight exquisitely physical aspects of high speed friction, the ballistic friction concept may be expected to become of future relevance to potential applications in nanosystems such as, e.g., nanoelectromechanical systems and nanomotors, as well as to other problems involving high speed gas collisions with solid surfaces.

Contact Person Maria Clelia Righi (mcrighi@unimore.it)

Collaborators M. Reguzzoni, M. Ferrario, A. Vanossi, R. Guerra, U. Tartaglino, E. Tosatti

ii) Onset of frictional slip by domain nucleation in adsorbed monolayers.

It has been known for centuries that a body in contact with a substrate will start to slide when the lateral force exceeds the static friction force. Yet the microscopic mechanisms ruling the crossover from static to dynamic friction are still the object of active research. Reguzzoni *et al.* have identified the atomistic processes that govern the slip onset for two interlocked surfaces by considering a xenon (Xe) monolayer sliding on a copper (Cu) substrate. This idealized system has been recently studied by experiments on the microscopic origin of friction, by way of an oscillating quartz crystal microbalance (QCM).

It has been observed that the monolayer of noble gas atoms adsorbed onto the metal surface could be set into relative sliding motion by the inertial force induced by the resonant oscillation. If the registry between xenon and copper had not been perfect, this result would not have come as a surprise. However, as the two systems are commensurate and the forces induced by the QCM are too weak to displace the Xe atoms from the minima of the substrate potentials, the question arises why sliding was initiated. Reguzzoni *et al.* recognized that atoms in the adsorbed layer do not move in parallel, but motion is initiated collectively by a group of atoms that have jumped from the initial minima to the next one. In particular, they suggested that frictional slip occurs by the nucleation of a small commensurate domain that then expands by displacing a domain wall. The energy barrier to nucleate a new commensurate domain can be estimated by comparing the energy gain associated with the slip with the energy cost needed to create the domain wall. Once a critical size of the new domain has been reached, the domain will keep growing spontaneously and the monolayer will set into motion.

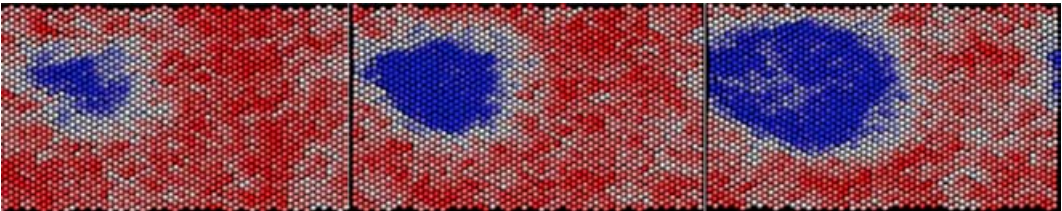


Figure 2.

The formation of a new commensurate domain prior to the global slip. The particle color indicates the distance from the substrate potential minima. Red particles are in the original minimum and become blue when they slip into the next minimum. Particles in white are part of the domain wall and are located outside the potential minima.

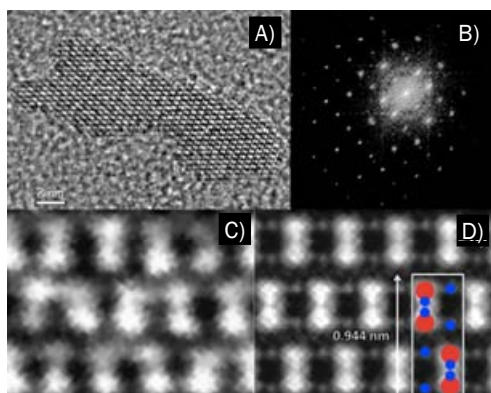
Related publications *Ballistic nanofriction*. R. Guerra, U. Tartaglino, A. Vanossi, and E. Tosatti, *Nature Materials* **9**, 634 (2010).

Onset of frictional slip by domain nucleation in adsorbed monolayers. M. Reguzzoni, M. Ferrario, S. Zapperi, and M.C. Righi, *PNAS* **107**, 1311 (2010).

Sub-ångström imaging of oxygen atoms in nanocrystals using electron diffraction

High-resolution imaging of low-atomic-number chemical elements using electron microscopy is challenging and may require the use of high doses of electrons. Electron diffractive imaging, which creates real-space images using diffraction intensities and phase retrieval methods, could overcome such issues, although it is also subject to limitations. Here, we show that a combination of electron diffractive imaging and high-resolution transmission electron microscopy can image individual TiO₂ nanocrystals with a resolution of 70 pm while exposing the specimen to a low dose of electrons. Our approach, which does not require spherical and chromatic aberration correction, can reveal the location of light atoms (oxygen) in the crystal lattice. We find that the unit cell in nanoscale TiO₂ is subtly different to that in the corresponding bulk.

High-Resolution Transmission Electron Microscopy (HRTEM) has revolutionized our understanding of nanoscale materials by identifying structure properties correlations at the atomic level. The spatial resolution achievable by TEM is related to the short wavelength of the high-energy electrons (e.g., 2.5 pm for 200 keV) used for imaging samples. However, despite technical progress achieved in the construction of modern microscopes the diffraction limit has not yet been approached due to the aberrations of electromagnetic lenses. A joint effort made by researchers of the Istituto di Cristallografia, Istituto Officina dei Materiali and National Nanotechnology Laboratory at the CnrNano have demonstrated that the imaging resolution of a HRTEM experiment can be improved by using an approach that bypasses such drawbacks. It relied on recording a phase-contrast HRTEM image of the target object together with the corresponding electron nano-diffraction (n-ED) pattern with a standard HRTEM microscope. While the resolution of the HRTEM image was limited to 0.19 nm, the n-ED pattern contained reflections corresponding to significantly smaller lattice spacings. The resolution of the n-ED pattern was hence much higher than that of the HRTEM image. A new phase retrieval algorithm was developed to extract the information contained in the n-ED pattern by using the information contained in the HRTEM image as input data. This approach is called electron diffractive imaging (EDI). Fig. 1 shows an individual crystalline TiO₂ (anatase) nanorod that was imaged by EDI at a record resolution of 70 pm, unambiguously revealing the presence and location of light atomic elements, namely oxygen, in the relevant tetragonal lattice. Subtle deformation of the anatase unit cell was also detected, which can



be responsible for some of the peculiar chemical-physical properties of these nanostructured TiO₂ materials. With EDI the study and understanding of matter at ultimate resolution is now possible using standard HRTEM microscopes.

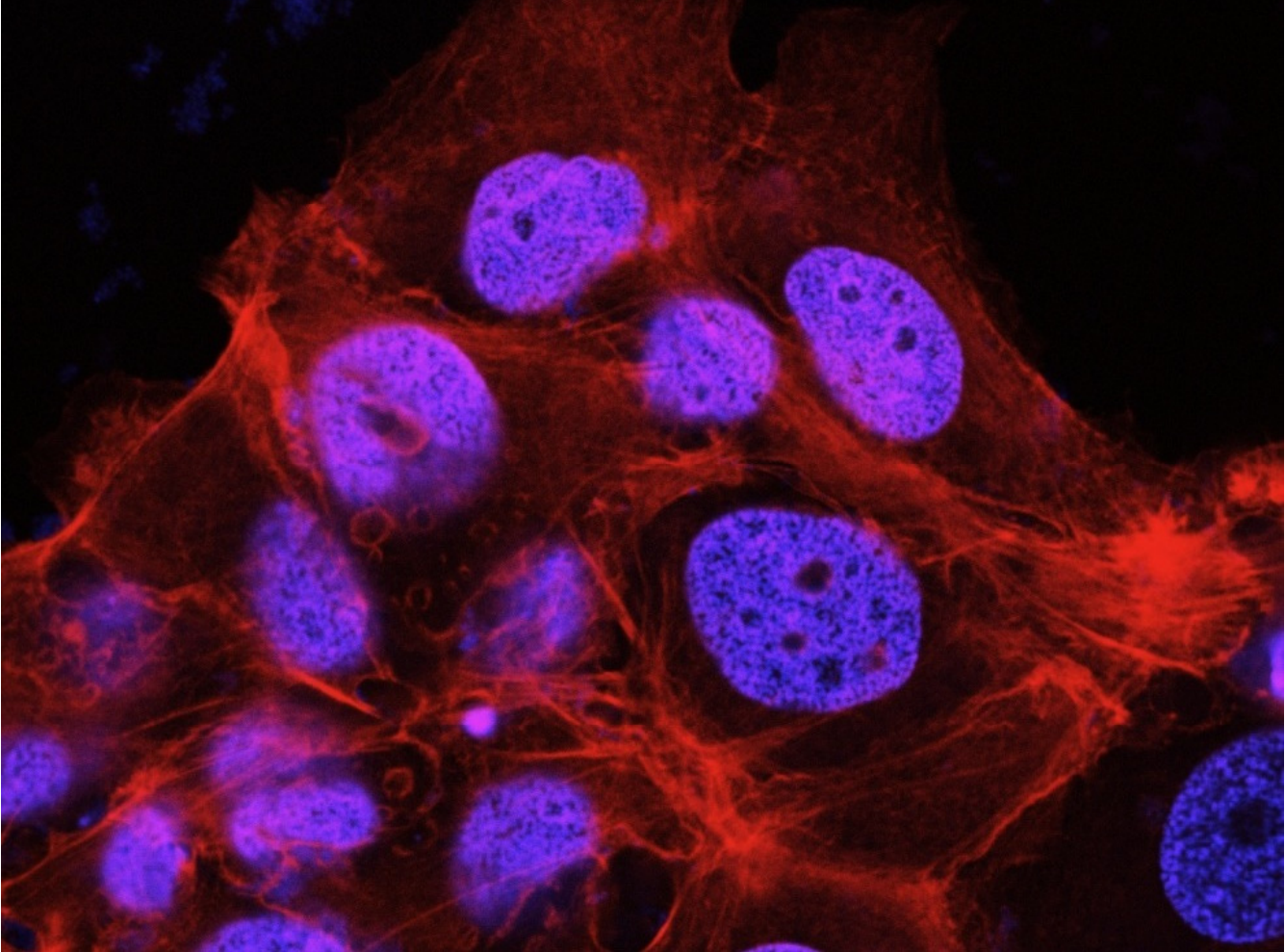
Figure 1.

A) HRTEM image of an anatase TiO₂ nanorod down the [100] zone axis; B) Combination of the fast Fourier transform (FFT) of A) with the n-ED pattern of the relevant nanorod after subtraction of the contribution of the amorphous carbon substrate; C) Magnified view of the HRTEM image contrast in A); D) EDI-retrieved image, where the rectangular box highlights the TiO₂ lattice along the [100] direction (blue: O atoms, red: Ti atoms).

Contact Person P. Davide Cozzoli (davide.cozzoli@unisalento.it)

Collaborators L. De Caro, E. Carlino, G. Caputo, C. Giannini

Related publication *Electron diffractive imaging of oxygen atoms in nanocrystals at sub-ångström resolution.* L. De Caro, E. Carlino, G. Caputo, P.D. Cozzoli, and C. Giannini, *Nature Nanotechnology* **5**, 360 (2010).



Highlights Nanobiotechnology

Autism and brain circuitry formation visualized at the two-photon microscope

By means of two-photon microscopy in vivo we have studied the morphological plasticity of excitatory neurons in a mouse model of genetic autism (Rett syndrome). Here, we have also demonstrated a cellular basis for the action of a putative therapeutic treatment for this disease.

Rett syndrome is a brain disease leading to severe invalidity. It is responsible, e.g., for autism, ataxia, epilepsy and respiratory difficulties. It is linked to the X chromosome and hits 1 girl out of about 10.000 in the first 18 months of life. The genetic background of this disease is well known: it is caused in about 90% of cases by a loss of function mutation of the gene MeCP2. Notwithstanding this knowledge, the cellular mechanisms at the basis of the pathology are not completely understood. The onset of Rett occurs at a time in which the nervous system is undergoing its most important period of post natal maturation. At this time the brain circuitry is perfected and the basis for the necessary machinery for memory and learning are posed. An important aspect of this developmental process is due to the morphological maturation of neurons.

In this study we have crossed a mouse model of Rett (the MeCP2 “knock-out” mouse) with a mouse line in which cortical neurons are made visible by the expression of the green fluorescent protein in a sparse set of excitatory neurons. By means of two-photon microscopy it is possible to visualize the finest details of neuronal morphology in the brain of an anesthetized mouse by imaging the superficial layers of the cortex through a window applied on the cranium.

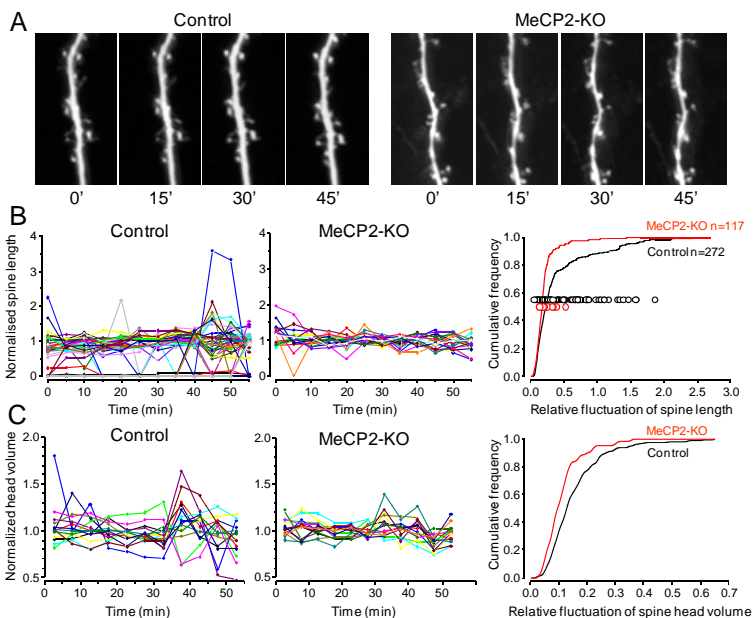


Figure 1.

In vivo two-photon imaging in young (4 weeks) mice.

A) Sample time lapse sequence from the somatosensory cortex of control and MeCP2 KO mice.

B,C) Quantification of length and volume of dendritic spines as functions of time. The fluctuations in the control mice (left) are clearly larger than in the Rett mice.

Contact Person Gian Michele Ratto (gianmichele.ratto@nano.cnr.it)

Collaborators S. Landi, E. Putignano, E.M. Boggio, M. Giustetto, T. Pizzorusso

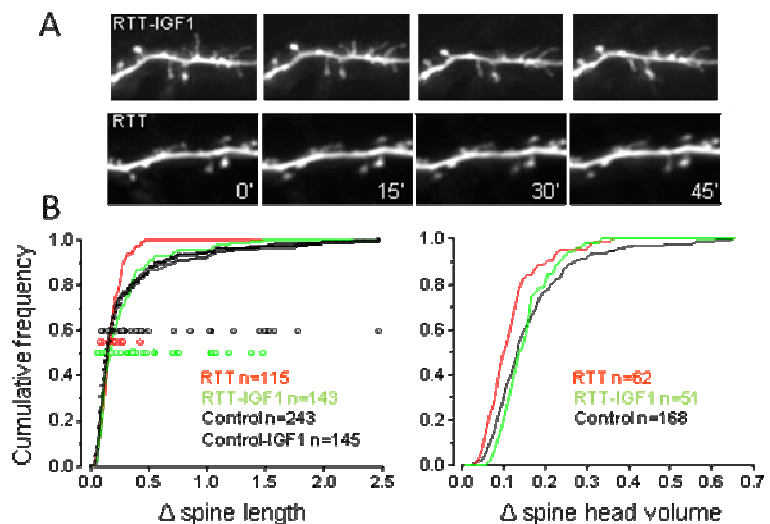
In the Rett mice we have studied the dynamics of the processes of anatomical reorganization that brings about the maturation of neuronal circuitry. More specifically, we have studied the micron-sized protusions (dendritic spines) placed on the dendrites of the excitatory neurons (Fig. 1). Each dendritic spine receives one excitatory sinapse from the upstream neuron: it is now clear that the dendritic spines are the main elementary computational element of the brain.

One of the most fascinating aspects of the physiology of dendritic spines is the strict function-form relationship that governs their activity. Changes in shape and position of dendritic spines always translate in changes of the synaptic efficacy. These processes of morphological and functional modifications are at the basis of the processes of memory and learning.

By means of two-photon microscopy it is possible to study the changes of dendritic spines in time. In the young mice, imaged during the ongoing maturation of brain circuitry, dendritic spines behave very differently compared to the diseased mice. Indeed, spines are extremely stable in the MeCP2 KO mice, at a developmental period in which spines should exhibit very high mobility, reflecting the continuous remodeling of circuitry (Fig. 1B). From these data a defect of synaptic plasticity emerges that could be interpreted as a precocious aging of the nervous system. Indeed, at an age in which in a healthy mouse structural and functional remodeling of the nervous system is still very active, a strong inhibition of these processes is detected in the Rett mouse. This early deficit appears early on the development stage and once it is "congealed" in the mature nervous system, it certainly limits its functioning.

However, this defective development might be not completely irreversible or not preventable. In other experiments we have shown that the injection of a trophic factor (the insulin-like trophic factor IGF1) has been capable to contrast the precocious interruption of dendritic spine mobility (Fig. 2).

Figure 2. Effects of the trophic factor IGF1 on dendritic spine dynamics in vivo. A) Two photon imaging in a Rett mouse one day after a single injection of IGF1 (upper images) or in control conditions (lower sequence). B) Cumulative distributions of dendritic spine length and volume show the recovery due to the treatment.



Related publication *The short-time structural plasticity of dendritic spines is altered in a model of Rett syndrome.* S. Landi, E. Putignano, E.M. Boggio, M. Giustetto, T. Pizzorusso, and G.M. Ratto, *Scientific Reports* **1**, 45 (2011).

Nanotopographic control of neuronal polarity

Interaction between differentiating neurons and the extracellular environment guides the establishment of cell polarity during nervous system development. Developing neurons read the physical properties of the local substrate in a contact-dependent manner and retrieve essential guidance cues. We employ simple geometrical rules to design a set of nanotopographies able to interfere with focal adhesion establishment during neuronal differentiation. Exploiting nanoimprint lithography techniques on cyclo-olefin-copolymer films, we demonstrate that by varying a single topographical parameter the orientation and maturation of focal adhesions can be finely modulated yielding independent control over the final number and the outgrowth direction of neurites. Taken together, this report provides a novel and promising approach to the rational design of biocompatible textured substrates for tissue engineering applications.

The mammalian neuronal network provides the best example of a highly polarized tissue whose functions depend on the underlying cell polarity. The initiation and engorgement of a nascent neurite are controlled by the establishment and maturation of focal adhesions (FAs), the integrin-based cellular structures that link the cell to the underlying substrate, at the tip of lamellipodia and filopodia. A mature FA can induce local actin polymerization and thus control the rearrangement of the cell shape. In a second step, the developing neurites test the surrounding environment searching the way toward their final targets in a process termed neurite pathfinding. Neuronal polarity establishment and neurite pathfinding are the most important processes to build a functional tissue during neuronal development and regeneration.

FAs generated by PC12 cells contacting flat substrates (between 12 and 24 h after NGF stimulation) are, on average, 1600 nm long and 900 nm wide. Importantly, on nanogratings with 500 nm wide ridges and grooves, FA establishment is restricted to individual ridges. This topographical constraint affects FA maturation by demoting the length increase in misaligned FAs, thus blocking their maturation, and by limiting the width increase in aligned FAs, while promoting their elongation. The net result of this cell-topography interaction is the selection of bipolar cells with two aligned neurites. Starting from these considerations, a set of nanogratings was produced, with constant groove size and depth (500 and 350 nm, respectively) and increasing ridge width, ranging from 500 nm (smaller than the typical FA length and width) to 2000 nm (larger than the typical FA length and width).

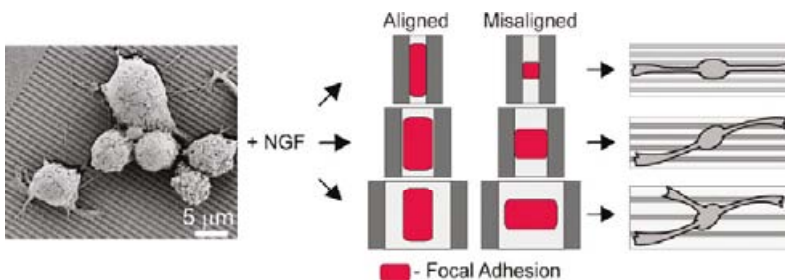


Figure 1. Nanotopographic control of neuronal polarity and neurite alignment by FA shaping.

Contact Person Marco Cecchini (marco.cecchini@nano.cnr.it)

Collaborators I. Tonazzini, E. Jacchetti, O. Vittorio, S. Meucci, F. Beltram, A. Ferrari

The rationale behind this design is that a gradual release of the topographic constraint would result in a modulation of neuronal polarity selection by allowing the maturation of misaligned FA (Fig. 1). As expected, nanogratings with ridge width smaller than the typical length of FAs (from 500 to 1500 nm) applied a topographical constraint leading to adhesion maturation only at the tip of aligned neurites while forcing the collapse of adhesions at the tip of misaligned ones. This yielded a fine modulation of neurite pathfinding and demonstrates that between 500 and 1500 nm the average neurite alignment can be controlled as a function of the lateral ridge sizes with an accuracy of $0.20 \pm 0.02^\circ$ over 10 nm. Nanogratings with increasing ridge width also allowed control over the average number of neurites per differentiating neuron. Nanogratings with the smallest ridge size (500 nm) strongly favored bipolar cells. The mechanism selecting bipolar cells was tolerant in the ridge-width range between 500 and 1000 nm. A transition to multipolarity was obtained increasing the ridge width to 1500 nm. This result demonstrated that neurite pathfinding and neuronal polarity establishment can be decoupled by pure topographical means (Fig. 2). The mechanisms controlling these processes were differently sensitive to ridge-width changes when contacting nanogratings. Neurite pathfinding was responsive to ridge-width variations between 500 and 1000 nm. Differently, the mechanism controlling neuronal polarity establishment senses variation in ridge width between 1000 and 1500 nm.

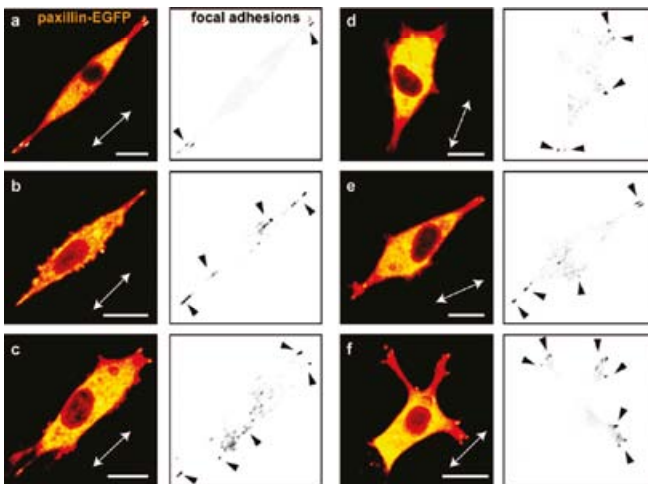


Figure 2.

Focal adhesion establishment by stimulated PC12 cells contacting nanogratings with increasing ridge width. Distribution of paxillin-EGFP fluorescent signal (between 12 and 24 h after NGF stimulation) in PC12 cells differentiating on nanogratings with ridge width corresponding to (a) 500 nm, (b) 750 nm, (c) 1000 nm, (d) 1250 nm, (e) 1500 nm or (f) 2000 nm. Scale bars correspond to 10 μ m.

In the right panel, inverted fluorescent signal at the cell-substrate interface pinpoints the corresponding regions of paxillin-EGFP accumulation (black spots).

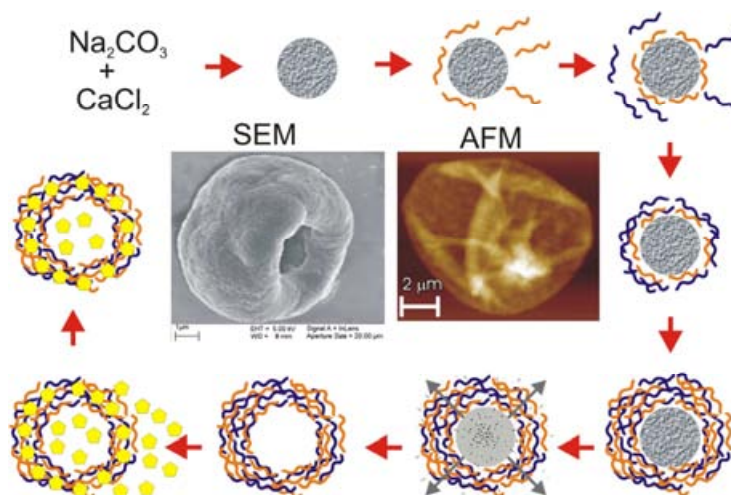
Related publication *Nanotopographic control of neuronal polarity.* A. Ferrari, M. Cecchini, A. Dhawan, S. Micera, I. Tonazzini, R. Stabile, D. Pisignano, and F. Beltram, *Nano Letters* **11**, 505 (2011).

Drug-loaded polyelectrolyte microcapsules for cancer cell targeting

In this review we overview novel nanotechnological nanocarrier systems for cancer therapy focusing on recent development in polyelectrolyte capsules for targeted delivery of antineoplastic drugs against cancer cells. Biodegradable polyelectrolyte microcapsules (PMCs) are supramolecular assemblies of particular interest for therapeutic purposes, as they can be enzymatically degraded into viable cells, under physiological conditions. Incorporation of small bioactive molecules into nano-to-microscale delivery systems may increase drug bioavailability and therapeutic efficacy at single cell level giving desirable targeted therapy. Layer-by-layer (LbL) self-assembled PMCs are efficient microcarriers that maximize the cell exposure to the drug, thus enhancing antitumor activity of neoplastic drug in cancer cells. They can be envisaged as novel multifunctional carriers for resistant or relapsed patients or for reducing dose escalation in clinical settings.

Packaging of drugs into micro- or nanocarriers has sparked great interest in biological validation of micro-to-nanoscale delivery systems for targeted therapy. Hollow microcapsules are of particular interest, as they can be fabricated via layer-by layer (LbL) assembly of oppositely charged polyelectrolyte multilayers of polysaccharides that are degraded by intracellular proteases or hydrolytic enzymes, around a sacrificial core of calcium carbonate that is dissolved by EDTA after deposition. Due to the versatility of electrostatic interactions, properties and functionalities of the resulting hollow capsules can be finely tuned in the nanometer range by varying capsule wall thickness and number and composition of the polymeric layers, hence their permeability in response to changes on pH, ionic strength or solvent. Several drugs have an intracellular target but they have a poor uptake when delivered in a soluble form or are lacking in solubility. However, specific targeting by drug molecules is also often needed to enhance the therapeutic efficiency or to avoid severe side effects.

Figure 1. Polyelectrolyte multilayer microcapsules. Consecutive adsorption of layer-by-layer assembled polyelectrolyte multilayers (red and blue) onto calcium carbonate microspheres (grey) is followed by dissolution of core templates by EDTA, and successive incubation with anticancer drug (IM, in yellow) in water solution for drug loading in the polymeric shells. SEM (left) and AFM (right) images of typically folded and air-dried hollow capsules are shown herein.



Contact Person Stefano Leporatti (stefano.leporatti@nano.cnr.it)

Collaborators V. Vergaro, F. Scarlino, C. Bellomo, R. Rinaldi, D. Vergara, M. Maffia, F. Baldassarre, G. Giannelli, X. Zhang, Y.M. Lvov

Several research groups have assessed cytotoxicity issues by performing in vitro cell-viability assays such as the MTT test or Trypan Blue. Reduced toxicity was observed even at elevated capsule concentrations: this is often attributed to aggregation of the capsules on top of the cells as a result of competition for space between capsules and cells. This effect limits the metabolism of the cells, and thus reduces their cytotoxicity. Recently Palamà *et al.* reported on PMCs and coated polymer microcolloids cytotoxicity and uptake by tumor cells. They showed that biosynthetic and biodegradable polyelectrolyte capsules and microcolloids are readily uptaken by three neoplastic model cellular lines (rat neuroblastoma, human cervix and breast cancer). Time-resolved MTT tests demonstrated also the low micro-carrier cytotoxicity and good cytocompatibility.

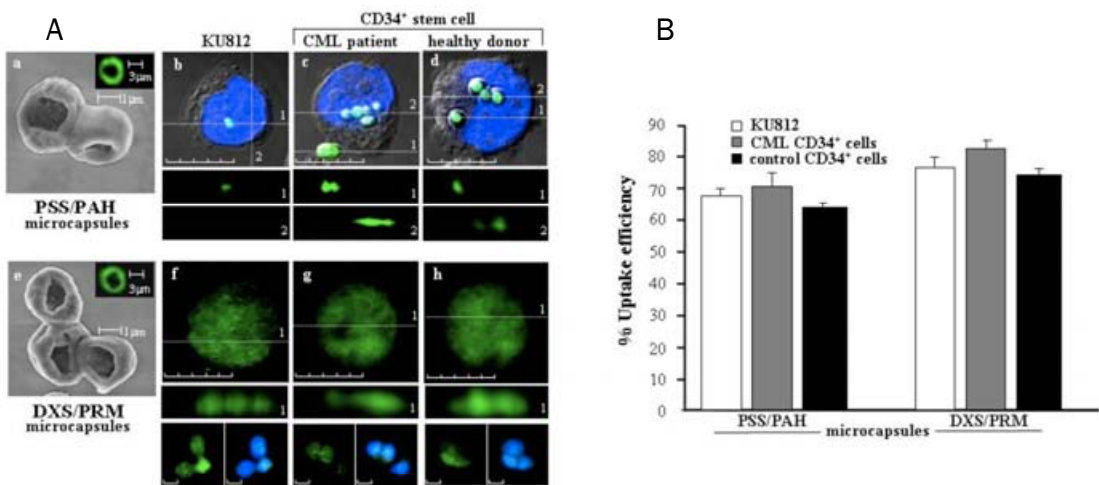


Figure 2.

A) Scanning Electron Microscope (SEM) micrographs of hollow microcapsules with (PSS/PAH)₃ (a) or (DXS/PRM)₃ (e) polyelectrolyte multilayers after CaCO₃ core dissolution (scale bar: 1 μm). Confocal images show the uptake of synthetic PSS/PAH (b, c, and d panels) or biodegradable DXS/PRM (f, g, and h panels) microcapsules, in KU812 leukemia cell line (b and f), and primary CD34⁺ cells freshly-isolated from CML patients (c and g) or healthy donors (d and h) after 3 hours of incubation. Additional fluorescence confocal images with DAPI merge of three cells were also reported for each cell-type upon uptake of DXS/PRM microcapsules (lower panels). B. Graphs of synthetic (PSS/PAH) and biodegradable (DXS/PRM) capsules uptake (percentage ratios of uptaken capsules) by KU812 (white squares), leukemic CD34⁺ cells (gray squares) or normal CD34⁺ cells (black squares).

Related publications

Imatinib-loaded polyelectrolyte microcapsules for sustained targeting of BCR-ABL+ leukemia stem cells. I.E. Palamà, S. Leporatti, E. de Luca, N. Di Renzo, M. Maffia, C. Gambacorti-Passerini, R. Rinaldi, G. Gigli, R. Cingolani, and A.M.L. Coluccia, *Nanomedicine* **5**, 419 (2010).

Multilayered Polyelectrolyte Capsules and Coated Colloids: Cytotoxicity and Uptake by Cancer Cells. I.E. Palamà, M.A.L. Coluccia, A. della Torre, V. Vergaro, E. Perrone, R. Cingolani, R. Rinaldi, and S. Leporatti, *Sci. Adv. Mater.* **2**, 138 (2010).

Drug-loaded polyelectrolyte microcapsules for sustained targeting of cancer cells. V. Vergaro, F. Scarlino, C. Bellomo, R. Rinaldi, D. Vergara, M. Maffia, F. Baldassarre, G. Giannelli, X.C. Zhang, Y.M. Lvov, and S. Leporatti, *Adv Drug Del Rev* **63**, 847 (2011).

Nanohybrids for drug delivery based on pH-responsive hydrogels and inorganic nanoparticles

In this study we have covalently attached various nanoparticles (NPs) to pH-responsive poly(2-vinylpyridine-co-divinylbenzene) nanogels. The conjugation was effected by means of a facile and robust one-step surfactant-free emulsion polymerization procedure. The NPs we employed are allyl-PEG capped inorganic NPs, including magnetic iron oxide (IONPs), fluorescent CdSe/ZnS quantum dots (QDs), and metallic gold (AuNPs of 5 and 10 nm). The characterization of their structural, magnetic and optical properties has revealed interesting features exploitable in various fields, among them the biomedical area.

We have developed a simple one-step procedure to co-polymerize allyl-polyethylene glycol functionalized inorganic nanocrystals. These are made of metallic like gold nanoparticles (AuNPs of 5 and 10 nm), superparamagnetic like iron oxide nanocrystals (IONPs) or semiconductor like CdSe/ZnS quantum dots (QDs). The nanocrystals have been conjugated, either individually or simultaneously, within poly(2-vinylpyridine-co-divinylbenzene) nanogels (Fig. 1).

The inclusion of the inorganic nanoparticles has been finely controlled during the micro-emulsion polymerization by the injection of the nanoparticles at a late stage of polymerization, when just polymeric radicals were present. The final products of the pH-responsive nanogels functionalized with nanoparticles preserve the pH-swelling behavior with a volume phase transition at pH 4.3 and a variation over the degree of swelling depending on the number of nanoparticles included. Furthermore, additional features are added by the insertion of different nanoparticles since both the magnetic response and the optical luminescence of the nanogels are strongly affected by the presence of QDs. In addition, gold nanoparticles exhibited radical quenching, thus affecting the final distribution of nanoparticles around the nanogel. In the case of gold-nanogel the typical plasmonic signature of gold nanoparticles is also recorded. These nanostructures might be exploitable as pH-responsive tools in drug delivery and sensor applications. For instance, in a recent work we have demonstrated the use of magnetic pH-responsive nanogels to transport and release short inference RNA sequences. In principle, this tool could be used in silencing interference RNA therapy. Indeed, the pH-mediated down-regulation of the green fluorescent protein has been demonstrated.

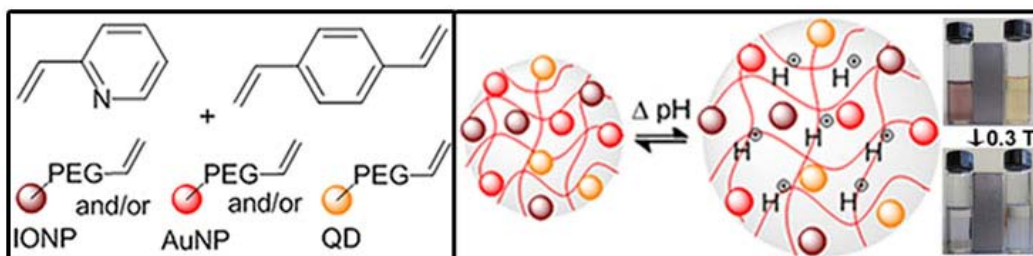


Figure 1.

Schematic view of the allyl-capped inorganic nanocrystals and vinyl pyridine divinyl benzene monomers used for the co-polymerization of inorganic nanocrystals with nanogel polymer, with subsequent acidic pH swelling. Image of the gold and magnetic functionalized nanobeads in solution before and after the application of a magnetic field of 0.3T.

Contact Person Teresa Pellegrino (teresa.pellegrino@nano.cnr.it)

Collaborators R. Cingolani, A. Riedinger, M. Pernia Leal, S.R. Deka, C. George, I.R. Franchini, A. Falqui

Related publications *Acidic pH-Responsive Nanogels as Smart Cargo Systems for the Simultaneous Loading and Release of Short Oligonucleotides and Magnetic Nanoparticles*. S. Deka, A. Quarta, R. Di Corato, A. Falqui, L. Manna, R. Cingolani, and T. Pellegrino, *Langmuir* **26**, 10315 (2010).

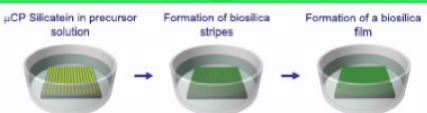
"Nanohybrids" Based on pH-Responsive Hydrogels and Inorganic Nanoparticles for Drug Delivery and Sensor Applications. A. Riedinger, M. Pernia Leal, S.R. Deka, C. George, I.R. Franchini, A. Falqui, R. Cingolani, and T. Pellegrino, *Nano Letters* **11**, 3136 (2011).

Bioinspired electrically-insulating silica films

Silica represent a key material for realization of microelectronic and optical components. We showed that silica microstructures and films can be obtained in a biomimetic way, using the micro-contact printing technology and a recombinant protein derived from sponges, named silicatein α . Protein micropatterns were successfully realized on silicon based substrates, and investigated by fluorescent microscopy after fluorescein-based staining. By using environmentally benign conditions, tetraethylorthosilicate was used as a precursor of the biomineralisation process, which was monitored over time by several complementary microscopy methods. The electrically-insulating properties of biosilica films were assayed for the first time, demonstrating the potential production of next generation electronic components utilizing biologic pathways and mild production conditions.

Silica films are ubiquitously used in many fields, e. g., as coatings for biomedical surfaces and devices (for tissue engineering, controlled drug delivery, surface modification, transplants, etc.), catalytic, diagnostic and sensing surfaces, composites, smart surfaces, optics, and optoelectronics (being optically transparent, as dielectric layer for interferential elements, for light-emitting devices, etc.), for microelectronics and nanoelectronics (as gate dielectric layers for field-effect transistors and other electronic devices).

Unfortunately, the commonly used production processes of silica surfaces, at both laboratory and industrial scales, are usually carried out by processing at high temperatures, extreme conditions of pressures, and strongly acid and basic environments. The controlled realization of silica patterns and the production of silica by low-cost, gentle biomineralization processes could be instead a powerful method for the environmentally-friendly realization of coatings and devices, because many living organisms are able to synthesize silica under mild, physiological conditions. Silicateins are peculiar proteins from sponges, able to catalyze the reaction of silica polymerization to give ordered structures. In the framework of the European Project "Biomineralization for lithography and microelectronics" (BIO-LITHO), we used for the first time recombinant silicateins to produce micropatterns and films on silicon, and to assess the electrically-insulating properties of the obtained biosilica. The proposed method extends biosilicification to the controlled fabrication of miniaturized silica elements by physiological processing conditions, which cannot be addressed by conventional technologies. Patterning silicatein and realizing different silica geometries can be particularly useful as a tool for electrical insulating of microscale building blocks in complex circuits. We showed how to microfabricate biosilica stripes and films just by tuning the incubation time in silica precursor solution. Recent works on biomedical applications of biosilica clear the way for its use as a new bioactive material.



The *Suberites domuncula* demosponge, and schematic illustrations of the steps for realizing biosilica structures.

Contact Person Dario Pisignano (dario.pisignano@nano.cnr.it)

Collaborators A. Polini, S. Pagliara, A. Camposeo, A. Biasco, H.C. Schröder, W.E.G. Müller

Related publication *Biosilica Electrically-Insulating Layers by Soft Lithography-Assisted Biomineralisation with Recombinant Silicatein*. A. Polini, S. Pagliara, A. Camposeo, A. Biasco, H.C. Schröder, W.E.G. Müller, and D. Pisignano, *Adv. Mater.* **23**, 4674 (2011).

Protein-surface interactions: insights from atomistic simulations

The interaction of proteins with inorganic surfaces and nanoparticles is pivotal in nanobiotechnology. A computational, atomistic description of this interaction can provide us with microscopic insights on its origin and nature, which are elusive to experimental investigation alone. We have set up and applied atomistic computational methodologies (ab initio and empirical) for the study of peptides and proteins on Au surfaces, that led to the disclosure of mechanisms of interaction and to the explanation of puzzling experimental results. In particular, by ab initio simulations we clarified how hydroxyl-amino acids interact with (and potentially recognize) the Au(111) surface. In another ab initio study, we explained the capability of the hydroxyl amino acid tyrosine to promote the synthesis of gold nanoparticles from chloroaurate ions.

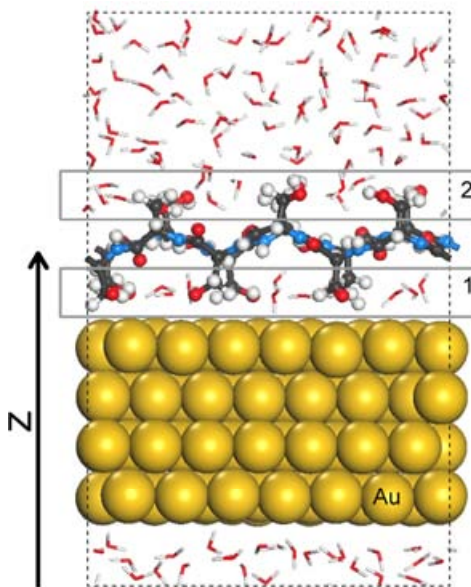
Understanding and controlling the interaction of proteins with inorganic surfaces and nanoparticles is a key task in nanobiotechnology. On the one hand, inorganic components within a biological system (e.g., nanoparticles for drug delivery, for diagnostics or accidentally uptaken; surgical implants) are readily covered with proteins, whose nature, orientation and subsequent conformational changes are determined by protein-inorganics interactions. On the other hand, development of applications where proteins are used in nanotechnology contexts (e.g., biomolecular electronics, peptide-based self-assembling, enzymatic biofuel cells) also requires a detailed understanding of such interactions. Experimentally probing the protein-surface interface at the microscopic level is a difficult task, and the available information is still limited.

Atomistic computational modeling therefore emerges as a useful complementary approach to shed light on the intimate nature of protein-surface interactions. We have developed and applied simulation strategies and tools to unravel the basic principles that govern the interaction of proteins and peptides with inorganic surfaces and nanoparticles. We use techniques at multiple levels, ranging from ab initio methods to rigid protein-surface docking, chained in a sequential multiscale approach.

Figure 1.

Ab initio simulations can explain fundamental aspects of protein-surface and protein-nanoparticle interactions.

Side-view of the protein-surface system investigated by AIMD simulations (peptide-Au and peptide-water interfaces are identified by rectangles). The 20 ps long simulation allowed us to highlight the nature of the peptide-surface interaction and the geometrical preferences that follow.



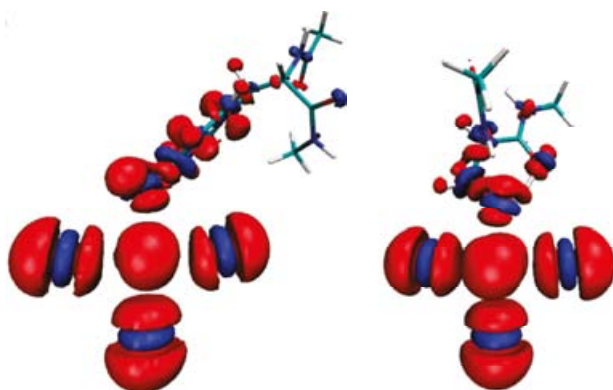
Contact Person Stefano Corni (stefano.corni@nano.cnr.it)

Collaborators R. Di Felice, A. Calzolari, A. Catellani, C. Cavazzoni, O. Carrillo, G. Cicero, L. Bellucci, G. Brancolini, M.E. Siwko, D. Toroz

Thanks to the extreme computing power secured by a European extreme computing initiative project, we were able to perform the first ab initio molecular dynamics (AIMD) simulation of a prototype protein on a gold surface in water (Fig. 1). We clarified the intimate nature of the interaction between gold and peptides rich in amino acids containing hydroxyl groups, showing that it can lead to the texture recognition. Moreover, we highlighted the role of the peptide hydration water, that acts as an integral part of the peptide itself. We also investigated by ab initio calculations how peptides can control the synthesis of gold nanoparticles (Fig. 2), explaining the puzzling differential behaviors of various hydroxyl amino acids in the early stages of nanoparticle formation. The computational tools developed by us and by our international coworkers are freely available to the academic community.

Figure 2.

Charge density difference between the reduced and the oxidized forms of tyrosine (left) and serine (right) complexes with Au. Tyrosine and serine are both natural hydroxyl amino acids. Our ab initio calculations revealed why tyrosine is able to reduce gold much more effectively than serine.



Related publications *Combined effects of metal complexation and size expansion in the electronic structure of DNA base pairs.* R. Di Felice and S. Corni, *J. Phys. Chem. Lett.* **2**, 1510 (2011).

Hydroxyl-Rich β -Sheet Adhesion to the Gold Surface in Water by First-Principle Simulations.

A. Calzolari, G. Cicero, C. Cavazzoni, R. Di Felice, A. Catellani, and S. Corni, *J. Am. Chem. Soc.* **132**, 4790 (2010).

Peptide synthesis of gold nanoparticles: the early steps of gold reduction investigated by density functional theory. D. Toroz and S. Corni, *Nano Lett.* **11**, 1313 (2011).



Highlights Nanoscience

A Josephson quantum electron pump

We report the experimental detection of charge flow in an unbiased InAs nanowire embedded in a superconducting quantum interference device (SQUID), in the absence of Coulombic effects. In this system quantum pumping may occur via the cyclic modulation of the phase of the order parameter of different superconducting electrodes. The symmetry of the current with respect to the enclosed magnetic flux and bias SQUID current is a discriminating signature of pumping. Currents exceeding 20 pA are measured at 250 mK, and exhibit symmetries compatible with quantum pumping. The SQUID voltage dependence of the current flowing through the nanowire shows a monotonic linear increase for small voltages and a suppression at large voltages, passing through a maximum at a voltage corresponding to a Josephson frequency of about 190 GHz. In the so-called adiabatic regime, i.e., where the pumped current varies linearly with frequency, we estimate some 10^{-3} electrons pumped per cycle. Furthermore, the current flowing through the nanowire shows a monotonic decrease upon increasing temperature which can be ascribed to the influence of thermal smearing as well as thermal-induced dephasing. A theoretical framework based on the dynamical scattering approach is employed to analyse the different mechanisms generating a direct current in the nanowire.

Mesoscopic charge pumping, a transport mechanism that relies on the explicit time-dependence of some properties of a nanoscale conductor, was envisaged theoretically a few decades ago. So far, nanoscale pumps have been realized only in systems exhibiting strong Coulombic effects, whereas evidence for pumping in the absence of Coulomb blockade has been elusive. Here we use the ac Josephson effect to induce periodically time-dependent Andreev reflection amplitudes in a hybrid normal-superconducting system. Andreev reflection is the quantum process for which an electron impinging from the normal side onto the interface between a normal metal and a superconductor is retroreflected as a hole (i.e., a time-reversed electron), which picks up the phase of the superconducting order parameter.

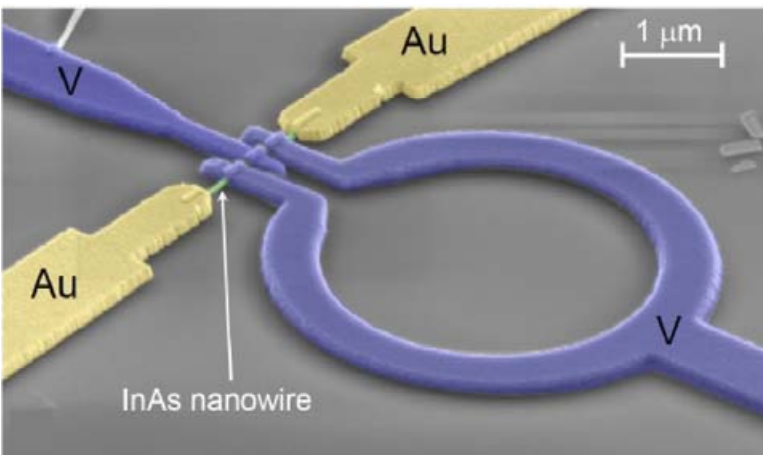


Figure 1.

An InAs nanowire (NW) is connected to three ≈ 250 -nm-wide V/Ti superconducting contacts forming two ≈ 50 -nm-long Josephson weak-links and realizing a superconducting quantum interference device (SQUID). Two Au/Ti leads, placed at relative distance of $\approx 1.5 \mu\text{m}$, are contacted to the ends of the NW to allow current detection. The structure was fabricated with electron-beam lithography and evaporation of metals.

Contact Person Fabio Taddei (fabio.taddei@nano.cnr.it)

Collaborators F. Giazotto, P. Spathis, S. Roddaro, S. Biswas, L. Sorba, M. Governale

The physical realization of this scheme is shown in Fig. 1 and consists of a heavily-doped InAs semiconducting nanowire (NW) on top of which three fingers of superconducting (S) vanadium (V) are deposited thus implementing a SQUID. Two Au normal-metal electrodes (N) are coupled to the ends of the NW to allow detection of the current I_{wire} flowing through the wire. Time-dependence, and possibly pumping, arises from biasing the loop with a current I_{SQUID} larger than the critical current I_c of the SQUID so that the phase differences $\phi_1(t)$ and $\phi_2(t)$ across the two Josephson junctions cycle in time at the Josephson frequency $\nu_J = V_{\text{SQUID}}/\Phi_0$, where V_{SQUID} is the voltage developed across the SQUID and Φ_0 is the flux quantum. In addition, $\phi_1(t)$ and $\phi_2(t)$ can be shifted by a constant term originating from an applied magnetic flux Φ threading the loop. This scheme has the advantage that no high-frequency signal needs to be brought to the sample thus simplifying the setup and minimizing the impact of stray capacitancies. The measurement is performed by grounding the N electrodes and sensing I_{wire} with an amperometer. The N and S parts of the circuit have no common ground therefore preventing any direct net charge transfer from the SQUID to the NW.

In general, I_{wire} is not expected to possess any definite parity with I_{SQUID} . In addition, the pumped current has no definite parity with Φ , although the flux-symmetric component of I_{wire} could be ascribed also to other mechanisms than pumping. Therefore, we focus on the component ($I_{\text{A,wire}}$) antisymmetric in Φ of the measured current, as it is predicted to be a fingerprint of quantum pumping in the system. Fig. 2A displays $I_{\text{A,wire}}$ versus Φ and I_{SQUID} at 250 mK. The Φ_0 -periodicity joined with the antisymmetry imply that $I_{\text{A,wire}}$ vanishes at $\Phi = \Phi_0/2$, while its sign and magnitude can be changed by varying Φ . Notably, $I_{\text{A,wire}}$ is almost symmetric in I_{SQUID} . The theoretical $I_{\text{A,wire}}$, calculated through a dynamical scattering approach assuming for the NW multiple independent modes, is shown in Fig. 2B. Although rather idealized, the model is an essential tool to predict the symmetries of the system. Remarkably, summing over many NW modes yields $I_{\text{A,wire}}$ which is almost symmetric in I_{SQUID} , in agreement with the experiment. The nature of the symmetries displayed by I_{wire} is therefore compatible with a quantum pumping mechanisms.

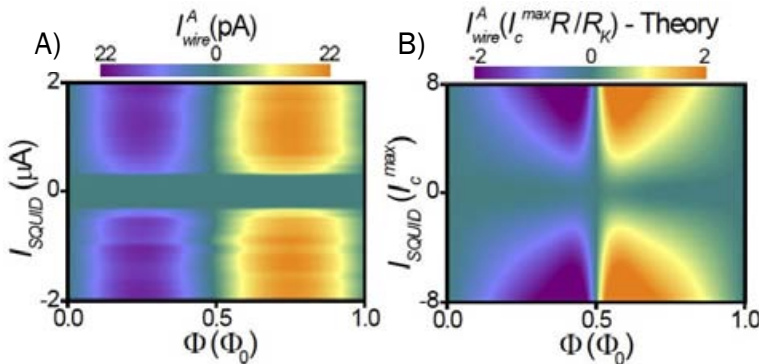


Figure 2.

A) Color plot of $I_{\text{A,wire}}$ versus I_{SQUID} and Φ . B) Color plot of the theoretical zero-temperature $I_{\text{A,wire}}$ versus I_{SQUID} and Φ . The calculation was performed assuming the same asymmetry between the Josephson junctions as in the experiment. $I_{c,\text{max}}$ is the sum of the critical currents of the two Josephson junctions, R is the total shunting SQUID resistance, and $R_K \approx 25.8 \text{ k}\Omega$ is the Klitzing resistance.

Related publication *A Josephson quantum electron pump.* F. Giazotto, P. Spathis, S. Roddaro, S. Biswas, F. Taddei, M. Governale, and L. Sorba, *Nature Physics* **7**, 857 (2011).

Few electron transport effects in InAs/InP nanowire transistors

Self-assembled nanowires (NWs) are emerging as a versatile and powerful tool for the investigation of transport phenomena at the nanoscale. NWs can be grown to form complex axial and radial heterostructures in which normally incompatible materials can be combined into advanced nanostructures. Recent activities focused on the realization of highly-tunable single-electron transistors based on InAs/InP NWs where electron orbitals can be strongly and controllably warped by means of an external electrostatic field. High-temperature Coulomb blockade operation and controlled manipulation of the quantum dot energy spectrum have been demonstrated, with perspectives in high-temperature single-electron devices and time-resolved single-spin control.

The metal-seeded growth of semiconductor NWs has emerged as a flexible and promising technology for the fabrication of self-assembled nanostructures, with a potential impact on innovative device applications. Different materials can be easily combined in individual high-quality single-crystal NWs, with significantly looser lattice-matching constraints with respect to alternative growth techniques. As a consequence, NW technology represents a unique research and development platform for fundamental physics investigation as well as for scalable electronics. NW-based single-electron devices – obtained either by using local gating or epitaxial barriers – have been so far one of the ambits where this nanofabrication technology excelled, leading to device architectures where a control of electron filling down to the last free electron can be routinely obtained. While tightly confined single-electron systems based on NWs have been demonstrated, their tunability has so far been limited and in practice the InAs/InP technology allowed observing clear Coulomb blockade effects only up to about the liquid He temperature. Even if scaling is expected to enhance both charging and quantum confinement, NWs with a diameter below 20-25nm tend to be insulating because of quantum confinement effects.

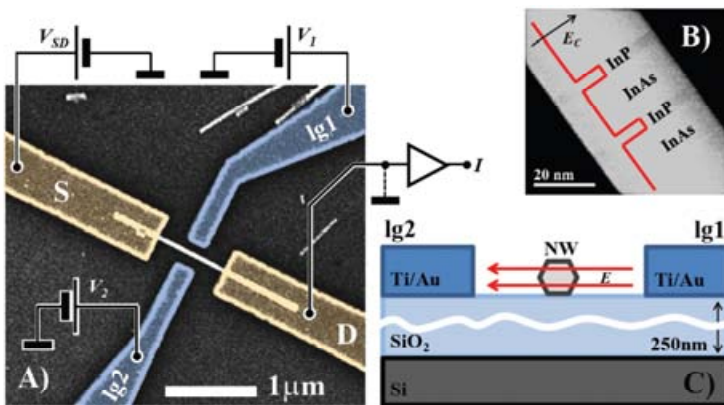


Figure 1.

A) Scanning electron micrograph of one of the studied devices with a sketch of the measurement setup in overlay. The nanowire is deposited on a SiO₂/Si substrate which can act as a backgate and it is contacted by two Ti/Au electrodes (yellow). Two gate electrodes at the two sides of the nanowire (blue) allow control of the electronic filling and the transverse electric field in the dot region. Gates are aligned to the position of the heterostructured dot.

B) Scanning transmission electron microscopy picture of one of the InAs/InP nanowires utilized for this research work. C) Cross-sectional view of the device. The two lateral electrodes can be used to control the electron filling in the dot and induce a transverse field.

Contact Person Stefano Roddaro (stefano.roddaro@iom.cnr.it)

Collaborators L. Romeo, A. Pescaglini, A. Pitanti, D. Ercolani, L. Sorba, F. Beltram

This leaves a limited margin for the enhancement of the QD's working temperature through bare scaling. Our recent research activities at NEST have demonstrated a novel electrostatic technique that exploits the hard-wall confinement potential of InAs/InP quantum dots (QDs) in order to dramatically modify the energy spectrum of the electron island controlling the transport through the device.

An example of the studied devices is depicted in Fig. 1: InAs/InP NWs with a diameter of about 45 nm are deposited on a Si/SiO₂ substrate where they are contacted by aligned e-beam lithography (Fig. 1A). One of the grown QD structures is visible in the scanning transmission electron microscopy (STEM) micrograph of Fig. 1B and contains two 5 nm thick InP barriers separated by a 20 nm long InAs island. Ohmic contacts are obtained by thermal evaporation of two GeAu/Au source (S) and drain (D) electrodes (yellow in Fig. 1A) located at a nominal distance of 800 nm. Two local gate electrodes (blue, Ig1, and Ig2 visible in panels A) and C) of Fig. 1) are also fabricated in correspondence to the QD and allow for the control of the electron population (in common biasing mode) and of a transverse electric field (in differential biasing mode) across the QD.

Thanks to the strongly non-parabolic shape of the hard-wall confinement potential of the InAs/InP QD, the transverse field can have a dramatic effect on the energy spectrum of the electron island. Indeed our experimental results demonstrated that a transverse electrical field can be highly effective in the manipulation of the orbitals in the QD. Fig. 2 shows how the addition energy for the third electron in the QD can be highly enhanced thanks to an artificial increase of the confinement energy of the second orbital of the QD with respect to the first one. Our results on current NWs allowed us to push the inter-level gap up to about 50 meV and the addition energy up to about 75 meV. This made it possible to observe very strong charging effects even at the liquid nitrogen temperature. Given such a result for a relatively large NW (50 nm diameter), room temperature operation appears to be at reach by bare scaling of our novel multigating technique. The same approach is also expected to allow for the investigation of exchange-driven spin effects at electrostatically-induced degeneracies between different electron orbitals.

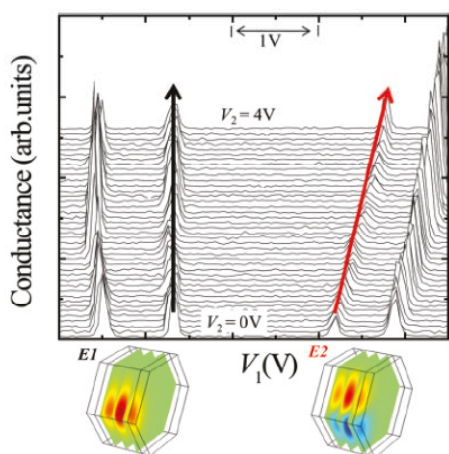


Figure 2.

The application of a transverse electric field on the QD enhances the Coulomb gap at a filling configuration corresponding to the full occupation of the first orbital in the island (level E1 visible at the bottom of the plot). In the specific measurement reported in figure, the transverse electrical field in the QD is estimated to go from zero (bottom curves) up to about 40keV/cm (top curves), based on a numerical simulations. The gap enhancement is consistent with the corresponding expected incremental quantum confinement effect between the first (left hand side below the plot) and second (right hand side below the plot) orbital.

Related publication *Manipulation of Electron Orbitals in Hard-wall InAs/InP Nanowire Quantum Dots.* S. Roddaro, A. Pesceglini, D. Ercolani, L. Sorba, and F. Beltram, *Nano Lett.* **11**, 1695 (2011).

Two-dimensional Mott-Hubbard electrons in an artificial honeycomb lattice

Artificial crystal lattices can be used to tune repulsive Coulomb interactions between electrons. We trapped electrons, confined as a two-dimensional gas in a gallium arsenide quantum well, in a nanofabricated lattice with honeycomb geometry. We probed the excitation spectrum in a magnetic field, identifying collective modes that emerged from the Coulomb interaction in the artificial lattice, as predicted by the Mott-Hubbard model. These observations allow us to determine the Hubbard gap and suggest the existence of a Coulomb-driven ground state.

In order to study quantum phenomena difficult to be directly investigated, scientists use artificially-designed systems - called quantum simulators - that can be controlled and manipulated in the laboratory. Quantum simulators have been developed quite recently and are based on different technologies (cold atoms, photonic crystals, trapped ions, single molecules on a clean metal surface, etc.). The artificial device we have developed is the first quantum simulator based on a semiconductor material and permits to observe the quantum behavior of electrons trapped in a honeycomb lattice. The most interesting phenomena occurring in condensed matter systems, such as ferromagnetism and high-temperature superconductivity, originate from mutual interactions among many degrees of freedom represented by electrons, lattice vibrations, spins, etc.

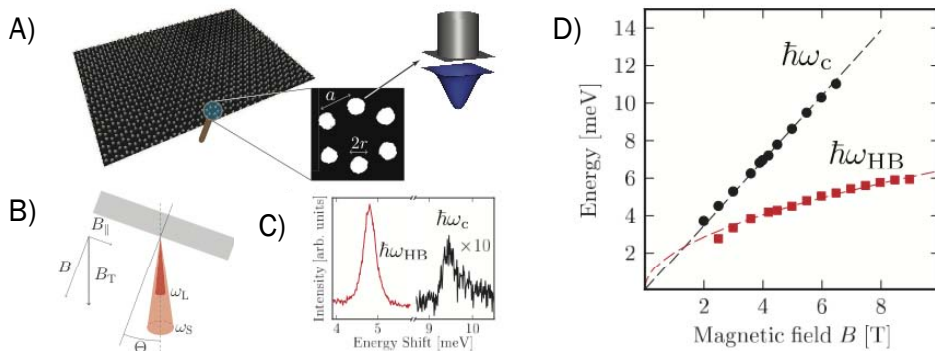


Figure 1.

A) Scanning electron microscopy (SEM) image of the semiconductor artificial lattice. An expanded view of the SEM image showing a single honeycomb cell ($2r \sim 60$ nm, $a \sim 130$ nm). The two-dimensional electron gas is positioned ~ 170 nm below the surface with a low-temperature mobility of 2.7×10^6 cm²/(V s). We also sketch a cartoon of the two-dimensional potential trap for electrons induced by the nanofabricated pillar at the surface. B) Geometry of the light scattering experiment: ω_{\perp} labels the incident (scattered) photon energy and $\theta = 5^\circ$ is the tilt angle. C) Resonant inelastic light scattering spectra showing the cyclotron mode and the new low-lying collective mode at $B = 5.48$ T and $T = 1.7$ K. d) Evolution of the energies of the cyclotron mode (black filled circles) and of the new collective mode at frequencies ω_{HB} (red filled squares) at $T = 1.7$ K. The black dashed line is a linear fit to the data using $\omega_c = eB/(m_b c)$. We find $m_b = 0.067 m_e$ with m_e the bare electron mass, in agreement with the bulk GaAs value. The red dashed line is a fit with $\omega_{\text{HB}} = \alpha B_{\perp}^{1/2}$.

Contact Person Marco Polini (marco.polini@nano.cnr.it)

Collaborators A. Singha, M. Gibertini, B. Karmakar, V. Pellegrini, S. Yuan, G. Vignale, M.I. Katsnelson, A. Pinczuk, L.N. Pfeiffer, K.W. West

These unique breakthroughs in scientific knowledge, which have led to silent revolutions in every-day life, pose a great challenge to humans since exact calculations of the behavior of the underlying complex systems are an impossible task, even for the more sophisticated and powerful computers. Quantum simulators help bypassing the problem, by replacing the “uncomputable” quantum system with a controllable artificial one, which is able to emulate the dynamics of the original system.

The simulator developed by us consists of a honeycomb lattice realized on the surface of a Gallium Arsenide (GaAs) heterostructure by advanced nanofabrication methods. The artificial honeycomb lattice structure replicates that of graphene, a material in which electrons behave in a peculiar way because of the crystal lattice geometry. Moreover, one can get the best out of the simulator as it is possible to modify at will some key parameters such as the lattice constant of the artificial lattice. This makes it possible to explore strong electron-electron interactions in graphene-like systems.

The prototype has been tested with a “first run” that generated within the crystal a peculiar state of the matter with intriguing low-energy collective excitations. This is the first step towards the realization of an innovative class of solid-state quantum simulators, which may soon help us understand some of the most complex quantum behaviors in the physics of matter.

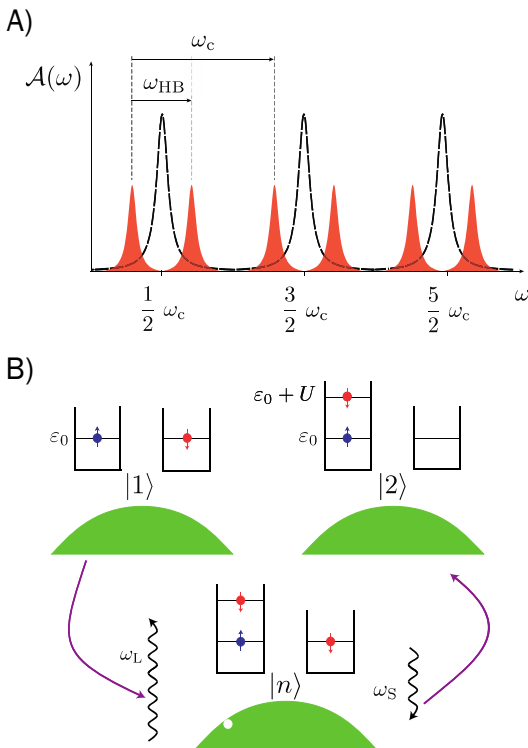


Figure 2.

A) A cartoon of the spectral function $A(\omega)$ of the patterned/unpatterned 2DEG (red/black). The Landau level peaks at $\omega = \omega_c(n + 1/2)$ are split by on-site Coulomb interactions into Hubbard lower and upper peaks, which are separated by $U \sim e^2/l_B$, where l_B is the magnetic length. B) The relevant electronic process which contributes to the Raman scattering cross section. The initial state is labeled by $|1\rangle$, the final state by $|2\rangle$, while the intermediate state with one hole and an extra electron is labeled by $|n\rangle$. The final excited state is separated from the ground state by the Hubbard charge gap U , i.e., by the energy cost of having two antiparallel spin electrons on the same site. In the intermediate state we have also depicted the absorbed (at frequency ω_L) and emitted (at frequency ω_S) photons. The square wells denote two neighboring minima of the artificial-lattice potential. The green areas denote valence-band electrons, which are assumed to be unaffected by the periodic modulation.

Related publication *Two-Dimensional Mott-Hubbard Electrons in an Artificial Honeycomb Lattice.* A. Singha, M. Gibertini, B. Karmakar, S. Yuan, M. Polini, G. Vignale, M.I. Katsnelson, A. Pinczuk, L.N. Pfeiffer, K.W. West, and V. Pellegrini, *Science* **332**, 1176 (2011).

All-optical control of the quantum flow of a polariton condensate

While photons are massless particles that, in vacuum, do not interact with each other, significant interactions, instead, appear in suitable nonlinear media, leading to hydrodynamic behaviours typical of quantum fluids. We demonstrate the generation and manipulation of vortex-antivortex pairs in a coherent gas of strongly dressed photons (polaritons) when flowing against an artificial potential barrier created and controlled by a light beam. The optical control of the polariton flow allows to reveal new quantum hydrodynamical phenomenologies such as the formation of vortex pairs upstream from the optical barrier, a case of ultrashort time excitation of the quantum flow, and the generation of vortices with counterflow trajectories. Moreover, it is possible to permanently trap and store quantum vortices generated hydrodynamically in the wake of a defect by using ad hoc potential geometries. These observations are theoretically supported by time-dependent simulations based on the non-equilibrium Gross-Pitaevskii equation.

As bosonic particles, polaritons have recently been demonstrated to undergo a phase transition to a Bose-condensed state. This has triggered the search for superfluid behaviors in polariton fluids, opening up new exciting possibilities. Recently, the study of nonlinear flow phenomena in polaritons has led to the observation of superfluidity, persistent circular flows and hydrodynamic nucleation of dark solitons. Photon-based polariton fluids, in particular, appear to be the most promising candidates for the study of quantum hydrodynamic effects and topological excitations such as vortices of quantized angular momentum.

In this context, polariton condensates may have the advantage of having large intrinsic nonlinearities as well as already being integrated in semiconductor chips. A quantum fluid encountering different kinds of obstacles may break its superfluid regime by the emission of topological excitations (vortices). This effect has recently been studied in ultra-cold atoms, and in a gas of resonantly generated polaritons hitting a natural defect in a sample.

This paper shows the potential of optical methods for the study, generation and manipulation of quantized vortices in a quantum fluid. With a full control over the parameters of an artificial obstacle sets in the trajectory of a polariton fluid running at velocities which allow for the superfluid regime to be violated, it is shown that the polariton condensate switches to a regime of turbulent motion. This regime is characterized by the emission of a pair of vortices which happens to appear upstream of the obstacle or along its equator (depending on the critical velocities), which is unique of quantum turbulent fluids. Many other behaviors of the polariton fluid are observed depending on the defect size and depth, including the observation of a quantum laminar flow in shallow obstacles and the bouncing of vortices in case of an abrupt barrier (Fig. 1). These outcomes demonstrate that by controlling the obstacle parameters it is possible to inspect the physics of the vortex nucleation process in unconventional regimes and reveal new effects.

Contact Person Daniele Sanvitto (daniele.sanvitto@nano.cnr.it)

Collaborators G. Gigli, S. Pigeon, A. Amo, D. Ballarini, M. De Giorgi, I. Carusotto, R. Hivet, F. Pisanello, V.G. Sala, P.S.S. Guimaraes, R. Houdré, E. Giacobino, C. Ciuti, A. Bramati

Moreover, by using particular geometries of the photonic potential, the possibility of trapping and storing vortices in an all-optical way is also demonstrated.

These observations confirm that polariton condensates are an alternative to ultra-cold atoms for the study of hydrodynamic turbulence effects in new regimes, and using solid-state samples that are operational up to room temperature. The all-optical control and trapping of vortices set the basis for the study of optical vortex lattices and their excitations.

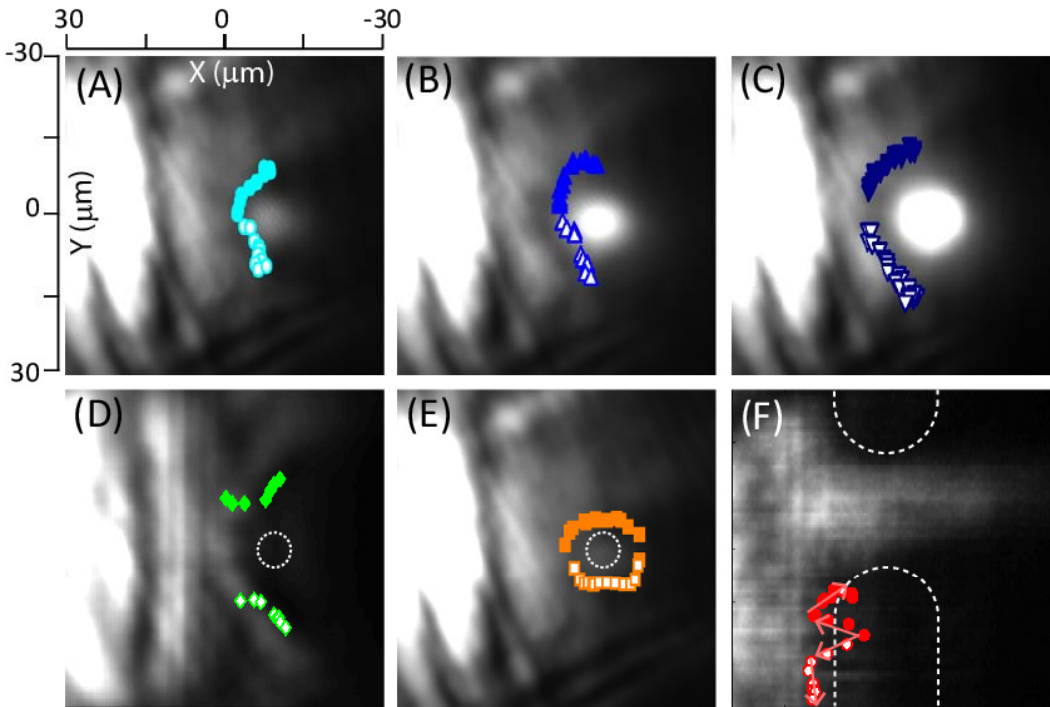


Figure 1.

Time-integrated real space emission patterns and corresponding vortex trajectories for different parameters of the injection density, barrier shape and depth. Vortex trajectories are from left to right. (A-C) show the effect of increasing the defect size while in (D) the polariton density is increased. In (E) the optical defect is shaped into a barrier with a 20 μm channel (boundaries shown by dotted lines). (F) shows the ultra-short reversible excitation of a quantum fluid when the obstacle is very shallow.

Related publication *Persistent currents and quantized vortices in a polariton superfluid.* D. Sanvitto, F.M. Marchetti, M.H. Szymańska, G. Tosi, M. Baudisch, F.P. Laussy, D.N. Krizhanovskii, M.S. Skolnick, L. Marrucci, A. Lemaître, J. Bloch, C. Tejedor, and L. Viña, *Nature Phys.* **6**, 527 (2010).

Propagation of spin information and entangled states in supramolecular dimers

Unlike direct- and super-exchange, spin interactions between magnetic centers through long organic groups still remains largely unexploited. Aromatic organic linkers are suitable candidates to create local interactions, and have been studied in the '80s and '90s within the quest for room temperature metallorganic magnets. Though the coupling between single paramagnetic ions had been already investigated in the literature, our challenge was to couple magnetically two (or more) complex molecules through heteroaromatic linkers without perturbing the properties of the individual units, and to achieve the propagation of the magnetic information at supramolecular (nanometer) scale. Furthermore, our aim was to understand how to achieve controlled switching of such interaction, acting on the atomic conformation of the linkers. The controlled introduction of exchange interactions between molecular building blocks represents a fundamental prerequisite for the investigation of inter-molecular correlations, and has allowed the experimental detection of entanglement between two heterometallic rings. Besides, it also represents a cornerstone of quantum-information processing based on the use of molecular spin-cluster qubits. In this perspective, we have recently developed a scheme for simulating a wide class of correlated quantum systems with translational invariance through ordered arrays of molecular spins, manipulated by means of spatially homogeneous fields.

The analysis by means of atomistic DFT and microSQUID magnetization experiments of a series of Cr₇Ni dimers, with general formula $[(Cr_7NiF_3(Etglu)(O_2C^iBu)_{16})_2L]$, with L being the heteroaromatic linker (see Fig. 1 for a sketch of the molecular structures of dimers), leads to the following conclusions:

- An alternation of spin polarization of the π orbitals when moving from one atom to the next, following bond paths, is present in all the linkers. Destructive interference between paths containing odd and even numbers of C/N atoms, leads to a very low spin-polarization of the orbitals in the inner region of the bipz. Electronic conjugation becomes less efficient as the number of bonds increases; consequently, the spin polarization in the inner region of the linker is larger for pyr than for bipy or bipyet, and reduces still further in bipytz.

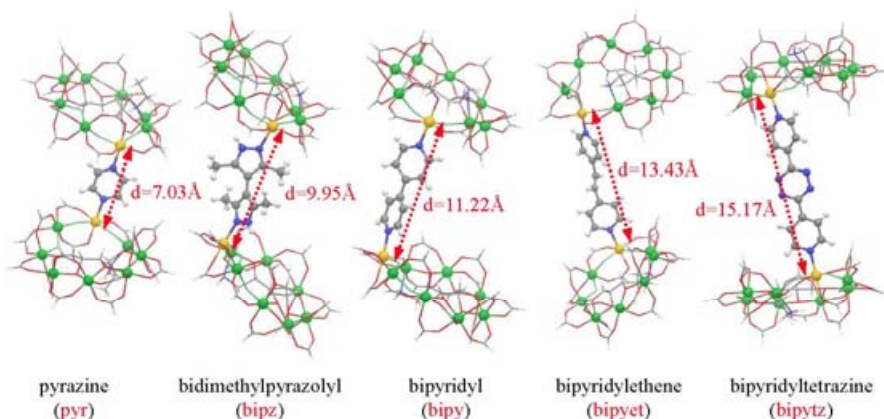


Figure 1. The molecular structures of Cr₇Ni dimers. The atoms of the linkers (N, blue; C, gray; H, white) and the metal ions in the rings (Ni, yellow; Cr, green) are highlighted; the inter-rings through-space Ni-Ni distances (d) are also given for each dimer.

Contact Person Valerio Bellini (valerio.bellini@nano.cnr.it)

Collaborators F. Troiani, A. Candini, G. Lorusso, M. Affronte, R.E.P. Winpenny, G.A. Timco, S. Carretta, P. Santini, G. Amoretti, W. Wernsdorfer

More quantitative indications can be extracted by mapping total energy calculations of different broken-symmetry spin configurations onto a microscopic spin Hamiltonian containing isotropic Heisenberg J exchange interactions between the Ni spin moments. The calculated J values are 367, 8, 48, 56 and 22 μeV for pyr, bipz, bipy, bipyet, and bipytz, respectively. The trend in the calculated J_s is fully supported by low-temperature microSQUID magnetization measurements.

- Maximum magnetic coupling would be achieved when the two cycles in the linker are coplanar, and overlap between π orbitals, and consequently conjugation, is at its maximum (see Fig. 2 B)). The variation of J as a function of the dihedral angle θ_d between the two cycles follows closely a $\cos^2\theta_d$ curve; interestingly enough, a similar behavior has been observed for the conductance through biphenyl junctions [*Nature* **442**, 904 (2006)]. Tuning of the spin propagation via the modification of θ_d , has been recently demonstrated experimentally.

- The control of intermolecular exchange between pairs of heterometallic rings can be exploited in order to observe quantum entanglement between complex molecules and to manipulate quantum information encoded in molecular spin-cluster qubits. In the first case, an antiferromagnetic coupling J between two heterometallic rings has allowed to detect equilibrium-state entanglement between them, through the use of magnetic susceptibility as an entanglement witness.

Here, the required J (about 40 mK) was smaller than the exchange coupling between ions within each ring but larger than the temperature at which the susceptibility measurements could be performed. The fine tuning of intermolecular exchange interactions can also represent a crucial resource in quantum simulation based on the use of molecular spin qubits. In particular, we have recently developed a scheme for simulating prototypical quantum Hamiltonians with translational invariance in arrays of molecular qubits, manipulated by means of spatially homogeneous fields. In the proposed scheme, the magnetic molecules play two distinct roles: (effective) two-level systems are used to encode the qubits; dimers (or oligomers) mediate the coupling between the qubits, and allow to switch it on and off if suitably driven from a non-magnetic to a magnetic state, or viceversa.

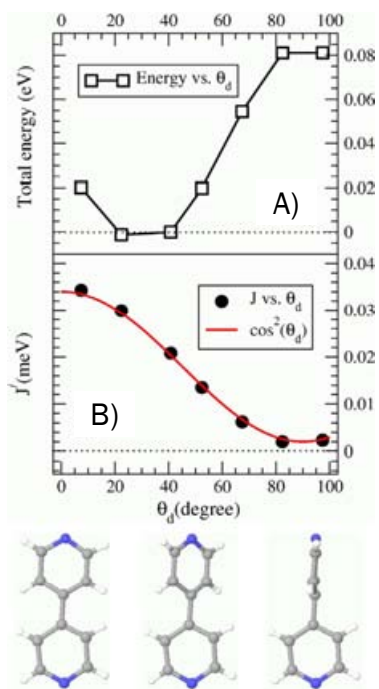


Figure 2.

A) Total energy and B) exchange interaction parameter J in the bipy-linked dimers, as a function of the dihedral angle θ_d between the two pyridine cycles.

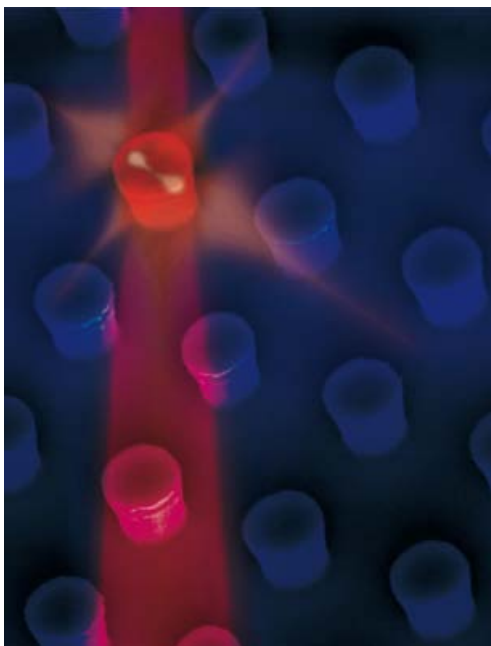
Related publications *Spin entanglement in supramolecular structures.* F. Troiani, V. Bellini, A. Candini, G. Lorusso, and M. Affronte, *Nanotechnology* **21**, 274009 (2010).

Propagation of spin information at supra-molecular scale through hetero-aromatic linkers. V. Bellini, G. Lorusso, A. Candini, W. Wernsdorfer, T.B. Faust, G.A. Timco, R.E.P. Winpenny, and M. Affronte, *Phys. Rev. Lett.* **106**, 227205 (2011).

Building an electron dimer molecule with light

We measure the quantum state of two electrons inside a semiconductor quantum dot in which the number of confined electrons is tuned by optical illumination. The two interacting electrons form a molecular dimer – similar to a diatomic molecule – and hence vibrate at the frequencies of the normal modes of the molecule. By comparing the spectrum of light scattered by the electrons with that predicted by exact-diagonalization calculations, we identify the breathing mode of the molecular dimer.

Two electrons have been trapped within an area of a few nanometers inside a semiconducting crystal nanostructure – a quantum dot. We measured for the first time their peculiar quantum state, which is known as an ‘electron molecule’ being very similar to that of a diatomic molecule.



This result has been obtained by employing a new technique to control the number of electrons in the quantum dot: one may add or remove electrons one by one from this ‘nano-trap’ by shining light on it by means of a laser beam (see Fig. 1 for a pictorial representation). Such precise method has made it possible to single out just two electrons as well as to measure the energy of their excitations. Theoretical calculations have clarified that the motion of the two electrons inside the dot has a vibrational character, being analogous to the one observed for the atoms of a diatomic molecule.

Figure 1.

Pictorial representation of the experiment: The frequencies of the vibrations of an electron molecule inside a quantum dot are measured by shining laser light on the dot and then collecting the scattered light. The number of electrons inside the quantum dot is controlled by tuning the intensity of a second independent laser beam.

Contact Person Massimo Rontani (massimo.rontani@nano.cnr.it)

Collaborators A. Singha, V. Pellegrini, A. Pinczuk, L.N. Pfeiffer, K.W. West

Electrons confined in quantum dots are important candidates for quantum computation: one challenge we face is their precise manipulation. Usually this is achieved by electrical control. However, in order to attach electric contacts to the quantum dot, one has to cover the crystal nanostructure with metallic layers. The technique we used has the same ability to inject single electrons but it is not invasive. In fact, manipulation by means of light does not affect the crystalline structure, allowing for the study of the inherent properties of the electrons inside the dot (Fig. 2). In contrast to previous optical experiments, it is now possible to consider the most simple interacting system, which is made of two electrons.

The electron molecule state was theoretically predicted but never directly measured so far. The motion of the electrons is ruled by the competition between two opposite effects: the repulsion between electric charges tends to keep electrons far apart whereas the quantum confinement of the nanostructure tends to make them stay close. The overall result is that the two electrons oscillate in a classical vibrational motion, as if they were connected by a spring. This study is the first measure of the fundamental frequency of the vibrational mode of the electron molecule.

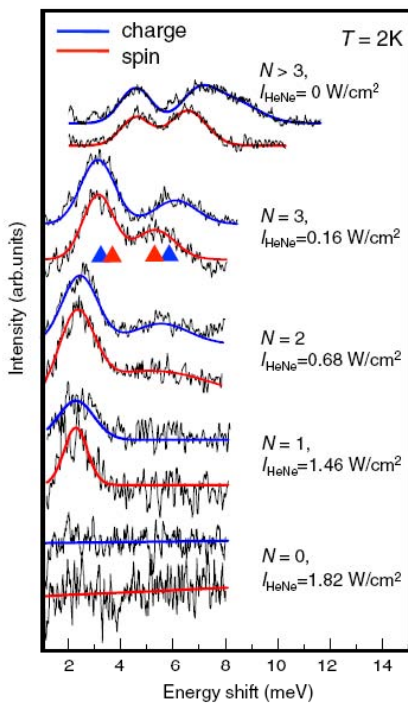
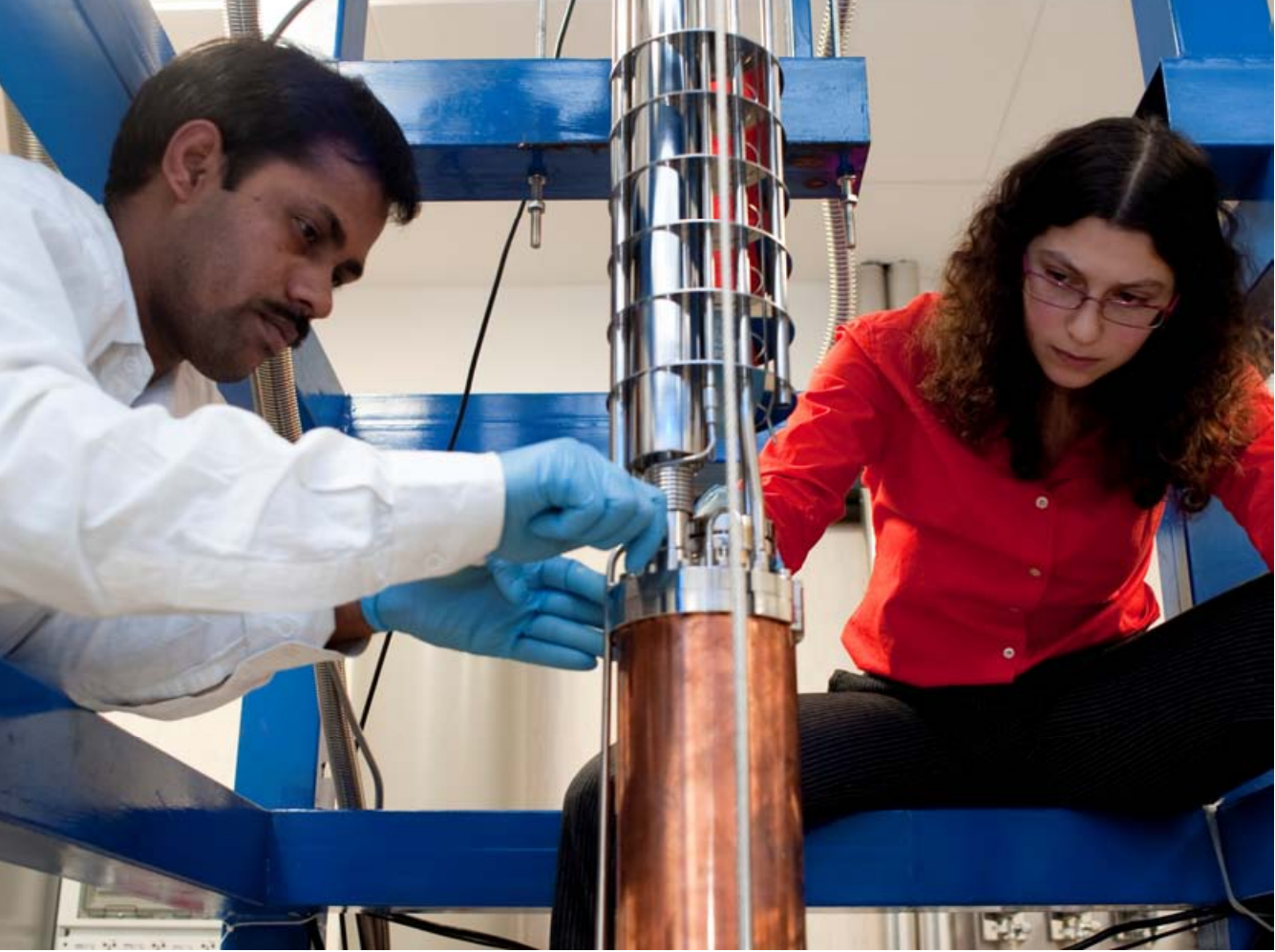


Figure 2.

Measured intensity of the light beam scattered by the quantum dots at frequencies (photon energies) different from those of the incoming laser beam. The experiment is performed at low temperature (2 Kelvin) to resolve the quantum states of the dot. The position of the peaks of the spectrum on the energy axis is a direct measure of the excitation energy of the vibrational modes of the electrons inside the dot. By varying the intensity of a second laser beam (labeled I_{HeNe}) one changes the average number N of electrons in the quantum dot. Blue and red curves point to different polarizations of collected light beams.

Related publication *Correlated electrons in optically tunable quantum dots: Building an electron dimer molecule.* A. Singha, V. Pellegrini, A. Pinczuk, L.N. Pfeiffer, K.W. West, and M. Rontani, *Phys. Rev. Lett.* **104**, 246802 (2010).



Equipment

The most advanced laboratory equipment for nano-fabrication and investigation of materials and devices at the nanoscale is available at the CnrNano centers, well-known for their strong tradition and expertise in experimental physics.

Laboratories in Modena, in particular, focus on micro- and nano-fabrication. Among their main set-ups, we point out electron microscopies with ion/electron beam lithography (FIB-SEM dual beam), scanning probe microscopies operating in different environments, laser tweezers, instrumentation for electron spectroscopies and microscopies of surfaces, cryo-magnetic facilities for transport studies, a tribology facility for the measurements of friction properties from the nano- to the microscale, and a cluster for scientific computation.

Facilities in Lecce include: labs for the growth of inorganic semiconductors (MBE, MOCVD and sputtering) and for the deposition of organics; nanofabrication lines (EBL, ICP-RIE, mask aligners/generator, soft lithography and nano-imprinting); characterization equipment, with an XRD, a SEM-FEG with an EDXS sensor, 6 AFMs, a UHV-STM, and a novel system combining AFM, confocal and TIRF microscopy; chemistry labs, for the synthesis and characterization of colloidal nanocrystals and organics; biotechnology labs, for bacterial and animal cell culture, and biochemistry/molecular biology; a high performance computing facility with servers and clusters for 4 Tflops.

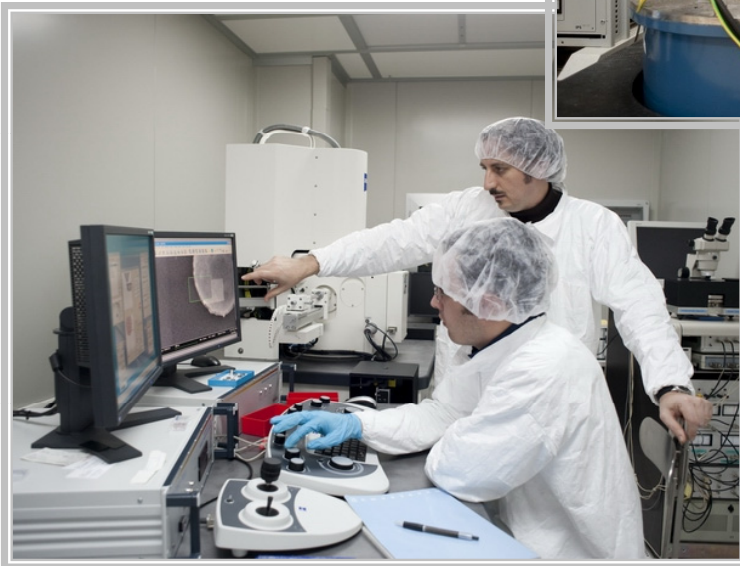
The laboratories in Pisa are characterized by several up-to-date facilities for device fabrication and advanced analysis (photo-I-V, C-V, spatially resolved optical analysis, FTIR, Raman, UHV-STM) in a broad range of experimental conditions (temperatures down to 10mK, magnetic fields up to 16T, laser sources from the ultra-violet to the far-infrared). Dilution fridges for magneto-optical studies at ultralow temperatures as well as CVD and CBE growth systems and low-temperature scanning probe facilities are also available.

Equipment



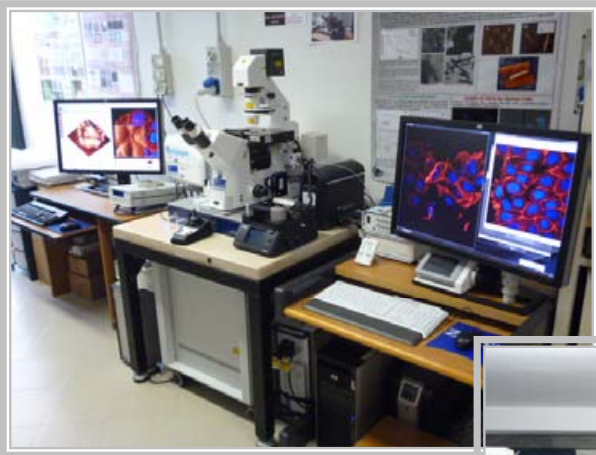
Chemical Beam Epitaxy facility dedicated to the growth of semiconductor nanowires.

Magneto-transport measurement equipment operating at 300mK and 12 Tesla.



Scanning Electron Microscope employed for imaging and electron beam lithography.

Equipment



CAT: a novel system combining AFM and optical (combined confocal and TIRF) microscopy.

Spatial and time-resolved optical set-up for photon emission and correlation measurements in the picosecond regime.



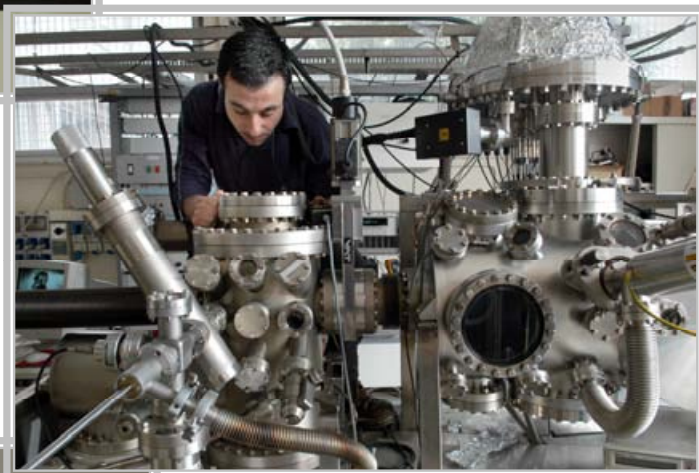
A multi-chamber cluster tool for the deposition of organic materials.

Equipment



EBL system based on a field emission SEM (Zeiss SIGMA) controlled by a Raith ELPHY Quantum pattern generator.

UHV system for the self-assembled growth of molecules on surfaces, equipped with XPS, LEED and HR-EELS characterization tools.



Dual beam FIB-SEM instrument (FEI STRATA DB235M) used for nanofabrication by FIB nanomachining and by electron and ion beam-induced deposition of conductive, insulating and magnetic materials from gas precursors.



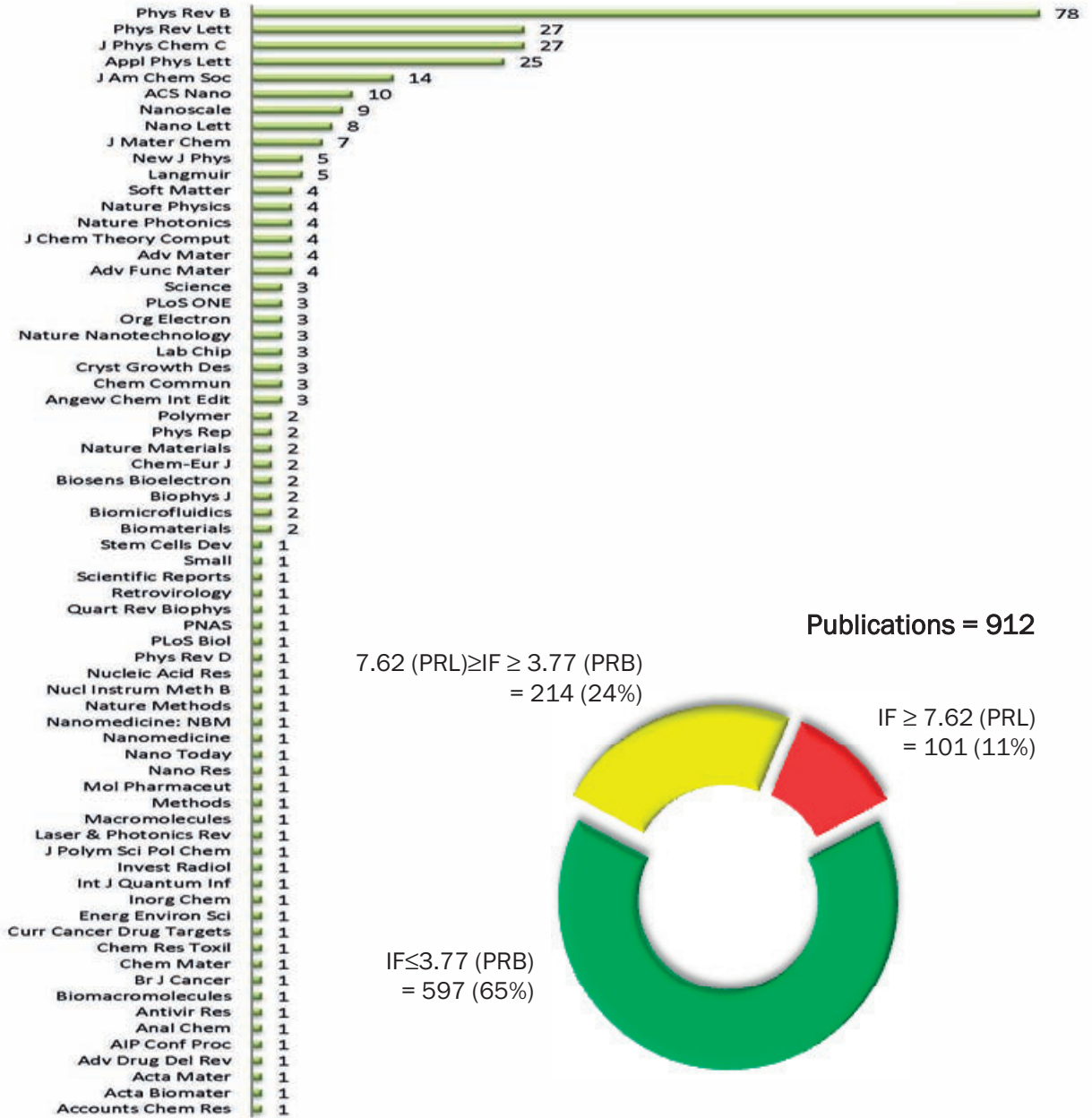
Publications

Publications

Details about the CnrNano publications are given as follows:

- the bar chart shows the number of publications in journals with Impact Factor ≥ 3.77 (*Physical Review B*'s JCR Impact Factor in 2010) according to their decreasing number;
- the ring chart represents the total number of publications sorted according to their impact factor. In elaborating our data, we chose two benchmarks: *Physical Review Letters*'s JCR impact factor in 2010 (7.62) and *Physical Review B*'s JCR impact factor in 2010 (3.77).

Publications by journals

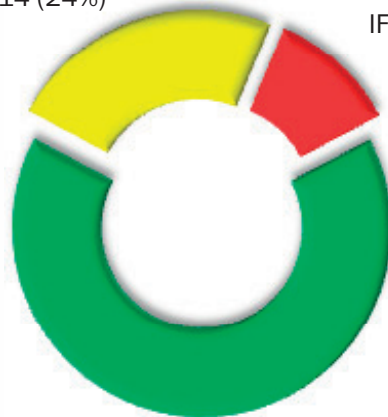


Publications = 912

$7.62 \text{ (PRL)} \geq \text{IF} \geq 3.77 \text{ (PRB)}$
= 214 (24%)

$\text{IF} \geq 7.62 \text{ (PRL)}$
= 101 (11%)

$\text{IF} \leq 3.77 \text{ (PRB)}$
= 597 (65%)



A list of publications from journals with $IF \geq 7.62$ (i.e., *Physical Review Letters*'s) ordered by their JCR 2010 IF is given.

A full and updated list of publications is available on the Institute website: <http://www.nano.cnr.it/> at the page "Publications".

Observation of plasmarons in quasi-freestanding doped graphene.

A. Bostwick, F. Speck, T. Seyller, K. Horn, M. Polini, R. Asgari, A.H. MacDonald, and E. Rotenberg. *Science* 328, 999 (2010).

Electron diffractive imaging of oxygen atoms in nanocrystals at sub-angstrom resolution.

L. De Caro, E. Carlino, G. Caputo, P.D. Cozzoli, and C. Giannini. *Nat Nanotechnol* 5, 360 (2010).

Highly conductive self-assembled nanoribbons of coordination polymers.

L. Welte, A. Calzolari, R. Di Felice, F. Zamora, and J. Gomez-Herrero. *Nat Nanotechnol* 5, 110 (2010).

Ballistic nanofriction.

R. Guerra, U. Tartaglino, A. Vanossi, and E. Tosatti. *Nat Mater* 9, 634 (2010).

Quasi-periodic distributed feedback laser.

L. Mahler, A. Tredicucci, F. Beltram, C. Walther, J. Faist, H.E. Beere, D.A. Ritchie, and D.S. Wiersma. *Nat Photonics* 4, 165 (2010).

Laser cooling of solids to cryogenic temperatures.

D.V. Seletskiy, S.D. Melgaard, S. Bigotta, A. Di Lieto, M. Tonelli, and M. Sheik-Bahae. *Nat Photonics* 4, 161 (2010).

Multiscale Modeling of Proteins.

V. Tozzini. *Accounts Chem Res* 43, 220 (2010).

Simultaneous intracellular chloride and pH measurements using a GFP-based sensor.

D. Arosio, F. Ricci, L. Marchetti, R. Gualdani, L. Albertazzi, and F. Beltram. *Nat Methods* 7, 516-U44 (2010).

Superconducting quantum interference proximity transistor.

F. Giazotto, J.T. Peltonen, M. Meschke, and J.P. Pekola. *Nat Phys* 6, 254 (2010).

Correlation-induced single-flux-quantum penetration in quantum rings.

A.J.M. Giesbers, U. Zeitler, M.I. Katsnelson, D. Reuter, A.D. Wieck, G. Biasiol, L. Sorba, and J.C. Maan. *Nat Phys* 6, 173 (2010).

An excitatory loop with astrocytes contributes to drive neurons to seizure threshold.

M. Gómez-Gonzalo, G. Losi, A. Chiavegato, M. Zonta, M. Cammarota, M. Brondi, F. Vetri, L. Uva, T. Pozzan, M. de Curtis, G.M. Ratto, and G. Carmignoto. *PLoS Biol* 8, e1000352 (2010).

Assembly of Colloidal Semiconductor Nanorods in Solution by Depletion Attraction.

D. Baranov, A. Fiore, M. van Huis, C. Giannini, A. Falqui, U. Lafont, H. Zandbergen, M. Zanella, R. Cingolani, and L. Manna. *Nano Lett* 10, 743 (2010).

Colloidal heterostructured nanocrystals: Synthesis and growth mechanisms.

L. Carbone and P.D. Cozzoli. *Nano Today* 5, 449 (2010).

Minimalist models for proteins: a comparative analysis.

V. Tozzini. *Quart Rev Biophys* 43, 333 (2010).

Shaping White Light Through Electroluminescent Fully Organic Coupled Microcavities.

M. Mazzeo, F. Della Sala, F. Mariano, G. Melcarne, S. D'Agostino, Y. Duan, R. Cingolani, and G. Gigli. *Adv Mater* 22, 4696 (2010).

Active Role of Oxide Layers on the Polarization of Plasmonic Nanostructures.
S. D'Agostino and F. Della Sala. *ACS Nano* 4, 4117 (2010).

Dynamical Formation of Spatially Localized Arrays of Aligned Nanowires in Plastic Films with Magnetic Anisotropy.

D. Fragouli, R. Buonsanti, G. Bertoni, C. Sangregorio, C. Innocenti, A. Falqui, D. Gatteschi, P.D. Cozzoli, A. Athanassiou, and R. Cingolani. *ACS Nano* 4, 1873 (2010).

Surface-Enhanced Raman Signal for Terbium Single-Molecule Magnets Grafted on Graphene.

M. Lopes, A. Candini, M. Urdampilleta, A. Reserbat-Plantey, V. Bellini, S. Klyatskaya, L. Marty, M. Ruben, M. Affronte, W. Wernsdorfer, and N. Bendiab. *ACS Nano* 4, 7531-7537 (2010).

Photoconduction properties in aligned assemblies of colloidal CdSe/CdS nanorods.

A. Persano, M. De Giorgi, A. Fiore, R. Cingolani, L. Manna, A. Cola, and R. Krahne. *ACS Nano* 4, 1646 (2010).

Surface effects on the atomic and electronic structure of unpassivated GaAs nanowires.

M. Rosini and R. Magri. *ACS Nano* 4, 6021 (2010).

Onset of frictional slip by domain nucleation in adsorbed monolayers.

M. Reguzzoni, M. Ferrario, S. Zapperi, and M.C. Righi. *PNAS* 107, 1311 (2010).

Delivery and Subcellular Targeting of Dendrimer-Based Fluorescent pH Sensors in Living Cells.

L. Albertazzi, B. Storti, L. Marchetti, and F. Beltram. *J Am Chem Soc* 132, 18158 (2010).

Single Amino Acid Replacement Makes *Aequorea victoria* Fluorescent Proteins Reversibly Photoswitchable.

R. Bizzarri, M. Serresi, F. Cardarelli, S. Abbruzzetti, B. Campanini, C. Viappiani, and F. Beltram. *J Am Chem Soc* 132, 85 (2010).

Architectural Control of Seeded-Grown Magnetic-Semiconductor Iron Oxide-TiO₂ Nanorod Heterostructures: The Role of Seeds in Topology Selection.

R. Buonsanti, V. Grillo, E. Carlino, C. Giannini, F. Gozzo, M. Garcia-Hernandez, A.M. Garcia, R. Cingolani, and P.D. Cozzoli. *J Am Chem Soc* 132, 2437 (2010).

Hydroxyl-Rich beta-Sheet Adhesion to the Gold Surface in Water by First-Principle Simulations.

A. Calzolari, G. Cicero, C. Cavazzoni, R. Di Felice, A. Catellani, and S. Corni. *J Am Chem Soc* 132, 4790 (2010).

Polarity-Sensitive Coumarins Tailored to Live Cell Imaging.

G. Signore, R. Nifosi, L. Albertazzi, B. Storti, and R. Bizzarri. *J Am Chem Soc* 132, 1276 (2010).

An Electrochemical Scanning Tunneling Microscopy Study of 2-(6-Mercaptoalkyl)hydroquinone Molecules on Au(111).

P. Petrangolini, A. Alessandrini, L. Berti, and P. Facci. *J Am Chem Soc* 132, 7445 (2010).

Deposition of functionalized Cr₇Ni molecular rings on graphite by liquid phase.

A. Ghirri, V. Corradini, C. Cervetti, A. Candini, U. del Pennino, G. Timco, R.J. Pritchard, C.A. Muryn, R.E.P. Winpenney, and M. Affronte. *Adv Funct Mater* 20, 1552 (2010).

Conductive nanostructures of MMX chains.

A. Guijarro, O. Castillo, L. Welte, A. Calzolari, P. J. Sanz Miguel, C. J. Gómez-García, D. Olea, R. Di Felice, J. Gómez-Herrero, and F. Zamora. *Adv Funct Mater* 20, 1451 (2010).

Neuronal polarity selection by topography-induced focal adhesion control.

A. Ferrari, M. Cecchini, M. Serresi, P. Faraci, D. Pisignano, and F. Beltram. *Biomaterials* 31, 4682 (2010).

The effect of alternative neuronal differentiation pathways on PC12 cell adhesion and neurite alignment to nanogratings.

A. Ferrari, P. Faraci, M. Cecchini, and F. Beltram. *Biomaterials* 31, 2565 (2010).

Homeotic proteins participate in the function of human-DNA replication origins.

L. Marchetti, L. Comelli, B. D'Innocenzo, L. Puzzi, S. Luin, D. Arosio, M. Calvello, R. Mendoza-Maldonado, F. Peverali, F. Trovato, S. Riva, G. Biamonti, G. Abdurashidova, F. Beltram, and A. Falaschi. *Nucleic Acids Res* 38, 8105 (2010).

Entanglement in supramolecular spin systems of two weakly coupled antiferromagnetic rings (purple Cr_7Ni).
A. Candini, G. Lorusso, F. Troiani, A. Ghirri, S. Carretta, P. Santini, G. Amoretti, C. Muryn, F. Tuna, G. Timco, E.J.L. McInnes, R.E.P. Winpenny, W. Wernsdorfer, and M. Affronte. *Phys Rev Lett* 104, 037203 (2010).

Teleportation-Induced Correlated Quantum Channels.
F. Caruso, V. Giovannetti, and G.M. Palma. *Phys Rev Lett* 104, 020503 (2010).

Dynamical phase transitions and instabilities in open atomic many-body systems.
S. Diehl, A. Tomadin, A. Micheli, R. Fazio, and P. Zoller. *Phys Rev Lett* 105, 015702 (2010).

Blockade and counterflow supercurrent in exciton-condensate Josephson junctions.
F. Dolcini, D. Rainis, F. Taddei, M. Polini, R. Fazio, and A.H. MacDonald. *Phys Rev Lett* 104, 027004 (2010).

Spin drag in an ultracold Fermi gas on the verge of a ferromagnetic instability.
R.A. Duine, M. Polini, H.T.C. Stoof, and G. Vignale. *Phys Rev Lett* 104, 220403 (2010).

Origin of Friction Anisotropy on a Quasicrystal Surface.
A.E. Filippov, A. Vanossi, and M. Urbakh. *Phys Rev Lett* 104, 074302 (2010).

Spontaneous Formation of Surface Antisite Defects in the Stabilization of the Sb-Rich GaSb(001) Surface.
C. Hogan, R. Magri, and R. Del Sole. *Phys Rev Lett* 104, 157402 (2010).

Capacities of Lossy Bosonic Memory Channels.
C. Lupo, V. Giovannetti, and S. Mancini. *Phys Rev Lett* 104, 030501 (2010).

Charged Oxygen Defects in SiO₂: Going beyond Local and Semilocal Approximations to Density Functional Theory.
L. Martin-Samos, G. Roma, P. Rinke, and Y. Limoge. *Phys Rev Lett* 104, 075502 (2010).

Cold-Atom-Induced Control of an Optomechanical Device.
M. Paternostro, G. De Chiara, and G.M. Palma. *Phys Rev Lett* 104, 243602 (2010).

Many-body orbital paramagnetism in doped graphene sheets.
A. Principi, M. Polini, G. Vignale, and M.I. Katsnelson. *Phys Rev Lett* 104, 225503 (2010).

Correlated electrons in optically-tunable quantum dots: Building an electron dimer molecule.
A. Singha, V. Pellegrini, A. Pinczuk, L.N. Pfeiffer, K.W. West, and M. Rontani. *Phys Rev Lett* 104, 246802 (2010).

Coherent detection of electron dephasing.
E. Strambini, L. Chirolli, V. Giovannetti, F. Taddei, R. Fazio, V. Piazza, and F. Beltram. *Phys Rev Lett* 104, 170403 (2010).

Observation of magnetophonon resonance of dirac fermions in graphite.
J. Yan, S. Goler, T.D. Rhone, M. Han, R. He, P. Kim, V. Pellegrini, and A. Pinczuk. *Phys Rev Lett* 105, 227401 (2010).

- Polariton Superfluids Reveal Quantum Hydrodynamic Solitons.
A. Amo, S. Pigeon, D. Sanvitto, V.G. Sala, R. Hivet, I. Carusotto, F. Pisanello, G. Leménager, R. Houdré, E. Giacobino, C. Ciuti, and A. Bramati. *Science* 332, 1167 (2011).
- Two-Dimensional Mott-Hubbard Electrons in an Artificial Honeycomb Lattice.
A. Singha, M. Gibertini, B. Karmakar, S. Yuan, M. Polini, G. Vignale, M.I. Katsnelson, A. Pinczuk, L.N. Pfeiffer, K.W. West, and V. Pellegrini. *Science* 332, 1176 (2011).
- Direct observation of a propagating spin wave induced by spin-transfer torque.
M. Madami, S. Bonetti, G. Consolo, S. Tacchi, G. Carlotti, G. Gubbiotti, F.B. Mancoff, M.A. Yar, and J. Akerman. *Nat Nanotechnol* 6, 635 (2011).
- ARTIFICIAL ATOMS Shape the wave.
M. Rontani. *Nat Mater* 10, 173 (2011).
- Molecular Spins for Quantum Information Technologies.
F. Troiani and M. Affronte. *Chem Soc Rev* 40, 3119 (2011).
- Advances in quantum metrology.
V. Giovannetti, S. Lloyd, and L. Maccone. *Nat Photonics* 5, 222 (2011).
- All-optical control of the quantum flow of a polariton condensate.
D. Sanvitto, S. Pigeon, A. Amo, D. Ballarini, M. De Giorgi, I. Carusotto, R. Hivet, F. Pisanello, V.G. Sala, P.S.S. Guimaraes, R. Houdre, E. Giacobino, C. Ciuti, A. Bramati, and G. Gigli. *Nat Photonics* 5, 610 (2011).
- Compositional mapping of semiconductor quantum dots and rings.
G. Biasiol and S. Heun. *Phys Rep* 500, 117 (2011).
- Physical properties of elongated inorganic nanoparticles.
R. Krahne, G. Morello, A. Figuerola, C. George, S. Deka, and L. Manna. *Phys Rep* 501, 75 (2011).
- A Josephson quantum electron pump.
F. Giazotto, P. Spathis, S. Roddaro, S. Biswas, F. Taddei, M. Governale, and L. Sorba. *Nat Phys* 7, 857 (2011).
- Quantum Metrology: Beauty and the noisy beast.
L. Maccone and V. Giovannetti. *Nat Phys* 7, 376 (2011).
- Drug-loaded polyelectrolyte microcapsules for sustained targeting of cancer cells
V. Vergaro, F. Scarlino, C. Bellomo, R. Rinaldi, D. Vergara, M. Maffia, F. Baldassarre, G. Giannelli, X.C. Zhang, Y.M. Lvov, and S. Leporatti. *Adv Drug Del Rev* 63, 847 (2011).
- Single-Molecule-Level Evidence for the Osmophobic Effect.
D. Aioanei, S. Lv, I. Tessari, A. Rampion, L. Bubacco, H. Li, B. Samorì, and M. Brucale. *Angew Chem Int Edit* 50, 4394 (2011).
- Multifunctional Trackable Dendritic Scaffolds and Delivery Agents.
R.J. Amir, L. Albertazzi, J. Willis, A. Khan, T. Kang, and C.J. Hawker. *Angew Chem Int Edit* 50, 3425 (2011).
- Microwave-Assisted Synthesis of Colloidal Inorganic Nanocrystals.
M. Baghbanzadeh, L. Carbone, P.D. Cozzoli, and C.O. Kappe. *Angew Chem Int Edit* 50, 11312 (2011).
- Band-Offset Driven Efficiency of the Doping of SiGe Core-Shell Nanowires.
M. Amato, S. Ossicini, and R. Rurali. *Nano Lett* 11, 594 (2011).
- Nanotopographic Control of Neuronal Polarity.
A. Ferrari, M. Cecchini, A. Dhawan, S. Micera, I. Tonazzini, R. Stabile, D. Pisignano, and F. Beltram. *Nano Lett* 11, 505 (2011).
- Manipulation of Electron Orbitals in Hard-Wall InAs/InP Nanowire Quantum Dots.
S. Roddaro, A. Pescaglioni, D. Ercolani, L. Sorba, and F. Beltram. *Nano Lett* 11, 1695 (2011).

Graphene Spintronic Devices with Molecular Nanomagnets.

A. Candini, S. Klyatskaya, M. Ruben, W. Wernsdorfer, and M. Affronte. *Nano Lett* 11, 2634 (2011).

Unit Cell Structure of Crystal Polytypes in InAs and InSb Nanowires.

D. Kriegner, C. Panse, B. Mandl, K.A. Dick, M. Keplinger, J.M. Persson, P. Caroff, D. Ercolani, L. Sorba, F. Bechstedt, J. Stangl, and G. Bauer. *Nano Lett* 11, 1483 (2011).

"Nanohybrids" Based on pH-Responsive Hydrogels and Inorganic Nanoparticles for Drug Delivery and Sensor Applications.

A. Riedinger, M. Pernia Leal, S.R. Deka, C. George, I.R. Franchini, A. Falqui, R. Cingolani, and T. Pellegrino. *Nano Lett* 11, 3136 (2011).

Peptide Synthesis of Gold Nanoparticles: The Early Steps of Gold Reduction Investigated by Density Functional Theory.

D. Toroz and S. Corni. *Nano Lett* 11, 1313 (2011).

Magnetic Nanocarriers with Tunable pH Dependency for Controlled Loading and Release of Cationic and Anionic Payloads.

N.C. Bigall, A. Curcio, M. Pernia Leal, A. Falqui, D. Palumberi, R. Di Corato, E. Albanesi, R. Cingolani, and T. Pellegrino. *Adv Mater* 23, 5645 (2011).

Biosilica electrically-insulating layers by soft lithography-assisted biomineralisation with recombinant silicatein.

A. Polini, S. Pagliara, A. Camposeo, A. Biasco, H.C. Schröder, W.E.G. Müller, and D. Pisignano. *Adv Mater* 23, 4674 (2011).

Evidence of gap modulation in DNA by complexation with metal ions.

E. Shapir, A.B. Kotlyar, G. Brancolini, R. Di Felice, and D. Porath. *Adv Mater* 23, 4290 (2011).

Multiplexed Sensing of Ions with Barcoded Polyelectrolyte Capsules.

L.L. del Mercato, A.Z. Abbasi, M. Ochs, and W.J. Parak. *ACS Nano* 5, 9668 (2011).

Multifunctional Nanobeads Based on Quantum Dots and Magnetic Nanoparticles: Synthesis and Cancer Cell Targeting and Sorting.

R. Di Corato, N.C. Bigall, A. Ragusa, D. Dorfs, A. Genovese, R. Marotta, L. Manna, and T. Pellegrino. *ACS Nano* 5, 1109 (2011).

Self-Assembled Monolayer of Cr₇Ni Molecular Nanomagnets by Sublimation.

A. Ghirri, V. Corradini, V. Bellini, R. Biagi, U. del Pennino, V. De Renzi, J.C. Cezar, C.A. Muryn, G.A. Timco, R.E.P. Winpenny, and M. Affronte. *ACS Nano* 5, 7090 (2011).

Tunneling magnetoresistance with sign inversion in junctions based on iron oxide nanocrystal superlattices.

C.I. Lekshmi, R. Buonsanti, C. Nobile, P.D. Cozzoli, R. Rinaldi, and G. Maruccio. *ACS Nano* 5, 1731 (2011).

Probing the Gate-Voltage-Dependent Surface Potential of Individual InAs Nanowires Using Random Telegraph Signals.

J. Salfi, N. Paradiso, S. Roddaro, S. Heun, S.V. Nair, I.G. Savelyev, M. Blumin, F. Beltram, and H.E. Ruda. *ACS Nano* 5, 2191 (2011).

The absorption properties of metal-semiconductor hybrid nanoparticles.

E. Shaviv, O. Schubert, M. Alves dos Santos, G. Goldoni, R. Di Felice, F. Vallée, N. Del Fatti, U. Banin, and C. Soennichsen. *ACS Nano* 5, 4712 (2011).

Highly efficient smart photovoltachromic devices with tailored electrolyte composition.

A. Cannavale, M. Manca, F. Malara, L. De Marco, R. Cingolani, and G. Gigli. *Energ Environ Sci* 7, 2567 (2011).

Photonic engineering of surface-emitting terahertz quantum cascade lasers.

L. Mahler and A. Tredicucci. *Laser & Photonics Rev* 5, 647 (2011).

- Hyperbranched TiO₂ Nanocrystals: Nonhydrolytic Synthesis, Growth Mechanism and Exploitation in Dye-Sensitized Solar Cells.
R. Buonsanti, E. Carlino, C. Giannini, D. Altamura, L. De Marco, R. Giannuzzi, M. Manca, G. Gigli, and P.D. Cozzoli. *J Am Chem Soc* 133, 19216 (2011).
- Anchor Group versus Conjugation: Toward the Gap-State Engineering of Functionalized ZnO(10-10) Surface for Optoelectronic Applications.
A. Calzolari, A. Ruini, and A. Catellani. *J Am Chem Soc* 133, 5893 (2011).
- A successful chemical strategy to induce oligothiophene self-assembly into fibers with tunable shape and function.
F. Di Maria, P. Olivelli, M. Gazzano, A. Zanelli, M. Biasiucci, G. Gigli, D. Gentili, P. D'Angelo, M. Cavallini, and G. Barbarella. *J Am Chem Soc* 133, 8654 (2011).
- A Cast-Mold Approach to Iron Oxide and Pt/Iron Oxide Nanocontainers and Nanoparticles with a Reactive Concave Surface.
C. George, D. Dorfs, G. Bertoni, A. Falqui, A. Genovese, T. Pellegrino, A. Roig, A. Quarta, R. Comparelli, M.L. Curri, R. Cingolani, and L. Manna. *J Am Chem Soc* 133, 2205 (2011).
- Surface supramolecular organization of a terbium (III) double-decker complex on graphite and its single molecule magnet behavior.
M. Gonidec, R. Biagi, V. Corradini, F. Moro, V. De Renzi, U. del Pennino, D. Summa, L. Muccioli, C. Zannoni, D.B. Amabilino, and J. Veciana. *J Am Chem Soc* 133, 6603 (2011).
- Water-Dispersible Sugar-Coated Iron Oxide Nanoparticles. An Evaluation of their Relaxometric and Magnetic Hyperthermia Properties.
L. Lartigue, C. Innocenti, T. Kalaivani, A. Awwad, M. del Mar Sanchez Duque, Y. Guari, J. Larionova, C. Guerin, J.L.G. Montero, V. Barragan-Montero, P. Arosio, A. Lascialfari, D. Gatteschi, and C. Sangregorio. *J Am Chem Soc* 133, 10459 (2011).
- Dielectric and Thermal Effects on the Optical Properties of Natural Dyes: A Case Study on Solvated Cyanin.
O.B. Malcioglu, A. Calzolari, R. Gebauer, D. Varsano, and S. Baroni. *J Am Chem Soc* 133, 15425 (2011).
- Live-cell-permeant thiophene fluorophores and cell-mediated formation of fluorescent fibrils.
I.E. Palamà, F. Di Maria, I. Viola, E. Fabiano, G. Gigli, C. Bettini, and G. Barbarella. *J Am Chem Soc* 133, 17777 (2011).
- Magnetic/Silica Nanocomposites as Dual-Mode Contrast Agents for Combined Magnetic Resonance Imaging and Ultrasonography.
M.A. Malvindi, A. Greco, F. Conversano, A. Figuerola, M. Corti, M. Bonora, A. Lascialfari, H.A. Doumari, M. Moscardini, R. Cingolani, G. Gigli, S. Casciaro, T. Pellegrino, and A. Ragusa. *Adv Funct Mater* 21, 2548 (2011).
- Soft Nanolithography by Polymer Fibers.
D. Tu, S. Pagliara, A. Camposeo, G. Potente, E. Mele, R. Cingolani, and D. Pisignano. *Adv Funct Mater* 21, 1140 (2011).
- Motion of Spin Polariton Bullets in Semiconductor Microcavities.
C. Adrados, T.C.H. Liew, A. Amo, M.D. Martin, D. Sanvitto, C. Anton, E. Giacobino, A. Kavokin, A. Bramati, and L. Viña. *Phys Rev Lett* 107, 146402 (2011).
- Persistent Spin Oscillations in a Spin-Orbit-Coupled Superconductor.
A. Agarwal, M. Polini, R. Fazio, and G. Vignale. *Phys Rev Lett* 107, 077004 (2011).
- Propagation of spin information at supra-molecular scale through hetero-aromatic linkers.
V. Bellini, G. Lorusso, A. Candini, W. Wernsdorfer, T.B. Faust, G.A. Timco, R.E.P. Winpenny, and M. Affronte. *Phys Rev Lett* 106, 227205 (2011).
- Phonon-Mediated Coupling of InGaAs/GaAs Quantum-Dot Excitons to Photonic Crystal Cavities.
M. Calic, P. Gallo, M. Felici, K.A. Atlasov, B. Dwir, A. Rudra, G. Biasiol, L. Sorba, G. Tarel, V. Savona, and E. Kapon. *Phys Rev Lett* 106, 277402 (2011).

Semiclassical Neutral Atom as a Reference System in Density Functional Theory.

L.A. Constantin, E. Fabiano, S. Laricchia, and F. Della Sala. *Phys Rev Lett* 106, 186406 (2011).

Electrostatic-field-driven alignment of organic oligomers on ZnO surfaces.

F. Della Sala, S. Blumstengel, and F. Henneberger. *Phys Rev Lett* 107, 146401 (2011).

Energy transport by neutral collective excitations at the quantum Hall edge.

E.V. Deviatov, A. Lorke, G. Biasiol, and L. Sorba. *Phys Rev Lett* 106, 256802 (2011).

Controlled coupling of spin-resolved quantum Hall edge states.

B. Karmakar, D. Venturelli, L. Chirolli, F. Taddei, V. Giovannetti, R. Fazio, S. Roddaro, G. Biasiol, L. Sorba, V. Pellegrini, and F. Beltram. *Phys Rev Lett* 107, 236804 (2011).

Sequential Projective Measurements for Channel Decoding.

S. Lloyd, V. Giovannetti, and L. Maccone. *Phys Rev Lett* 106, 250501 (2011).

Closed Timelike Curves via Postselection: Theory and Experimental Test of Consistency.

S. Lloyd, L. Maccone, R. Garcia-Patron, V. Giovannetti, Y. Shikano, S. Pirandola, L. A. Rozema, A. Darabi, Y. Soudagar, L.K. Shalm, and A.M. Steinberg. *Phys Rev Lett* 106, 040403 (2011).

Molecular Nanomagnets as Quantum Simulators.

P. Santini, S. Carretta, F. Troiani, and G. Amoretti. *Phys Rev Lett* 107, 230502 (2011).

Onset and Dynamics of Vortex-Antivortex Pairs in Polariton Optical Parametric Oscillator Superfluids.

G. Tosi, F.M. Marchetti, D. Sanvitto, C. Anton, M.H. Szymanska, A. Berceanu, C. Tejedor, L. Marrucci, A. Lemaître, J. Bloch, and L. Viña. *Phys Rev Lett* 107, 036401 (2011).



Projects and Grants

Most of the research activity at CnrNano is supported by funding obtained through competitive calls, witnessing the prominent role of the Institute in the international scientific arena and the wide scope of our research. Details about projects running in 2010-2011 are given following this order: project name, type of call, coordinator, CnrNano principal investigator (these may coincide), start and ending dates, website (if available).

European Projects

NANOTAIL. Hybrid nanocrystals exhibiting advanced and tailored properties. FP6-MOBILITY1.3 Marie Curie Host Fellowships - Transfer of knowledge (TOK). Foundation for Research and Technology, GR (A. Lappas); CnrNano NNL (P.D. Cozzoli). 2006-2010. <http://www.iesl.forth.gr/programs/nanotail/>

PROETEX. Protection E-Textiles: micronanostructured fibre systems for emergency disaster wear. FP6-2004-IST-4-026987. CnrNano S3 (A. Bonfiglio). 2006-2010. <http://www.proetex.org/index.htm>

DNA-Nanodevices. ICT FET-Open, FP6-029192. Tel Aviv University, IL (A.B. Kotlyar); CnrNano S3 (R. Di Felice). 2006-2010.

Single NANO-HYBRID. Properties and optical response of single hybrid semiconductor-metal nanoparticles. European NanoSci-Era. Université Lyon 1 (F. Vallee); CnrNano S3 (R. Di Felice). 2007-2010. <http://www.uni-mainz.de/FB/Chemie/NanoSciEra/>

SPIDME. Spintronic Devices for Molecular Electronics. FP6-NEST NEST-2004-ADV. CnrNano NNL (G. Maruccio). 2006-2010. <http://spidme.nanophysics.it/public/>

DEDOM. Development of Density Functional Methods for Organic-Metal Interaction. ERC Starting Grant 2007. CnrNano NNL (F. Della Sala). 2008-2013. <http://www.theory-nnl.it/dedom/>

MOLSPINQIP. Molecular spin Clusters for Quantum Information Processes. ICT-2007.8.0 FET Open. CnrNano S3 (M. Affronte). 2008-2011. <http://www.molspinqip.org/>

NANOSCI-EPLUS. Transnational call for collaborative proposals in basic nanoscience research. FP7-NMP. Centre National de la Recherche Scientifique, FR (J.L. Robert); CnrNano (E. Molinari). 2008-2012.

ROC. Radiochemistry on chip. NMP-2007-3.2-2. CnrNano NNL (R. Rinaldi). 2008-2011. <http://www.roc-project.eu/site/>

SYSTEX. Platform for Smart Textiles and Wearable Microsystems. ICT-2007.3.6 Micro/nanosystems. Universiteit Gent, BE (L. Vanlangenhoven); CnrNano S3 (A. Bonfiglio). 2008-2010. <http://www.systemex.org/>

MaECENAS. Nanoscale Optical-to-Mechanical Energy Conversion: Coupling Nano-Object with Light Powered Molecular Lifters. European NanoSci-Era. University of Ferrara, IT (M.A. Rampi), CnrNano S3 (S. Corni). 2009-2012.

MAGNIFYCO. Magnetic nanocontainers for combined hyperthermia and controlled drug release. FP7-NMP-2008-1.1-1. CnrNano NNL (T. Pellegrino). 2009-2012. <http://www.magnifyco.eu/>

AFM4NanoMed&Bio. European network on applications of Atomic Force Microscopy to NanoMedicine and Life Sciences. COST Action TD1002. CNRS Marcoule, FR (P. Parot); CnrNano S3 (P. Facci). 2010-2014. <http://www.afm4nanomedbio.eu/home.aspx>

HY SUNLIGHT. Optical properties of Hybrid organic/inorganic nanoparticles for photovoltaic applications: toward a predictive computational approach. FP7-PEOPLE-2009-IIF. CnrNano S3 (G. Goldoni). 2010-2012.

INDEX. Indirect Excitons: Fundamental Physics and Applications. FP7-PEOPLE-2011-ITN. CNRS Montpellier, FR (M. Vladimirova); CnrNano S3 (M. Rontani). 2011-2014. <http://indexitn.ges.univ-montp2.fr/>

Q-NET. Quantum-Nano-Electronics Training. FP7-PEOPLE-2010-ITN. Université Joseph Fourier Grenoble 1, FR; CnrNano NEST (F. Giazotto). 2011-2015.

National Projects

Dalle molecole al comportamento: comprendere le basi neurobiologiche della plasticità e dell'apprendimento. FIRB 2004. CnrNano NNL (F. Calabi). 2006-2010.

ITALNANONET. FIRB 2006. Cnr-Instm (R. Psaro); CnrNano S3 (P. Facci); CnrNano NNL (G. Gigli); CnrNano NEST (R. Bizzarri). 2009-2012.

Fenomeni quantistici in punti quantici a semiconduttore. FIRB Italia/Canada 2007. CnrNano NEST (F. Beltram); CnrNano S3 (E. Molinari). 2007-2011.

Semiconduttori unidimensionali autoassemblati e loro applicazioni dispositivi. FIRB Italia/Canada 2007. CnrNano NEST (F. Beltram). 2007-2012.

Nanostrutture unidimensionali di semiconduttore e dispositivi microfluidici. FIRB 2005 Accordi Bilaterali Italia/USA. CnrNano NNL (D. Pisignano). 2006-2010.

IPERFREQUENZE. FIRB Idee progettuali 2006. Cnr-Imm (A. Siciliano); CnrNano NNL (A. Passaseo, M. De Vittorio). 2007-2010.

POLIFLEX. Display piatti e relativi componenti elettronici anche su supporto flessibile. FIRB 2006. CnrNano NNL (D. Pisignano). 2007-2011.

Bioprotesi articolari innovative per l'ortopedia. FIRB 2005 "PNR-Programma Nazionale della Ricerca". Cnr-Istec; CnrNano NNL (D. Pisignano). 2007-2010.

Nanobiotecnologie per dispositivi e sensori innovativi applicabili a genomica e post-genomica quali ad esempio dispositivi opto-elettronici e nano-biosensori ibridi a lettura ottica e/o elettronica. FIRB 2004. CnrNano NNL (R. Cingolani). 2005-2010.

EC-SPECTRA. Sviluppo dell'ambiente elettrochimico nel calcolo delle spettroscopie di nano-sistemi ibridi. FIRB Futuro in Ricerca 2008. CnrNano S3 (A. Ferretti). 2010-2013.

Nanofibre polimeriche attive multifunzionali per la fotonica e l'elettronica. FIRB Futuro in Ricerca 2008. CnrNano NNL (D. Pisignano). 2010-2014.

Nanofibre Biomedicali per Ingegneria Tissutale basata su Cellule Staminali Renali. FIRB 2008 MERIT. CnrNano NNL (D. Pisignano). 2010-2013.

PLASMOGRAPH. Plasmons and Terahertz devices in graphene. FIRB Futuro in Ricerca 2010. CnrNano NEST (M. Polini). 2011-2014. <http://www.plasmograph.it/>

Projects & Grants

Processi di micro- e nano- fabbricazione avanzati per la realizzazione di dispositivi o apparati funzionali per applicazioni nel campo dell'elettronica, della fotonica, della micromeccanica e della biosensoristica. MIUR FAR. CnrNano NNL (R. Rinaldi). 2006-2010.

Nanocarriers for Cancer Therapy. MAE 2010 Italia-USA. CnrNano NNL (S. Leporatti). 2008-2010.

Proprietà elettroniche di nanostrutture basate sul grafene/Electronic properties of graphene-based nanostructures. MAE 2010 Italia-USA. CnrNano NEST (V. Pellegrini); CnrNano S3 (E. Molinari). 2009-2010.

Effetti della manipolazione della via di trasduzione ERK sulla plasticità strutturale della via cortico-striatale in vivo mediante microscopia a due fotoni. PRIN 2008. CnrNano NEST (G.M. Ratto). 2010-2014.

Sviluppo di proteine fluorescenti per nanoscopia ottica orientata allo studio di dinamiche cellulari. PRIN 2008. University of Genoa (A.G. Diaspro); CnrNano NEST (V. Tozzini). 2010-2013.

Trasporto quantistico in monostrati di grafene corrugato e rilassamento di spin in punti quantici di grafene. Accordo di cooperazione scientifica Cnr - CSIC (ES). CnrNano NEST (M. Polini). 2009-2010.

Energie da fonti rinnovabili. Progetto interdepartimentale Cnr. CnrNano NNL (G. Gigli). 2011-2014.

Una strategia di nanofabbricazione controllata per la manipolazione ottica di stati a pochi elettroni in dispositivi fotonici a quantum dot. PRIN 2008. Politecnico di Torino (F. Rossi); CnrNano NEST (V. Pellegrini). 2010-2012.

Crescita e caratterizzazione microscopica di dispositivi ad effetto di campo basati su nanofili a semiconduttore. PRIN 2009. Università di Napoli (F. Tafuri); CnrNano NEST (L. Sorba). 2011-2013.

Friction and adhesion of nano-particles on surfaces. PRIN 2008. University of Padova (G. Mistura); CnrNano S3 (S. Zapperi and G. Paolicelli). 2010-2012.

Controlling the structure and function of metal supported organometallic nanostructures. PRIN 2008. University of Rome La Sapienza (M.G. Betti); CnrNano S3 (R. Di Felice). 2009-2012.

Spintronic devices for mass-scale electronics. MAE 2010 Italia-India. CnrNano NNL (G. Maruccio). 2008-2010.

Innovative catalytic patterns for nanowire growth. MAE 2010 Italia-India. CnrNano NEST (S. Heun). 2008-2010.

Regional Projects

SAFEMEAT. Innovazioni di processo e di prodotto per incrementare i profili di sicurezza e per diversificare la gamma dei prodotti (freschi e stagionati) a base di carne suina. Regione Puglia. Cnr Dipartimento Agroalimentare; CnrNano NNL (R. Rinaldi). 2011-2014.

Biosensor-based assay for high-throughput quantitative screening of chloride transport. Regione Toscana "Bando Salute 09". CnrNano NEST (D. Arosio). 2010-2012.

Sviluppo e realizzazione di biochip per la diagnostica molecolare e la tipizzazione di virus patogeni umani (HPV, HCV, COXSACKLE B) PS 105. Strategico Regione Puglia. CnrNano NNL (R. Rinaldi). 2009-2012.

PHOEBUS. Regione Puglia. CnrNano NNL (G. Gigli). 2009-2011.

Development of a diamond film detector for UV detection. Regione Puglia. Cnr-Imip, Bari; CnrNano NNL (A. Passaseo). 2009-2010.

WAFITECH. Laboratorio regionale per le nuove nano e biotecnologie per la filtrazione dell'acqua: design e costruzione di membrane biomimetiche per applicazioni industriali, commerciali e ambientali. Regione Puglia. University of Bari (G. Calamita); CnrNano NNL (A. Camposeo). 2009-2012.

AEROCOMP. Studio Preliminare di Materiali Nanocompositi per Applicazioni Aeronautiche (Progetto DM 48391). DHITECH FAR. CnrNano NNL (A. Athanassiou). 2008-2012.

OLED. Nuovi sorgenti OLED per l'illuminazione. DHITECH FAR. CnrNano NNL (G. Gigli). 2008-2012.

INTERMECH. Interlaboratorio per la Meccanica Avanzata. Regione Emilia Romagna "Laboratori strategici". University of Modena and Reggio Emilia (A.O. Andrisano); CnrNano S3 (U. del Pennino). 2008-2010.

PROMINER. Progetto per le micro e nanotecnologie in Emilia Romagna. Regione Emilia Romagna "Laboratori strategici". CnrNano S3 (E. Molinari). 2008-2010.

Costituzione di una banca di cellule staminali adulte renali per la promozione degli studi sulle cellule staminali e loro applicazione pratica e progettazione e realizzazione di un dispositivo su chip per dialisi. Regione Puglia. Consorzio CARSO; CnrNano NNL (D. Pisignano). 2007-2011.

PONAMAT. Sviluppo di materiali nanocompositi polimerici innovativi per applicazioni in ottica elettronica e sensoristica. Regione Puglia. ENEA; CnrNano NNL (D. Pisignano). 2006-2011.

Other Funding Agencies

Development of cytochrome c assay marker of ischemia/reperfusion damage to the heart. Istituto Europeo di Oncologia - Bando Fondazione Umberto Veronesi. CnrNano NNL (R. Rinaldi). 2011-2012.

MOPROSURF Modeling protein-surface interaction. IIT Istituto Italiano di Tecnologia Seed. CnrNano S3 (S. Corni; R. Di Felice). 2010-2013. <http://www.moprosurf.nano.cnr.it/>

Modena-Columbia partnership on Carbon-based nanoscience. Fondazione Cassa di Risparmio di Modena "Internazionalizzazione". CnrNano S3 (E. Molinari). 2008-2010.

Theory of Switching and imaging molecular magnets on surfaces. Fondazione Cassa di Risparmio di Modena "Internazionalizzazione". CnrNano S3 (F. Manghi). 2010-2012.

Multi-scale modelling DNA. Fondazione Cassa di Risparmio di Modena "Internazionalizzazione". CnrNano S3 (R. Di Felice). 2010-2012.

Few-body Physics of cold Fermi atoms. Fondazione Cassa di Risparmio di Modena "Internazionalizzazione". CnrNano S3 (M. Rontani). 2010-2012.

MARINE Materiali ad Indice di rifrazione negativo nel visibile e criteri per l'invisibilità. Ministero Difesa. University of Rome La Sapienza; CnrNano NNL (A. Passaseo). 2010-2013.

UdR IIT @ NNL. IIT Istituto Italiano di Tecnologia. CnrNano NNL (R. Rinaldi). 2006-2011.





Collaborations

Selected Collaborations

- Brazil** Marília J. Caldas and Helena M. Petrilli, *Universidade de São Paulo, São Paulo.*
- Canada** Harry E. Ruda, *University of Toronto, Toronto.*
- Denmark** Birthe B. Kragelund, *University of Copenhagen, Copenhagen.*
- Finland** Jukka Pekola, *Aalto University, Aalto.*
- France** Alberto Bramati and Elisabetta Giacobino, *Université Pierre et Marie Curie, Paris*; Cristiano Ciuti, *Université Paris Diderot, Paris*; Wolfgang Wernsdorfer, *CNRS Institut L. Néel, Grenoble.*
- Germany** Tommaso Calarco, *Institut für Quanteninformationsverarbeitung, Universität Ulm, Ulm*; Gianaurelio Cuniberti, *Technische Universität Dresden, Dresden*; Hans-Joachim Freund, *Fritz-Haber-Institut der Max-Planck-Gesellschaft, Berlin*; Alfred Leitenstorfer and Rupert Huber, *University of Konstanz, Konstanz*; Werner E. G. Müller, *Johannes Gutenberg Universität, Mainz*; Heinz C. Schröder, *Johannes Gutenberg Universität, Mainz*; Turbomole GmbH, *Karlsruhe*; Rebecca Wade, *EML and University of Heidelberg, Heidelberg.*
- Greece** Demetrios Anglos and Maria Farsari, *FORTH, Heraklion.*
- India** Giridhar U. Kulkarni, *Jawaharlal Nehru Centre for Advanced Scientific Research, Bangalore*; Anushree Roy, *Indian Institute of Technology, Kharagpur.*
- Iran** Reza Asgari, *Institute for Research in Fundamental Sciences (IPM), Tehran.*
- Israel** Danny Porath and Uri Banin, *Hebrew University of Jerusalem, Jerusalem*; Gideon Schreiber and David Cahen, *Weizmann Institute of Science, Rehovot*; Eyal Zussman, *Technion – Israel Institute of Technology, Haifa.*
- Italy** Franca Albertini, *Imem-Cnr, Parma*; Giorgio Biasiol, *Iom-Cnr, Trieste*; Federico Boscherini, *Università di Bologna, Bologna*; Laura Cancedda, *Istituto Italiano di Tecnologia, Genova*; Massimo Capobianco and Maria Luisa Navacchia, *Isof-Cnr, Bologna*; Giorgio Carmignoto, *Istituto Neuroscienze-CNR, Padova*; Mauro Gemmi, *Center for Nanotechnology Innovation@NEST, Istituto Italiano di Tecnologia, Pisa*; Dario Gerace, *Università di Pavia, Pavia*; Gianfranco Pacchioni, *Università di Milano-Bicocca, Milan*; Saverio Pascazio, *Università di Bari, Bari*; Tommaso Pizzorusso, *Università di Firenze and Istituto Neuroscienze-CNR, Florence*; Giancarlo Salviati, *Imem-Cnr, Parma*; Giuseppe Santoro and Alessandro Silva, *SISSA, Trieste*; Diederik Wiersma and Paolo De Natale, *Cnr-Ino, Florence.*

- New Zealand** Michele Governale, *Victoria University of Wellington, Wellington.*
- Poland** Joanna Trylska, *University of Warsaw, Warsaw.*
- Portugal** Dmitry Isakov, *University of Minho, Braga.*
- Russia** Vadim Khrapai, *Institute of Solid State Physics, Russian Academy of Sciences, Chernogolovka.*
- Spain** Francisco Guinea, *CSIC, Madrid*; Jordi Hernandez-Borrell, *University of Barcelona, Barcelona*; Fabrice Laussy and Francesca Marchetti, *Universidad Autónoma de Madrid, Madrid*; Javier Luque, *Universitat de Barcelona, Barcelona*; Fernando Luis, *Instituto de Ciencia de Materiales de Aragón, CSIC-Universidad de Zaragoza, Zaragoza*; Felix Ritort, *University of Barcelona, Barcelona*; Angel Rubio, *Universidad del Pais Vasco, Donostia-San Sebastian*; Felix Zamora and Julio Gomez-Herrero, *Universidad Autónoma de Madrid, Madrid.*
- Sweden** Yi Luo, *Royal Institute of Technology, Stockholm.*
- Switzerland** Jérôme Faist, *ETH, Zurich*; Aldo Ferrari, *ETH, Zurich*; Atac Imamoglu, *ETH, Zurich*; Ernst Meyer, *University of Basel, Basel.*
- The Netherlands** Yaroslav Blanter, *TU Delft, Delft*; Rembert A. Duine and Hendricus T.C. Stoof, *Utrecht University, Utrecht*; Mikhail I. Katsnelson, *Radboud University of Nijmegen, Nijmegen.*
- United Kingdom** Asa H. Barber, *Queen Mary University of London, London*; Julia M. Yeomans, *University of Oxford, Oxford*; Carol C. Perry, *Nottingham Trent University, Nottingham*; David A. Ritchie, *University of Cambridge, Cambridge*; Peter Spearman, *Kingston University, London*; Vlatko Vedral, *University of Oxford, Oxford*; Richard E.P. Winpenney, *University of Manchester, Manchester.*
- USA** Alessio Accardi, *Cornell University, New York NY*; Marco Buongiorno Nardelli, *University of North Texas, Denton TX*; Subha Das, *Carnegie Mellon University, Pittsburgh PA*; Yuris A. Dzenis, *University of Nebraska-Lincoln, Lincoln NE*; Miguel Fuentes Cabrera, *Oak Ridge National Laboratory, Oak Ridge TN*; Mark Hybertsen, *Columbia University and Brookhaven National Laboratory, New York NY*; Allan H. MacDonald, *University of Texas, Austin TX*; Loren Pfeiffer, *Princeton University, Princeton NJ*; Aron Pinczuk, *Columbia University, New York NY*; Eli Rotenberg, *Advanced Light Source, Lawrence Berkeley National Laboratory, Berkeley CA*; Lu Sham, *University of California San Diego, San Diego CA*; Giovanni Vignale, *University of Missouri, Columbia MO*; David A. Weitz, *Harvard University, Cambridge MA.*





CnrNano Life

2010

June

CERIA 2010 (Modena)

On June 23-25, 2010, S3 scientists organized a *Workshop on Cerium Oxide* (CERIA 2010) in Modena. It brought together scientists working in the field of cerium oxide, to discuss, share ideas, establish new collaborations and consolidate the existing ones about this metal oxide. The workshop was mostly focused on studies of model systems, like ultrathin films and surfaces, with contributions on more realistic systems (e.g., nanoparticles and powdered catalysts). The workshop was attended by about 30 scientists from all over Europe, and a second edition was held in 2011 in Spain.



CERIA
2010

October

Kick-off Meeting



The Nanoscience Institute originates from the merging of three well-established research centers that shared a common scientific background and a long story of collaborations. In the Tuscan countryside, at Villa Guinigi, Matraia (Lucca) on October 4-5, the Institute kick-off meeting was held. It was attended by about 100 researchers of the Institute, who gathered to present and discuss their science, by way of talks and of a poster session. The isolated setting helped them know each other and set the basis for the building of the CnrNano community.

Festival della Scienza

CnrNano contributed to Festival della Scienza 2011, the major Italian event of science dissemination, with *Orizzonti Sonori*, a hands-on laboratory on the physics of sound. Visitors familiarized with the physics of waves and experimented the inner connections between physics and music through a collection of lab benches and interactive stations co-designed by CnrNano researcher Carlo Andrea Rozzi.



November

Cnr Sole24 Ore Award



On November 8, a CnrNano research group led by Luana Persano collected a prestigious award for promising high-tech business ideas, supported by Cnr and the major Italian financial newspaper *Sole24Ore*. Persano and colleagues Andrea Camposeo, Alessandro Polini, and Vanna Sciancalepore, were awarded for "SM&T", a start-up business idea focused on the design and production of innovative substrates for in-vitro stem cell culture. They were also awarded a "Premio Comunicazione" for showing the best skills in presenting and communicating their idea.

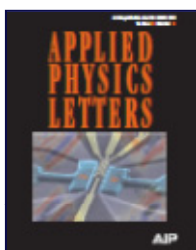
Professione Fisica

The next generation of nanoscientists: researchers from CnrNano are committed to bring their frontier research experience in nanoscience directly to the high-school environment. To this purpose they contributed to *Professione Fisica*, a workshop on physics careers for students held yearly in Modena, aimed at showing the high-school student the opportunities and challenges of a curriculum in physics and possibly in nanoscience studies. During the two-day event, students had the chance to meet physics graduates who described their professional experience; at the same time a number of teachers participated in an update course on the latest research in nanoscience and related technologies.

2011

March

Applied Physics Letters and Journal of Microscopy Cover Articles



Vittorio Pellegrini, Francesco Giazotto, Lucia Sorba, and Fabio Beltram earned the cover of Applied Physics Letters with the article *Quantum dot spectroscopy of proximity-induced superconductivity in a two-dimensional electron gas* [*Appl.Phys.Lett.* 98, 132101 (2011)]. Claudia Menozzi gained the cover of Journal of Microscopy with the article *Fibre-top atomic force microscope probe with optical near-field detection capabilities* [*J. Microsc.* 242, 10 (2011)], about a fibre-top technology that can be used for the development of a new generation of hybrid probes.



Blow-up. Images from the nanoworld in Verona

How do people imagine the nanoworld looks like? What do scientists see with their instruments? More than 3,000 visitors had these questions answered as they visited *Blow-up. Images from the nanoworld*, an exhibition resulting from the interaction between CnrNano scientists' and a photographer's work. Completely designed and produced by CnrNano, and displayed in Verona after several previous shows, the exhibition is a visual journey into the dimension of nanoscience that shows to the public images which are usually accessible only to few, as they are intended for research labs.

The artistic touch of photographer Lucia Covi shed new light on CnrNano scientific images and these do now challenge the viewer's imagination.



April

1st Seminar of the Seminar Institute Series



Beside the seminars occurring weekly in the different centers, the CnrNano Institute organizes a common series of seminars, focused on common-interest topics, and hold in one of the Centers by prominent scientists.

The seminars are usually video transmitted so to be available to researchers all around the Institute. The Seminar series was inaugurated by the lecture of professor Angel Rubio (ETSF and UPV/EHU, San Sebastian, Spain) about "Photo-induced dynamical processes in nanostructures, biomolecules and oxides", in Modena. It was attended by 80 researchers from the different sites.

June

Marie Curie, Hertha Ayrton and others

"Nothing in life is to be feared, it is only to be understood. Now is the time to understand more, so that we may fear less". One hundred years after her Nobel awarding, the fortunes and commitment in the life of Marie Curie are still food for thought on the complex relations between science and society. CnrNano organized a roundtable discussion on Marie Curie's legacy on the occasion of the staging of a piece about Marie Curie's life, written by CnrNano scientist Stefano Ossicini, at Teatro Cittadella, Modena.



Fare Fisica, a summer school for high-school students (Modena)



To give high school students an opportunity to get a foot in the door of a research environment, CnrNano in collaboration with University of Modena and Reggio Emilia, hosted *Fare Fisica*, a summer school for high school juniors. More than 40 high-school students attended college-level classes and complete hands-on research taught by faculty members and CnrNano scientists for six stimulating days. The free-of-charge program and the in-campus accommodation for the non residential students provided a truly academic and scientist-like experience.

Since the program met a highly positive response from both teachers and students, CnrNano intends to make it a yearly event to boost student interest in science careers.

August

National School on the Physics of the Matter (Erice)

All that matters: more than 120 attendees of the summer school and workshop entitled *Quantum phenomena in Graphene, other low-dimensional materials, and optical lattices* made it clear the ever-growing relevance of these issues. Co-organized by CnrNano and held in the prestigious Ettore Majorana Foundation and Centre for Scientific Culture in Erice (Sicily) from July 26 to August 7, the event intended to summarize some of the developments in the field of quantum phenomena in graphene, topological insulators and cold atoms in optical lattices, and explore possible practical applications.



September

ITQW 2011, (Badesi, Sardinia)



In the September 11-17 week, the 11th edition of the *International Conference on Intersubband Transitions in Quantum Wells* took place in Badesi, Sardinia. For the first time in 20 years, the event was held in Italy and Cnr-Nano was deeply involved in the organization, with Alessandro Tredicucci acting as conference chair (together with Gaetano Scamarcio from Bari University) and Miriam Vitiello chairing the program committee.

The conference drew over a hundred participants from all over the world, including a few researchers from Sendai in Japan, who were able to attend despite the grave natural disaster that had hit the area just a few months before. Among other advances, the new record-high temperatures of operation for THz quantum cascade lasers were first presented here by MIT scientists.

The European Researcher's night in Lecce



For one night, everybody can be a scientist. The *Researchers' Night* is a Europe-wide event that brings together the public at large and researchers once a year. In 2011 it took place on September 23 in over 800 venues of 320 European cities of 32 countries. Researchers from CnrNano contributed to the successful *Notte dei Ricercatori* in Lecce, where people had the unique opportunity to discover research facilities, to use the most recent technologies and instruments with the guidance of scientists, to watch demonstrations and simulations, and to exchange ideas with the researchers.

WESSS Workshop (Lecce)

In view of targeting common-interest topics, CnrNano decided to organize 3 workshops open to its own researchers and to top-level scientists. The first workshop of the series was the *WESSS Workshop on entanglement in solid state systems*, held in Lecce on September 24-26. Scientists expert in different fields met to compare approaches and strategies leading to the control of entanglement in different solid state quantum systems.

Workshop on "Photovoltaics: new frontiers and applications" (Lecce)

The second common Institute workshop was also held in Lecce, from September 28 to 30, and showed photovoltaics, solar cells and light harvesting as keywords. The *Workshop on Photovoltaics: New frontiers and applications* put together scientists and stakeholders to discuss the different design aspects of 3rd-generation photovoltaic cells.



The central themes faced were the core of hybrid/organic cells such as Dye Sensitised Solar Cells (DSSC), cells based on colloidal inorganic nanocrystals, inorganic wires, etc. New materials, device structures and fabrication processes were also debated by the 70 participants, who could also enjoy a wonderful social program based on the local traditions.

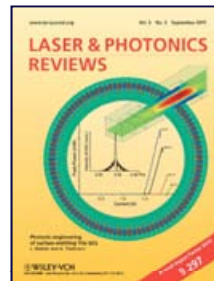
CnrNano scientists write about graphene in *Le Scienze*

In the September issue of *Le Scienze*, the Italian edition of *Scientific American*, an article appeared about graphene written by the CnrNano scientists Vittorio Pellegrini and Marco Polini. In *Laboratorio grafene* they took an in-depth look at the role of graphene in cutting-edge science and at its importance in fundamental physics.



Cover Article: Laser & Photonic (NEST)

CnrNano researcher Alessandro Tredicucci hits the cover of Laser & Photonic Reviews journal with the article *Photonic engineering of surface-emitting terahertz quantum cascade lasers* [Laser & Photonics Reviews 5, 647 (2011)].



October

NANOLAB for secondary school science teachers



Nanoscience as a gateway to engaging students in cutting-edge research, to introducing the basics of the modern physics of matter in a practical and interdisciplinary way, to connecting fundamental science and technology. To this extent CnrNano contributed to NANOLAB, an educational project developed by the Physics Department of the University of Modena and Reggio Emilia.

The NANOLAB team, composed of researchers and academic tutors, plan life-long training courses on nanoscience, and organize laboratories addressed to school teachers and focused on the insertion of nanoscience in high-school and undergraduate curricula. Lab experiments are indeed conceived for average school laboratories, and are provided with extensive teacher's guides, videos, software and background materials.

December

HYEX 2011 International Workshop on Hybrid Excitations in Nano-Materials (Modena)

On December 18, CnrNano welcomed in Modena the participants to the *International Workshop on Hybrid Excitations in Nano-Materials*, co-funded by Fondazione Cassa di Risparmio di Modena, for scientists active in the synthesis and spectroscopy of hybrid nano-objects, theoreticians and computational physicists. In the four days of talks and poster presentations, the 40 attendees analyzed the current situation in the field of hybrid excitations in composite materials at the nano-scale, and discussed open problems, challenges and the most promising directions.



Outreach and
communication

As a publicly funded organization, CnrNano has both the interest and the responsibility to inform the society on its activities, by disseminating results and by making its cutting-edge science understandable. A great number of activities aimed at communicating its innovative research and informing a range of audiences, from high-school students, to journalists, to policymakers, are therefore developed. Scientists and staff have worked together to publicize CnrNano scientific work via press campaign; to engage with schools and the general public; to build relationships with media and policymakers; to increase awareness about science in general.

Media Relations

Since the Institute foundation, a newborn Communication Office, working in agreement with the Cnr Press Office, has been able to establish sound relationships with media specialists, to provide information about important CnrNano research results and to promote CnrNano scientists as outstanding experts. In 2010-2011 the Communication Office issued 19 press releases that led to a quite widespread presence of CnrNano news in general and scientific press, both traditional and web, as well as on radio and tv. The Communication Office also hosts journalists' visits to CnrNano laboratories and organizes interviews with scientists.

Outreach Activities

CnrNano also supported a number of outreach initiatives directed at the wider scientific community, as well as journalists, students, teachers, and general public, aimed at different audiences, sharing knowledge about nanoscience and more generally raising awareness on the impact of science on society. Thanks to the active involvement and commitment of its scientific community, CnrNano was able to:

- sponsor and host a summer school for high-school students on physics and physics of matter (*Fare Fisica*, Modena, June 2011)
- participate to a workshop on physics careers for students (*Professione Fisica*, Modena, November 2010)
- take part in an educational programme supporting secondary school science teachers for the integration of nanoscience in high-school and undergraduate curricula (*Nanolab*, Modena, 2010-2011)

- submit presentations at scientific festivals and science popularization events, including a hands-on activity for the Festival della Scienza, the major science event in Italy (Genoa, November 2010), and a dissemination event for the European Researcher's night, the annual dissemination event organized all over Europe (Lecce, September 2011).
- showcase a self-produced cultural project, *Blow-up. Images from the nanoworld*, an exhibition of scientific images of nanoscale objects resulting from the interaction between a photographer's experience and CnrNano scientists' work. (Verona, March 2010; <http://blowup.nano.cnr.it/>).



PISA NEST

NEST
Piazza San Silvestro 12
56127 Pisa, Italy

+39 050 509418

segreteria.nest@nano.cnr.it



LECCE NNL

NNL
Via Arnesano
73100 Lecce, Italy

+39 0832 298239

segreteria.nnl@nano.cnr.it



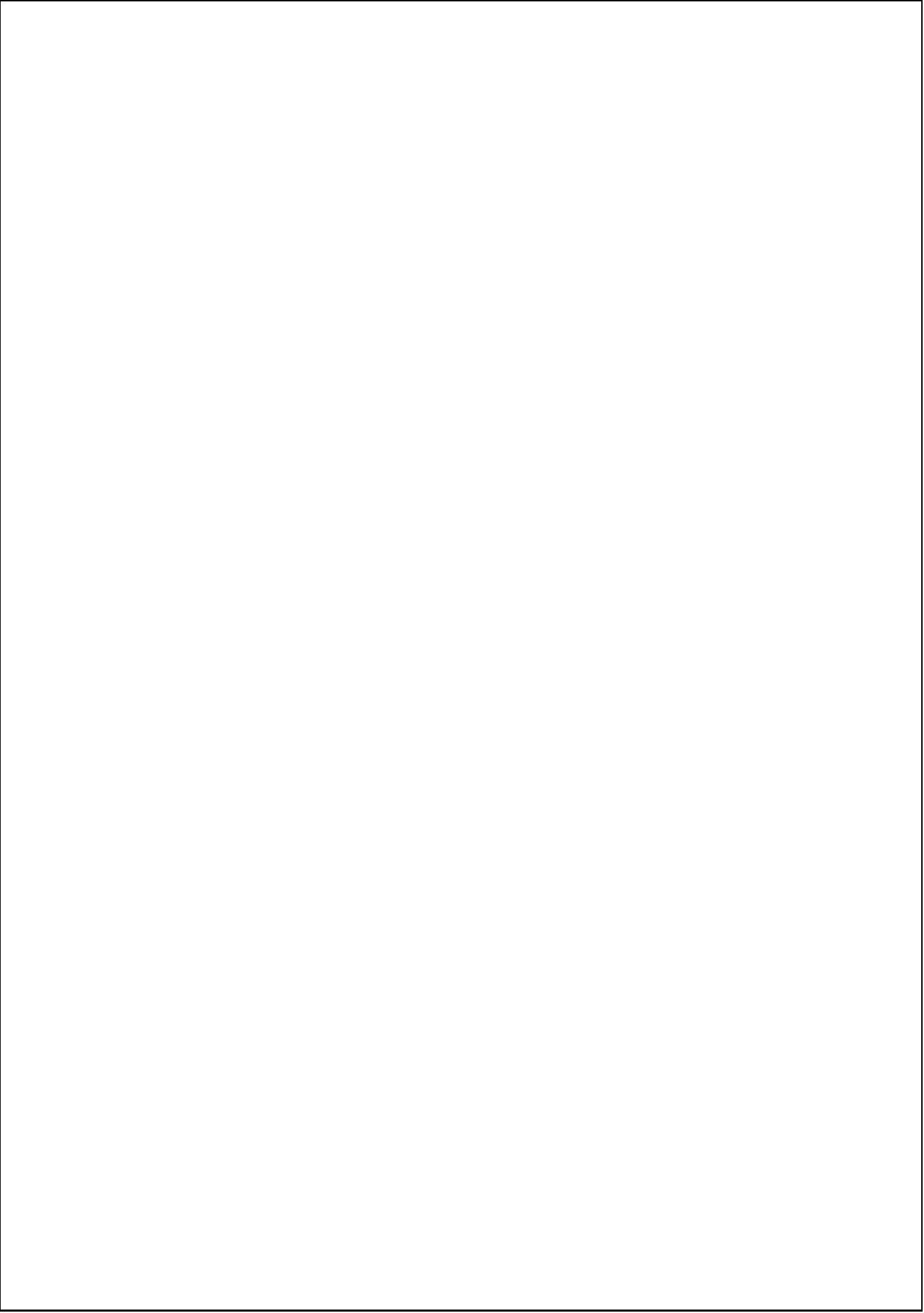
MODENA S3

S3
Via Campi 213/A
41125 Modena, Italy

+39 059 2055629

segreteria.s3@nano.cnr.it







 **CNRNANO**

ISTITUTO NANSCIENZE CONSIGLIO NAZIONALE DELLE RICERCHE

Pisa NEST, Lecce NNL, Modena S3
www.nano.cnr.it